90-05056/

Manitoba
Energy and Mines
Geological Services

Geological Paper GP87-1

Quaternary Stratigraphy and Overburden Geochemistry in the Phanerozoic Terrane of Southern Manitoba

By E. Nielsen
Winnipeg, 1989

Energy and Mines

Hon. Harold J. Neufeld
Minister

Ian Haugh
Deputy Minister

Minerals Division

Sobharam Singh
Assistant Deputy Minister

Geological Services
W.D. McRitchie
Director

TABLE OF CONTENTS

	Page
INTRODUCTION	1
METHODS OF INVESTIGATION	2
Field Methods	2
Heavy Mineral Separation	2
Textural Analysis and Pebble Counts	2
Clay Separation and Geochemistry	2
RESULTS OF INVESTIGATION	4
Balmoral-Komarno Area	4
Location and topography	4
Bedrock geology	4
Quaternary geology	4
Drift thickness	4
Ice flow	4
Inwood till	4
Komarno till	4
Proglacial sediments	10
Drift-ice turbate	10
Geochemistry	18
Tills	18
Glaciolacustrine sediments	22
Drift-ice turbate	22
Conclusions	22
Moosehorn-Gypsumville Area	24
Location and topography	24
Bedrock geology	24
Quaternary geology	24
Drift thickness	24
Ice flow	24
Inwood till	24
Komarno till	25
Proglacial sediments	25
Iceberg turbate	25
Geochemistry	32
Tills	32
Glaciolacustrine sediments	32
Iceberg turbate	32
Conclusions	32
Swan Lake-Dawson Bay Area	32
Location and topography	32
Bedrock geology	36
Quaternary geology	36
Drift thickness	36
Ice flow	38
Older till	38
Zelena Till	38
Arran Till	38
Iceberg turbate	41
Postglacial sediments	41
Geochemistry	41
Older till	41
Zelena Till	47
Arran Till	47
Iceberg turbate	47
Postglacial sediments	47
Conclusions	47
CONCLUSIONS AND RECOMMENDATIONS	62

Page

ACKNOWLEDGEMENTS 63
REFERENCES 64
APPENDIX I: Results of geochemical analysis on samples from the Balmoral-Komarno area 66
APPENDIX II: Results of geochemical analyses on samples from the Moosehorn-Gypsumville area 71
APPENDIX III: Results of geochemical analysis on samples from the Swan Lake-Dawson Bay area 73

FIGURES

Figure 1: Location of the three sampling areas vi
Figure 2: Galena float from southern Manitoba 1
Figure 3: Sampling sites in the Balmoral-Komarno area 3
Figure 4: Aerial photograph showing till and glaciolacustrine plains 6
Figure 5: Bedrock geology of the Balmoral-Komarno area 6
Figure 6: Surficial geology of the Balmoral-Komarno area 7
Figure 7: (A) Striated pavement indicating ice flow toward 130° 8
(B) Details of striae oriented toward 135° 8
Figure 8: (A) Fluted till plain west of Balmoral 9
(B) Till plain showing intersecting flutes 9
Figure 9: Crossing striae showing ice flow toward 170° and 140° 10
Figure 10: Stratigraphic cross-sections 11
Figure 11: Komarno till overlying Inwood till 12
Figure 12: Grain size distribution of Inwood till, Komarno till and drift-ice turbate 13
Figure 13: Scanning electron photomicrograph of Inwood till 16
Figure 14: Pebble fabric of Kormarno Till 16
Figure 15: Stratigraphy of glaciolacustrine sediments 17
Figure 16: Stony lake clays south of Argyle 17
Figure 17: Laminated stony lake clay with dropstones 17
Figure 18: Flow fold and disturbed bedding related to slumping 19
Figure 19: Distribution of iceberg and inshore drift-ice furrows 20
Figure 20: Intersecting iceberg furrows 21
Figure 21: Inshore drift-ice scouring southeast of South Shoal Lake 21
Figure 22: Cross-section of an iceberg furrow 22
Figure 23: Iceberg turbate comprising Komarno till and clay 24
Figure 24: Relative unconfined strength in drift-ice turbate and Inwood till 26
Figure 25: Phases of iceberg and iceberg turbate formation 26
Figure 26: Frequency distribution of trace elements and carbonate content 27
Figure 27: Till sample locations in the Moosehorn-Gypsumville area 31
Figure 28: Bedrock geology of the Moosehorn-Gypsumville area 33
Figure 29: Surficial geology of the Moosehorn-Gypsumville area 34
Figure 30: Drumlinoid ridges oriented toward 155° west of Mantagao Lake 35
Figure 31: Flutes oriented toward 140° in the Spearhill area 35
Figure 32: Summary of striae directions 36
Figure 33: Grain size distribution of Inwood till, Komarno till and iceberg turbate 37
Figure 34: Iceberg furrows near St. Martin Station 38
Figure 35: Stratigraphy near St. Martin Station 40
Figure 36: Cross-section of an iceberg furrow 40
Figure 37: Iceberg turbate exposed in Figure 36 41
Figure 38: Frequency distribution of trace elements and carbonate content 42
Figure 39: Sampling sites in the Swan Lake-Dawson Bay area 46

Page

Figure 40: The Manitoba escarpment and Porcupine Hills as seen from Swan Lake 47
Figure 41: Bedrock geology of the Swan Lake-Dawson Bay area 48
Figure 42: Winnipegosis reef south of Dawson Bay 49
Figure 43: Brine spring south of Dawson Bay 49
Figure 44: Swan River sandstone concretion, Kettle Hills 49
Figure 45: Shale outcrop along the Manitoba escarpment 49
Figure 46: Surficial geology of the Swan Lake-Dawson Bay area 51
Figure 47: Striae oriented toward 250° 52
Figure 48: Grain size distribution of the older till, Zelena Till, Arran Till and iceberg turbate 54
Figure 49: Hummocky stagnation moraine, Porcupine Hills 55
Figure 50: Zelena Till overlying deformed sand in hummocky stagnation moraine 55
Figure 51: Fossiliferous sand and gravel overlying Arran Till 56
Figure 52: Slumped Arran Till (a) overlying clay (b) and Arran Till (c) 56
Figure 53: Frequency distribution of trace elements and carbonate content 57

TABLES

Table 1: Summary of statistics for pebble counts on selected samples from all areas 5
Table 2: Summary statistics for the geochemical data from the Balmoral-Komarno area . . 23
Table 3: Summary statistics for the trace element geochemical data for the Paleozoic bedrock formations 25
Table 4: Summary statistics for the geochemical data from the Moosehorn-Gypsumville area 39
Table 5: Summary statistics for the geochemical data from the Swan Lake-Dawson Bay area 53

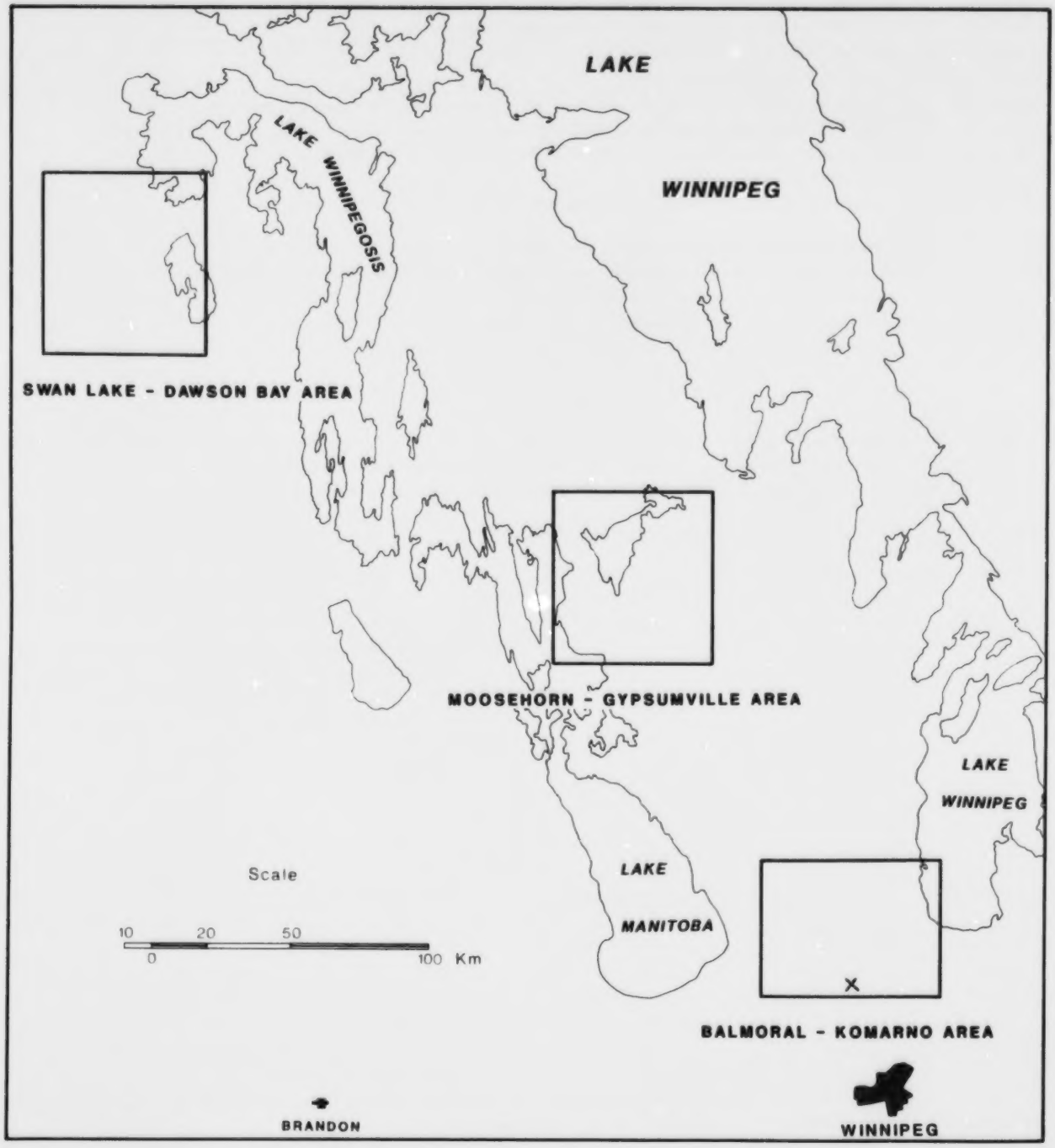

Figure 1: Location map showing the three till sampling areas and the location of the galena float (x).

INTRODUCTION

There has been relatively little published on work done in the Phanerozoic terrane of southern Manitoba in response to the discovery of galena float near Balmoral in the early 1960s. Stevenson (1973) and Evans (1976) undertook analyses of brine water from springs found along the west side of Lake Winnipegosis, and of birch twigs (*Betula papyrifera*) and soil samples, (A horizon) from the Red Deer River area. Six of the 90 twig and soil samples collected from 45 sites were anomalous, (twigs up to 15 400 ppm Zn, soil up to 700 ppm Zn). Follow-up drilling on semi-coincident birch twig and soil anomalies showed no evidence of sulphide mineralization.

Overburden geochemical and Quaternary stratigraphic studies have been undertaken in selected areas of the Phanerozoic terrane of southern Manitoba (Fig. 1) in response to the discovery of the Doan galena pebble (Fig. 2) near Balmoral (McCabe, 1969). Lead isotope ratios of the galena pebble indicates it was derived from a Phanerozoic source (Gale, in prep.). It was hypothesized that the source lay in the Phanerozoic terrane of southern Manitoba and that the erratic had been transported to Balmoral by glaciers moving through the region during the late Pleistocene.

The Paleozoic terrane of southern Manitoba was considered a favourable area for lead-zinc mineralization as there are areas of carbonate breccias, reef development, karst and paleokarst topography, several unconformities, Precambrian structures in the subsurface and extensive areas of dolomitization.

To find the source of the galena float two lines of investigation were undertaken: 1) Phanerozoic drill core, from the Manitoba Energy and Mines drill core library, was analyzed for base metals (Gale, in prep.), and 2) detailed overburden geochemistry and Quaternary stratigraphic analysis were carried out in the area where the galena erratic was found and in the up-ice direction. The results of the latter study is the subject of this report.

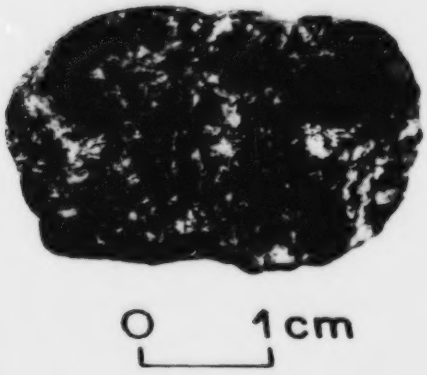

Figure 2: Doan galena pebble from Balmoral.

METHODS OF INVESTIGATION

Field Methods

A total of 372 backhoe pits, ranging between approximately one and five metres in depth, were dug in three main areas, namely the Balmoral-Komarno area in the southern Interlake, the Moosehorn-Gypsumville area in the central Interlake and the Swan Lake-Dawson Bay area in the northern Westlake area (Fig. 1). All the major lithosomes were sampled at least once in each area. Till was sampled in every hole but glaciolacustrine sediments were sampled in only a few places. The backhoe pits were dug along road allowances and were variously spaced between 0.25, 0.5 and 1 mile apart.

In each area the glacier flow direction was determined from striations and the orientation of flutes. The surficial geology of each area was mapped from airphotos or acquired from pre-existing maps.

Each sample consisted 25 kgs collected for heavy mineral separation, 8 kgs collected for textural analyses and pebble counts, and 0.5 kg collected for geochemistry.

Heavy Mineral Separation

Each 25 kg sample was disaggregated in a cement mixer until a muddy slurry was produced. The slurry was passed through a 2 mm screen and the less than 2 mm fraction was collected in a plastic garbage container. This fraction was subsequently passed over a shaker table where the heavy mineral fraction was concentrated. The coarser than 2 mm fraction was visually inspected for galena and sphalerite before being discarded. The results of the heavy mineral study is the topic of a separate report (Gale, in prep.).

Textural Analysis and Pebble Counts

The 8 kg sample was air dried, weighed and disaggregated using a wooden mallet before being dry sieved on a 4 mm screen. The coarse fraction was washed and sieved at 1 phi intervals between -5 phi and -2 phi. The 4-16 mm size-fraction was retained for pebble counting. The fine fraction, (<4 mm), was sieved and pipetted at 1 phi intervals between -2 phi and 8 phi using the procedure outlined by Folk (1968).

Clay Separation and Geochemistry

A 100 gm split from the 0.5 kg sample was disaggregated in 1 litre of distilled water using a milk-shake mixer. The silt and clay fraction was decanted into a 1 litre centrifuge bottle and centrifuged at 750 r.p.m. for 3 minutes. The <2 micron fraction was decanted into another 1 litre centrifuge bottle and centrifuged at 2300 r.p.m. for 15 minutes. After decanting the water the <2 micron fraction was scraped from the bottle, dried and crushed, and submitted for geochemical analysis. The reasons for using the clay-sized fraction are documented in Shilts (1975, 1976, 1977), Klassen and Shilts (1977), and summarized by DiLabio *et al.* (1982) and Shilts (1984).

The clay-sized fraction of the samples was analyzed for Cu, Pb, Zn, Ni, Co, Cr, Fe, Mn and Ba by atomic absorption spectrophotometry after hot nitric-hydrochloric acid extraction. The lower detection limits for all the elements are 1 or 2 ppm, except iron which has a detection limit of 0.1 per cent.

The carbonate content (CO_3) of the silt plus clay fraction was determined using the Leco furnace.

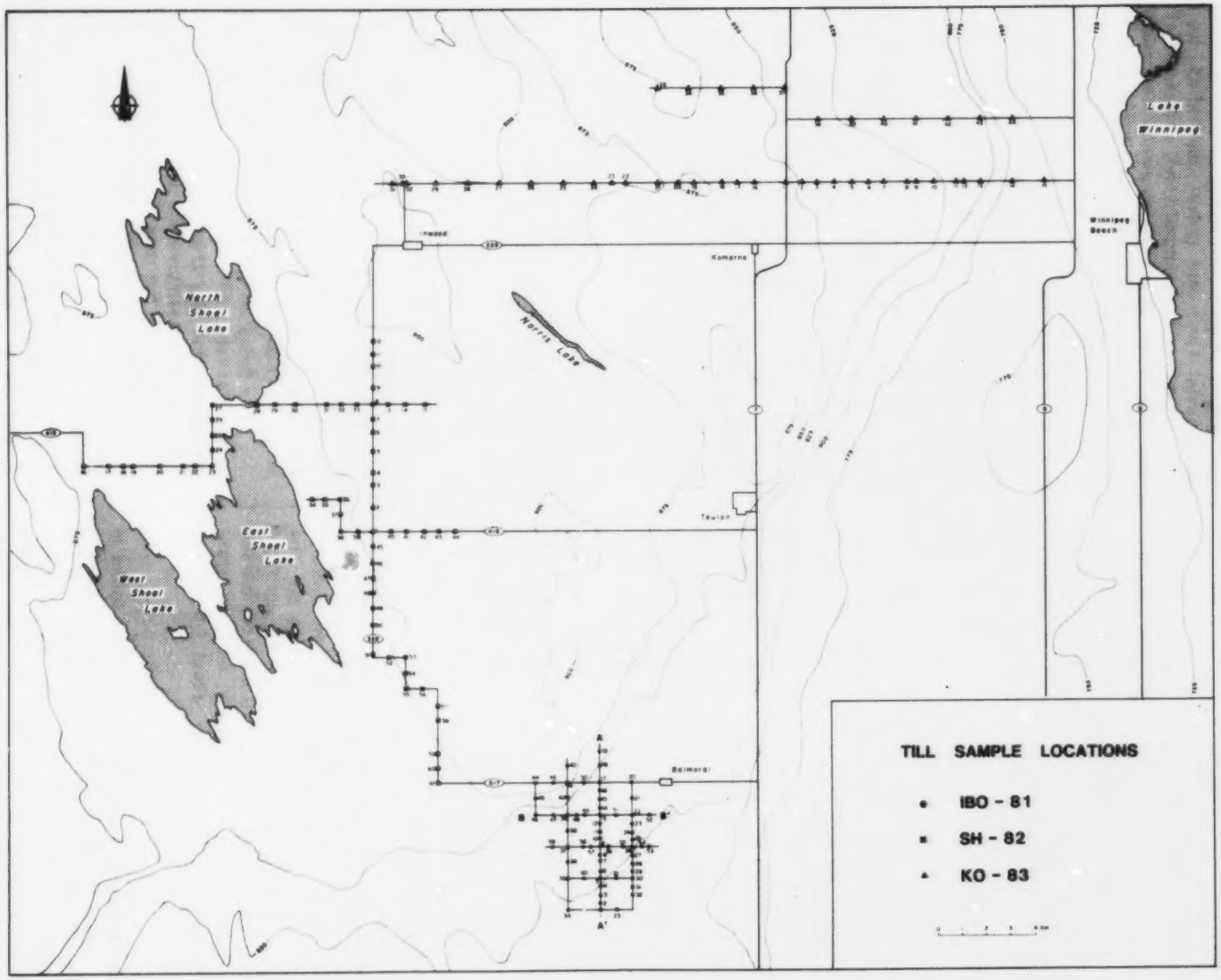

Figure 3: Sampling sites in the Balmoral-Komarno area. The Doan galena pebble was found near site IBO-81-55. Contours in feet.

RESULTS OF INVESTIGATIONS

Balmoral-Komarno Area

Location and topography

This sampling area is situated in the southern Interlake in the region where the Doan galena pebble (McCabe, 1969) was found (Fig. 3).

Elevations range from 275 m (asl) at Inwood down to the level of Lake Winnipeg at 218 m. The local relief is only about 1-2 m except for the prominent scarp that crosses the area from the northeast to the southwest. This scarp, reaching a height of over 20 m northeast of Teulon, separates a till plain to the northwest from a glaciolacustrine plain to the southeast (Fig. 4).

Bedrock geology

The area is underlain by the north-south trending Ordovician and Silurian outcrop belt. In order of decreasing age (east to west) the strata comprise the Selkirk and Fort Garry members of the Red River Formation, and the Gunn, Penitentiary, Gunton and William members of the Stony Mountain Formation. The Stonewall Formation overlies the Stony Mountain Formation. The Red River, Stony Mountain and Stonewall formations, of Ordovician age, are overlain by the Silurian age Interlake Group (Fig. 5; Manitoba Mineral Resources Division 1979).

The Ordovician Red River, Stony Mountain and Stonewall formations comprise dolomitic limestone and dolostones with only minor shale in the Gunn Member. The upper Stony Mountain Formation, Stonewall Formation and Interlake Group are mainly dolomite.

Variations in the degree of dolomitization and the effect it has had on weathering of bedrock resulted in the prominent scarp that crosses the area. The dolomitic limestone to the east and southeast has weathered recessively, whereas more dolomitic terrane to the west has been more resistant to erosion.

Quaternary geology

Drift thickness

Quaternary sediments reach a maximum thickness of over 40 m on the glaciolacustrine plain northeast of Komarno (Fig. 6). On the till plain, the overburden thickness is somewhat less than on the glaciolacustrine plain, averaging between 10 and 20 m with some areas having less than 10 m of overburden (Betcher, 1986). In the present study, only the upper part of the stratigraphic sequence, about 1-5 m, was investigated.

Ice flow

Bedrock outcrops are scarce and were found in only five areas. Striae in these areas record ice flow between 105° and 180° (Fig. 7). The majority of the striae record ice flow toward the southeast, parallel to the direction recorded by the flutes on the till plain (Fig. 8A). Crosscutting relations of intersecting flutes north of North Shoal Lake indicate southerly (170°) ice flow as followed by southeasterly ice flow (Fig. 8B). These ice flow directions are corroborated by crossing striae oriented in the same general directions (Fig. 9).

Eight major lithosomes, including two tills, glaciofluvial sand and gravel, ice rafted diamicton, clay, iceberg turbate, littoral sand, and recent alluvium were identified. The tills, proglacial sediments, and iceberg turbate are described in detail as only they relate to the dispersal of erratics.

Inwood till

The lowest stratigraphic unit encountered is an over-consolidated till named Inwood till (Fig. 10). This till is easily differentiated because it is harder than any other sediments in the area. Inwood till is believed to have been deposited by southerly (170°) flowing ice.

Inwood till was intersected in 143 backhoe pits in this area. In the field the till is identified by the compactness and pinkish grey colour (5YR 8/1). It is homogeneous and fissile and has an abundance of striated carbonate clasts (Fig. 11).

Granulometrically, the till is composed of a range of grain sizes but with a predominance of silt (Fig. 12). The fine till components are angular and composed mainly of carbonate fragments of varying sizes with little pore space (Fig. 13). The 4-16 mm pebble fraction comprises mainly locally derived Paleozoic carbonate clasts. The mean Precambrian clast content of the 79 samples analyzed is 18% (Table 1).

Komarno till

The till plain in the western Manitoba Interlake from Lake St. Martin in the north to Gimli and the Shoal Lakes in the south is fluted. The flutes are up to 10 km long and 400 m wide and are oriented toward the southeast (Fig. 8). These streamlined forms are parallel in the north but fan out in the south and southeast. The flutings are widespread on topographic high areas of the Interlake and are also found on topographic high areas around Libau, southeast of Lake Winnipeg (Nielsen and Matile, 1982a), and along the eastern side of the Lake Terrace Plain, southeast of Winnipeg. The flutes terminate near an ice margin situated near Windy Lake in southeastern Manitoba (G. Matile, pers. comm. 1988).

The flutes on the Interlake plain consist of 0.5-2 m of relatively soft diamicton in places mixed with glaciolacustrine clay (Fig. 11). This diamicton, termed Komarno till, resembles the underlying Inwood till in texture (Fig. 12) but may be differentiated from it by the presence of olive grey glaciolacustrine clay inclusions, a slightly darker colour, and more importantly a lower consolidation. The presence of horizontal fissility, a discontinuous boulder pavement at the contact with the underlying Inwood till, the fluted surface (Fig. 8) and the southeasterly fabric (Fig. 14) indicate the

Table 1: Summary statistics for pebble counts on selected samples from all areas

Balmoral - Komarno

	Inwood till		Komarno till		Drift-ice turbate	
	% Pe	% Carb	% Pe	% Carb	% Pe	% Carb
Mean	18.0	82.0	16.5	83.5	15.6	84.4
S.D.	2.9	2.9	3.4	3.4	3.0	3.0
Min.	12.0	73.9	10.2	77.8	6.8	78.2
Max.	26.1	88.0	22.2	89.8	21.8	93.2
Range	14.1	14.1	12.0	12.0	15.0	15.0
n. obs.	79	79	26	26	57	57

Moosehorn - Gypsumville

	Inwood till		Komarno till		Iceberg turbate	
	% Pe	% Carb	% Pe	% Carb	% Pe	% Carb
Mean	15.8	84.2	14.1	85.9	17.1	82.9
S.D.	3.6	3.6	1.7	1.7	3.0	3.0
Min.	9.6	78.1	10.6	84.0	11.9	79.0
Max.	21.9	90.4	16.0	89.4	21.0	88.1
Range	12.3	12.3	5.4	5.4	9.1	9.1
n. obs.	22	22	9	9	9	9

Swan Lake - Dawson Bay

	Zelena till					Arran till					Iceberg turbate				
	% Pe	% Carb	% Shale	% SS	% Tert	% Pe	% Carb	% Shale	% SS	% Tert	% Pe	% Carb	% Shale	% SS	% Tert
Mean	26.4	66.1	7.1	1.4	1.2	9.0	90.3	3.0	1.5	0.6	7.3	92.7	-	-	-
S.D.	5.7	6.5	7.0	1.7	0.7	4.4	5.9	3.6	1.1	0.4	3.5	3.5	-	-	-
Min.	9.8	48.0	1.1	0.2	0.4	2.9	63.6	0.3	0.3	0.3	1.2	86.5	-	-	-
Max.	32.6	77.2	25.9	5.9	1.8	21.1	97.1	11.9	3.7	1.0	13.5	98.8	-	-	-
Range	22.8	29.2	24.8	5.7	1.4	18.2	33.5	11.6	3.4	0.7	12.3	12.3	-	-	-
n. obs.	20	20	18	13	4	67	67	10	11	3	10	10	-	-	-

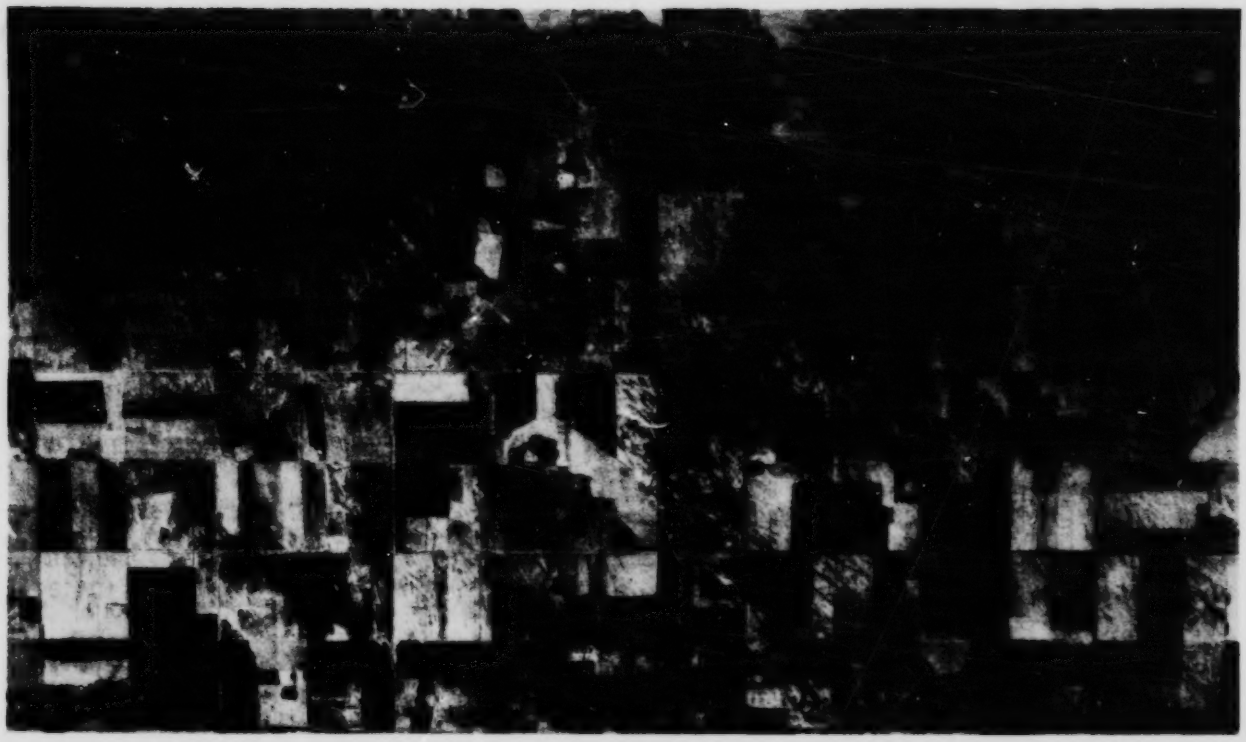

Figure 4: Aerial photograph showing the till plain and glaciolacustrine plain near Balmoral where the Doan galena pebble was found (arrow). Note the flutes (a) on the till plain and the widespread iceberg furrows (b).

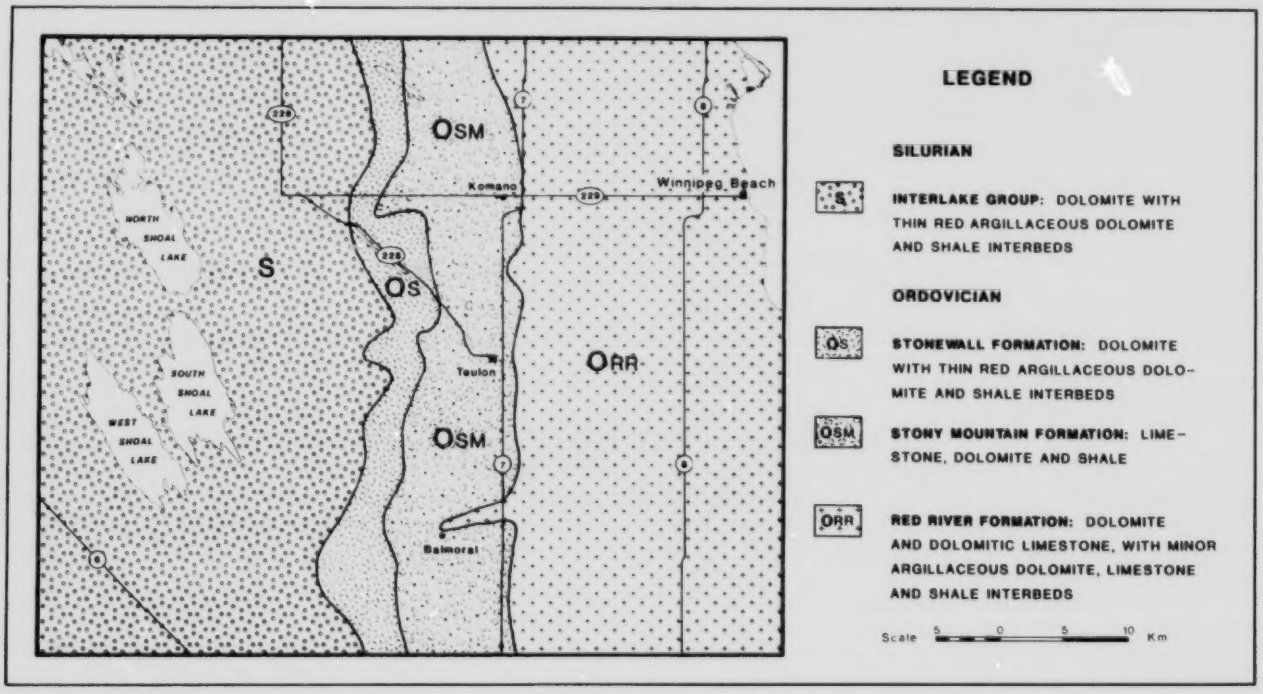

Figure 5: Bedrock geology of the Balmoral-Komarno area (from Manitoba Mineral Resources Division, 1979 and Betcher, 1986).

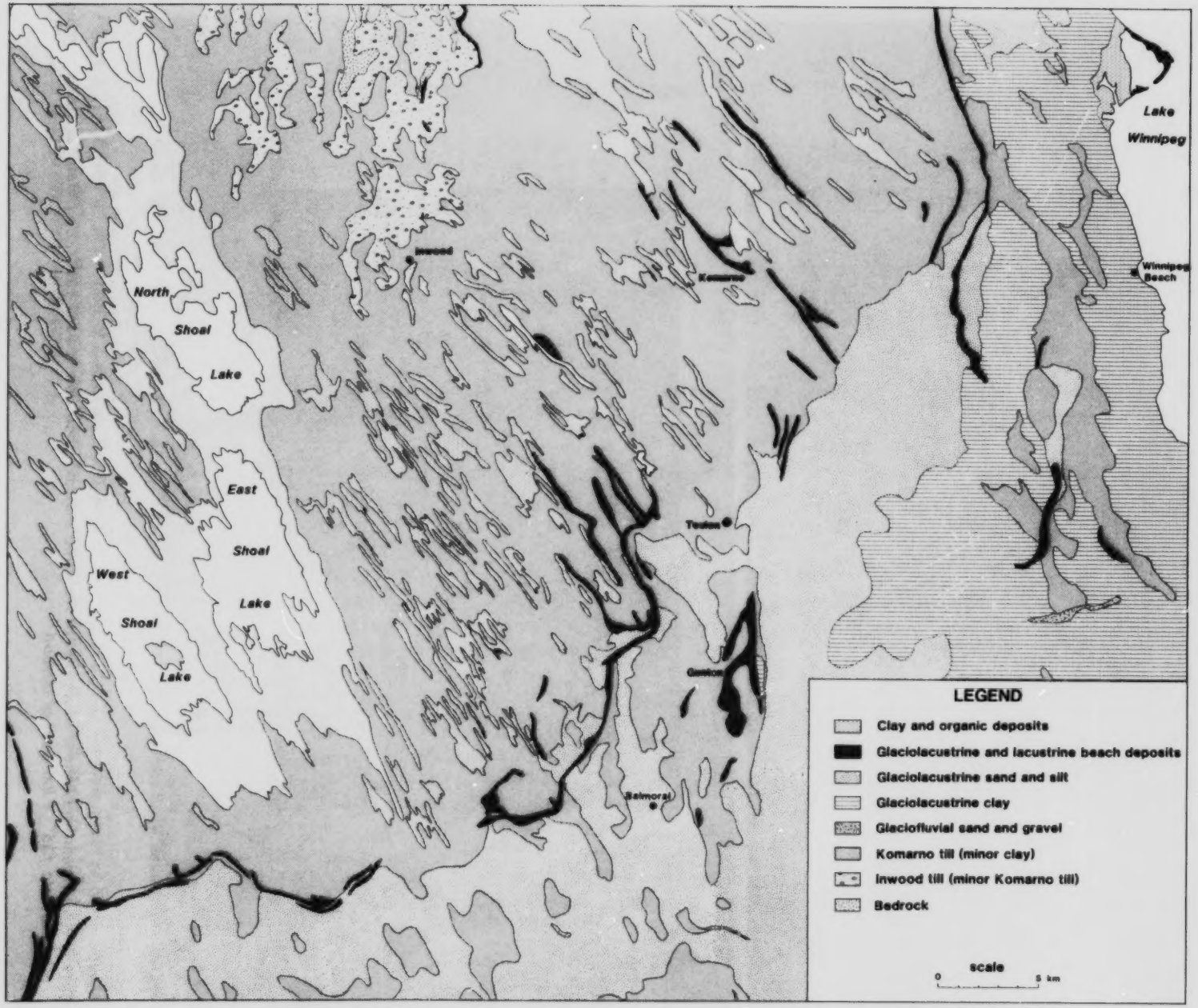

Figure 6: Surficial geology of the Balmoral-Komarno area. Modified from Pratt et al. (1961).

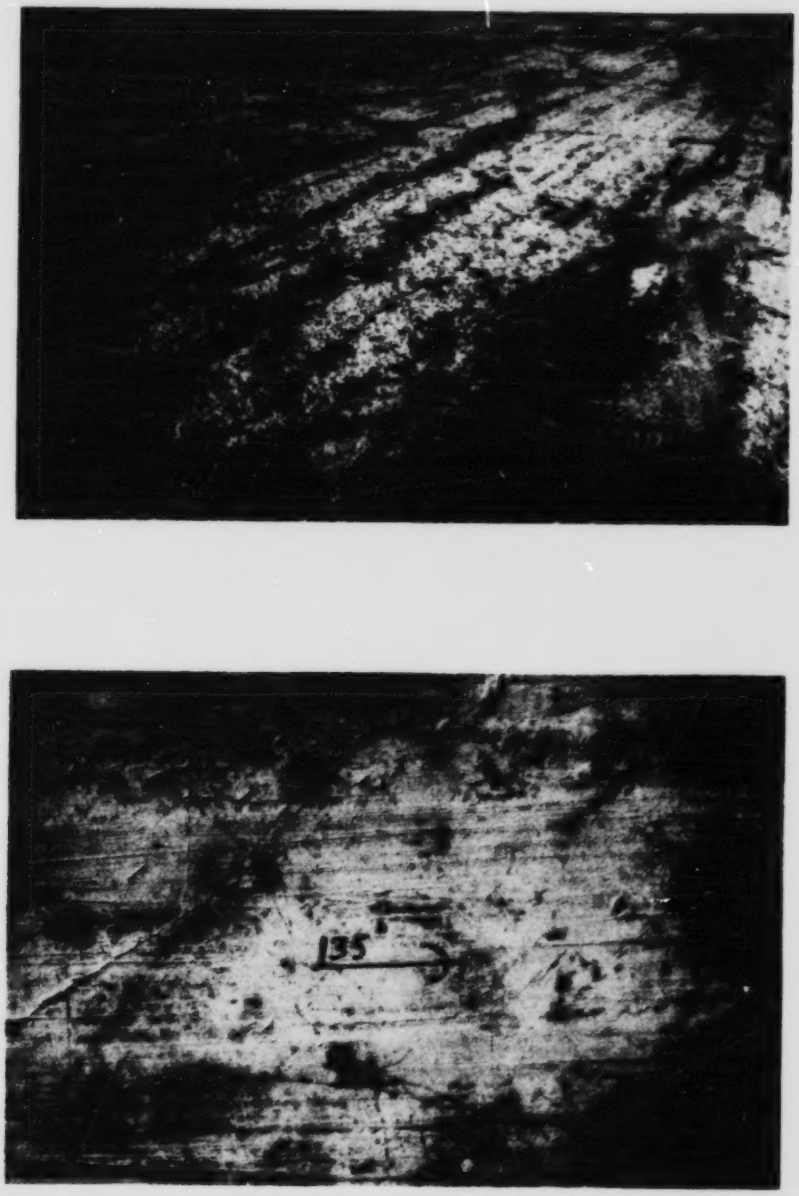

Figure 7: (A) Striated pavement southwest of Komarno indicating ice flow toward 130°. (B) Details of striae oriented toward 135°, 1 km west of Inwood.

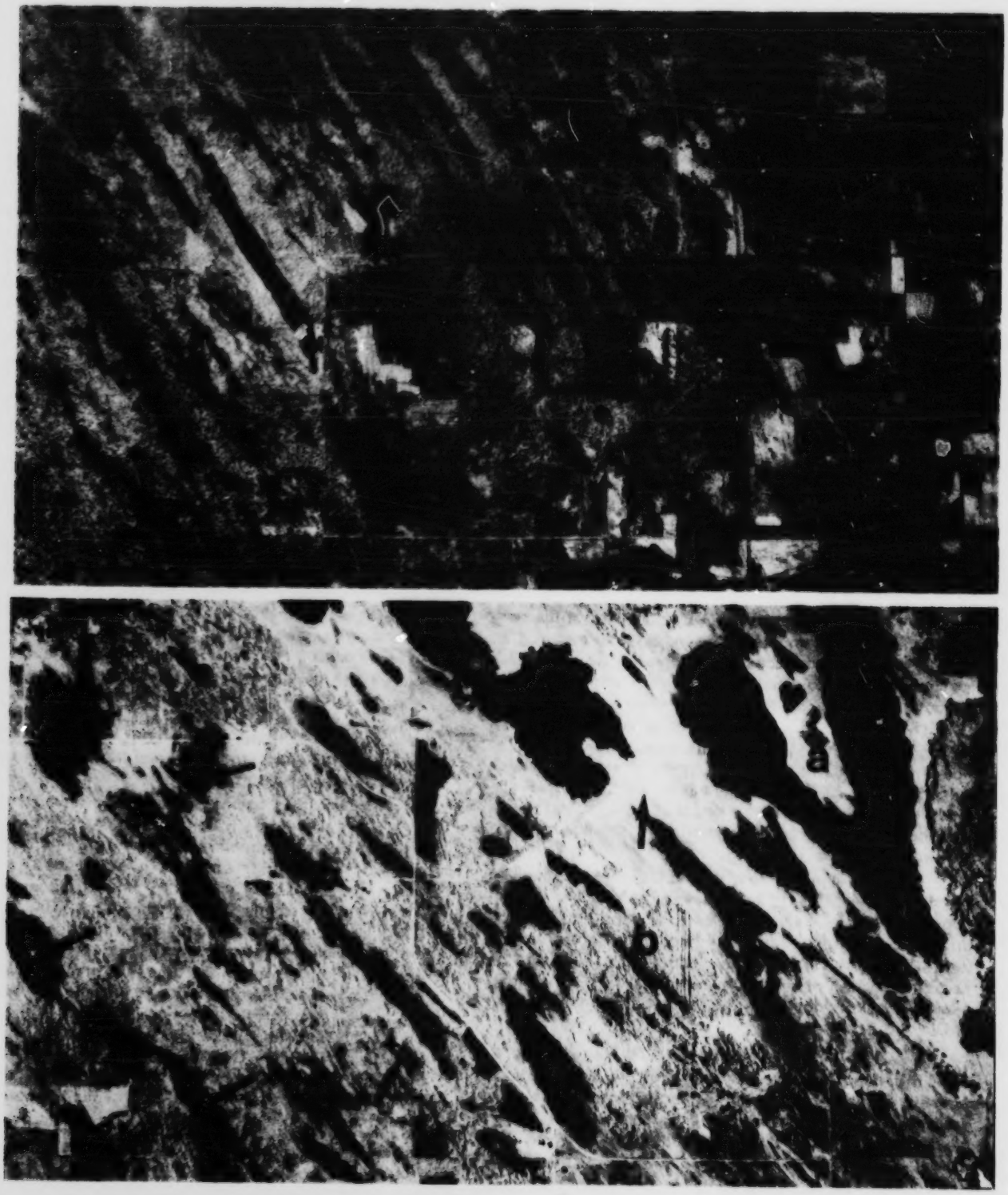

Figure 8: (A) Fluted till plain west of Balmoral. The flutes are oriented 140°. (B) Till plain north of North Shoal Lake showing early flutes (a) oriented towards 170° cut by flutes (b) oriented towards 130°. Parallel drift-ice furrows are indicated by arrows.

Figure 9: Crossing striae at Gunton indicating ice flow toward 170° and 140°.

Komarno till was deposited subglacially. The clay inclusions in the Komarno till are widespread but do not occur every where indicating the ice flow that deposited this till was into an ice marginal lake.

On the glaciolacustrine plain, Komarno till overlies hard Inwood till or softer glaciolacustrine stony lake clay (Fig. 10). It is generally overlain by glaciolacustrine sediments including stony lake clay and coarser textured littoral sediments. In places, the Komarno till resembles ice proximal glaciolacustrine diamicton and it may be difficult to differentiate the two (see later section).

Granulometrically Komarno till is similar to the underlying Inwood till (Fig. 12). The pebble composition of Komarno till is variable, reflecting the problem of classifying samples. Generally, Komarno till has fewer distantly travelled Precambrian clasts (16.5%) than the underlying Inwood till indicating different provenances for the two tills (Table 1).

The long linear flutes, the lack of consolidation of the till, the presence of lake clay inclusions and the topographic control on the ice flow (radiating fan) are features reminiscent of the Cochrane Till in northern Ontario (Hughes, 1965). These similarities suggest the Komarno till was deposited by surging of the ice margin, a conclusion corroborating the theoretical considerations of Clayton *et al.* (1988).

Proglacial sediments

Proglacial sediments deposited in glacial Lake Agassiz overlie Komarno till. These sediments are generally thin and largely reworked by icebergs on the till plain, and widespread but poorly exposed on the glaciolacustrine plain.

On the glaciolacustrine plain the proglacial sediments consist of two distinct facies, a pinkish grey (5YR 8/1) diamicton facies with interbedded rhythmites overlain by an olive grey (5YR 4/1) clayey facies (Fig. 15).

The diamicton facies is texturally similar to the underlying till. It occurs in beds ranging in thickness from less than 1 cm to more than a metre (Fig. 16). Dropstones comprising both rocks and lumps of till are common (Fig. 17).

The thinner, dark, fine textured portions of the rhythmites are interpreted as having been deposited during the winter when Lake Agassiz was frozen. The thicker, lighter and coarser textured part of the rhythmites was deposited during the summer months when sediment influx into Lake Agassiz was greatest. Although some of these couplets may be varves there is abundant evidence of penecontemporaneous slumping in the form of flow folds (Fig. 18A) and disturbed bedding (Fig. 18B), (not to be confused with iceberg grounding structures), suggesting at least some of these rhythmites are distal turbidites.

The olive grey facies overlying the diamicton (Fig. 15) is clayey and poorly laminated where it occurs in thick sections, and contains relatively fewer dropstones than the diamicton. It occurs both as laminae, 1-2 cm thick, interbedded with diamicton, and in places as accumulations 10 cm or more in thickness. The general succession of proglacial sediments recorded in Figure 15 is one of ice marginal retreat and decreasing glacier influence. The gravel at the base is glaciofluvial subaqueous outwash deposited in an ice contact environment. The gravel is overlain by stony lake clay (diamicton) deposited primarily by ice rafting and from suspension. The clay bed was deposited almost wholly from suspension in deep water with little or no influence of ice. The sand at the top of the section records the final regression of Lake Agassiz.

Drift-ice turbate

The Inwood till, Komarno till and proglacial sediments have in places been modified by drift-ice forming a layer of turbate 0.5-3 m or more thick over most of the Balmoral-Komarno area and the southern Interlake in general. This is evident by the abundance of drift-ice furrows on both the till plain and the glaciolacustrine plain (Fig. 4). Furrows formed by drifting ice are com-

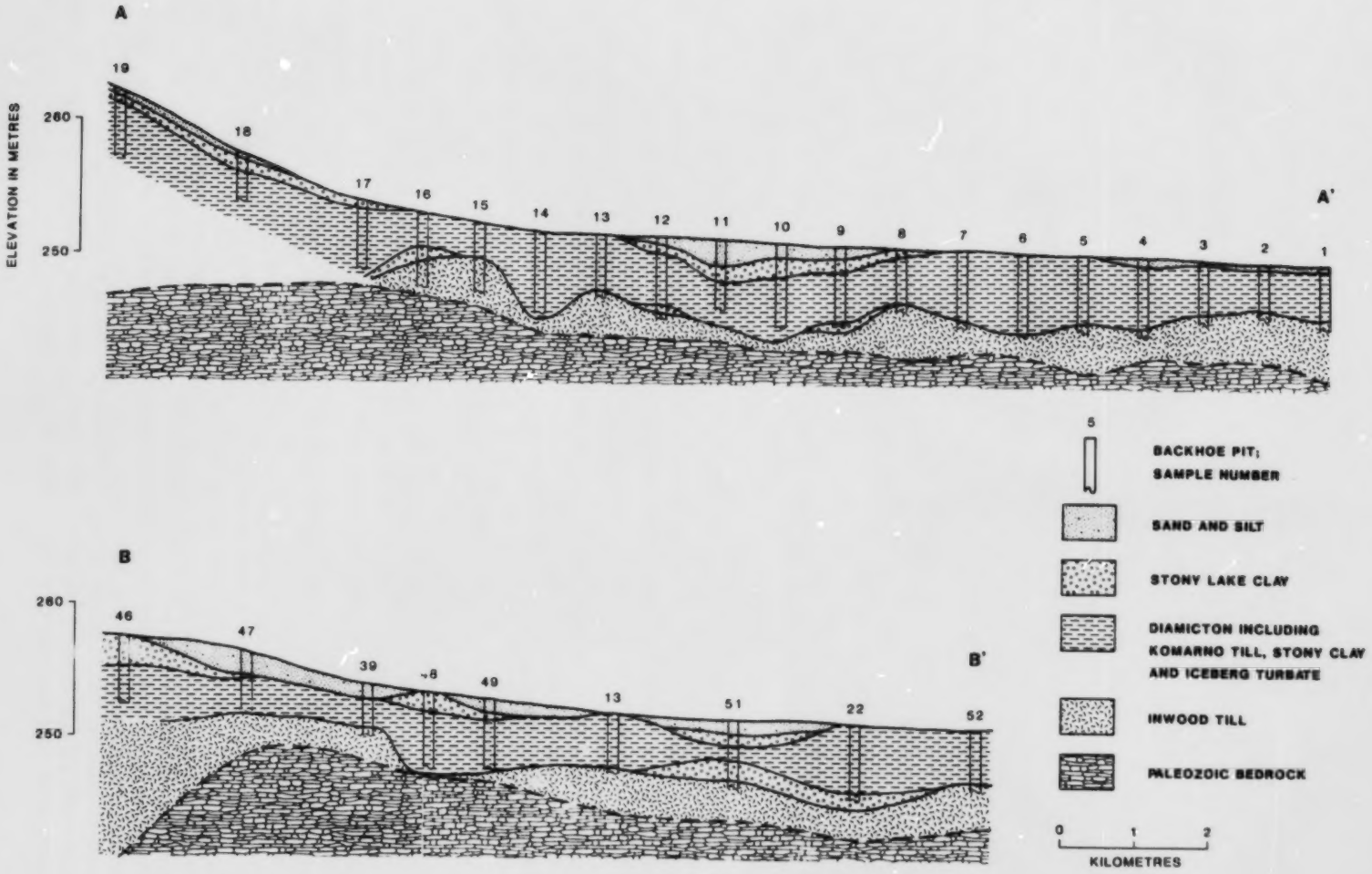

Figure 10: Stratigraphic cross-sections of Quaternary sediments in the Balmoral area. See Figure 3 for the location of the profiles.

Figure 11: Komarno till (a) overlying Inwood till (b) at site KO 32. Note the clay inclusions in the Komarno till.

mon in both offshore Lake Agassiz sediments and in till up to an elevation of about 275 m (900') (Fig. 19). They are generally not found at elevations above 275 m presumably because the water was too shallow. On the glaciolacustrine plain furrows are commonly buried or eroded in areas where near shore processes were active during the recession of Lake Agassiz. Two types of drift-ice furrows, those formed by iceberg keels (Fig. 20) and those formed by inshore ice (Fig. 21) are recognized in the area.

The iceberg plough marks or furrows are generally about 30 m wide and from 0.5 to 6 km long with low berms less than a metre high on both sides. They are found at elevations between 230 m (750') and 275 m (900'). On the till plain the iceberg furrows are most obvious in low swampy areas where they are accentuated by standing water (Fig. 20). In better drained areas, the furrows are highlighted by long narrow curvilinear clearings that are too wet to grow trees. The furrows curve and intersect forming a crisscross network of low depressions on the till plain. On the glaciolacustrine plain the furrows are filled with Lake Agassiz silt as can be seen around Komarno (Fig. 19, Fig. 22) and, as a result of differential compaction between the silt infill and the surrounding clay, the furrows form ridges (Nielsen and Matile, 1982a). The differences in the texture and resulting lower permeability of the surrounding clay compared to the furrow infill may also cause increased water ponding in the furrows. This has lead to a higher water content and increased volumes of the furrow infill and also helps in the formation of ridges (C.M.T. Woodsworth-Lynas and R. Lien, pers. comm. 1987).

Furrows formed by inshore ice are short and straight compared to the iceberg furrows (Fig. 21) which is seasonal ice forming pressure ridges in water generally less than 30 m deep (B.R. Pelletier, pers. comm.,1989). The inshore ice furrows appear to occur exclusively on the till plain between elevations of 259 m (850') and 268 m (880') in the western part of the region (Fig. 19). They occur only on the west sloping terrain in the southern Interlake. The inshore furrows were in places formed by multiple keels resulting in numerous adjacent parallel depressions (Fig. 8 A and B). In places where the scouring was intense, individual furrows may be difficult to discern giving the landscape a mottled or stippled appearance on air photographs (Fig. 21). The stippling is due to small clumps of trees growing on the remains of the berms. The little clumps of trees have furrows on three or more sides. The parallel furrows, elevation restrictions and areal distribution suggests these furrows were not formed by icebergs but rather by seasonal drift-ice pushed up into pressure ridges.

The furrows are generally oriented southeasterly, subparallel to the flutes in the underlying till surface. The orientation may be related to the predominant wind direction during deglaciation (Hochheim, 1982), or to the ice flow direction and the orientation of the calving ice margin.

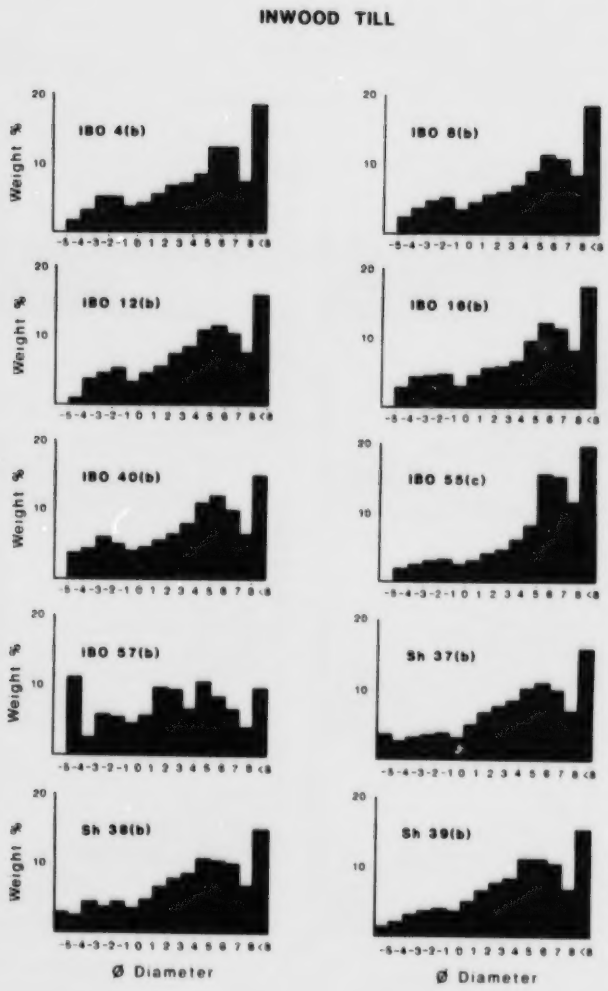

Figure 12: Histograms showing the grain size distribution of Inwood till, Komarno till and drift-ice turbate from the Balmoral-Komarno area.

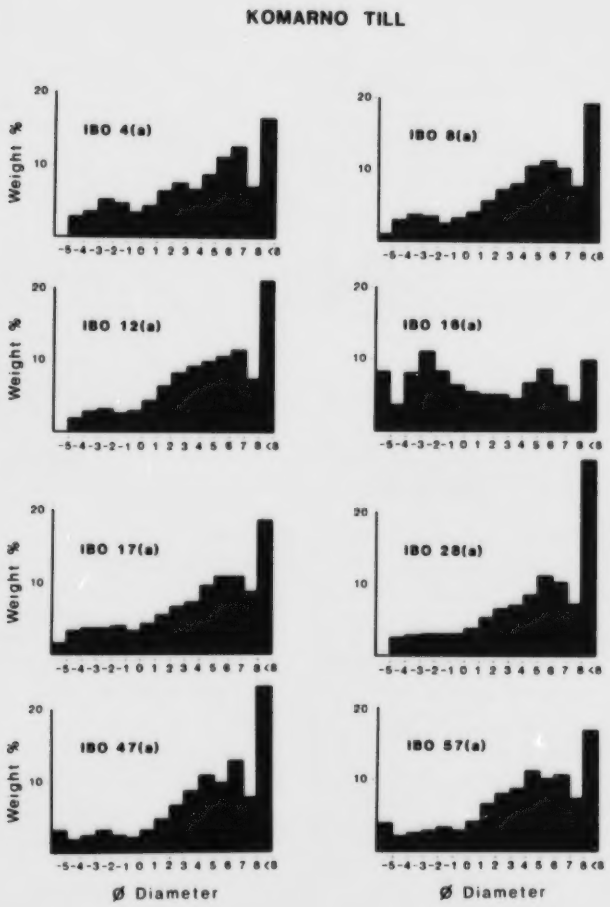

Figure 12: Continued.

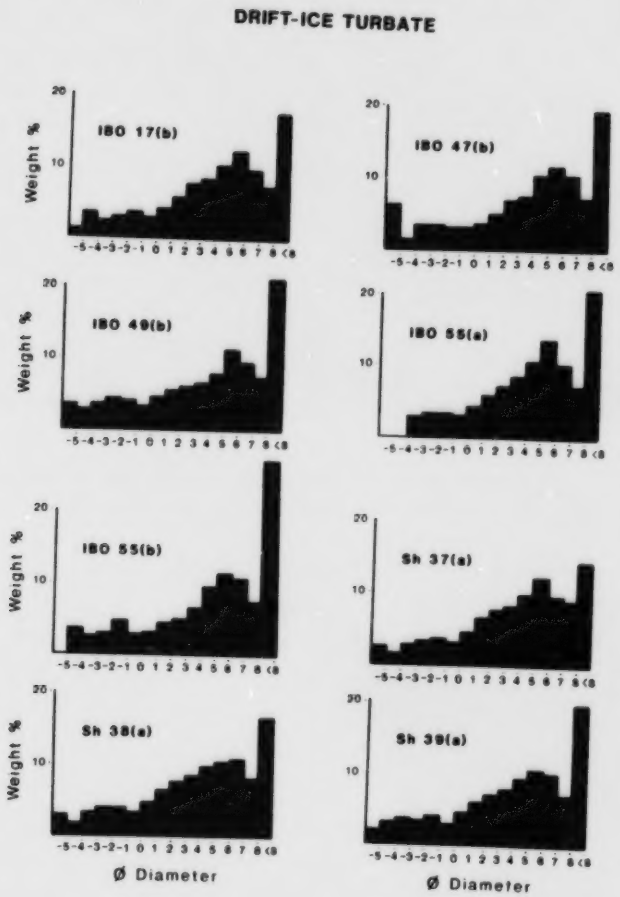

Figure 12: Continued.

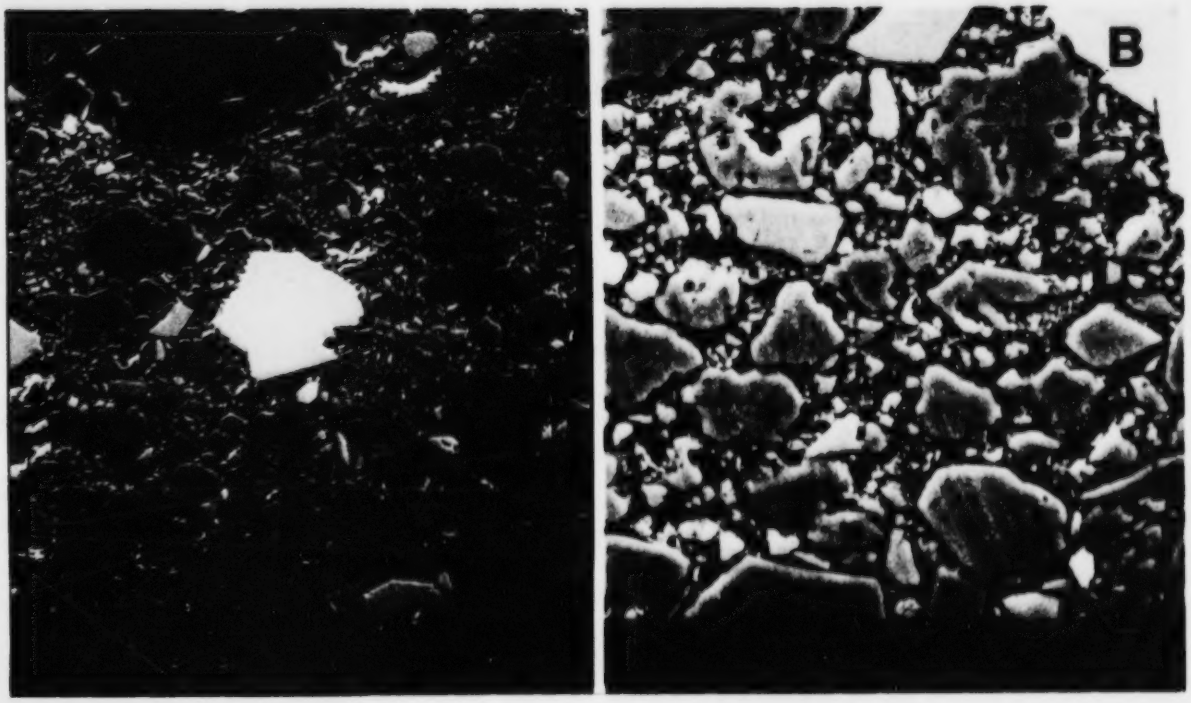

Figure 13: (A) Scanning electron photomicrograph of Inwood till (site Sh7(b)) showing the fine texture, angular components and tight packing. (B) Detail of Inwood till in (A). The scale bar is 10 microns.

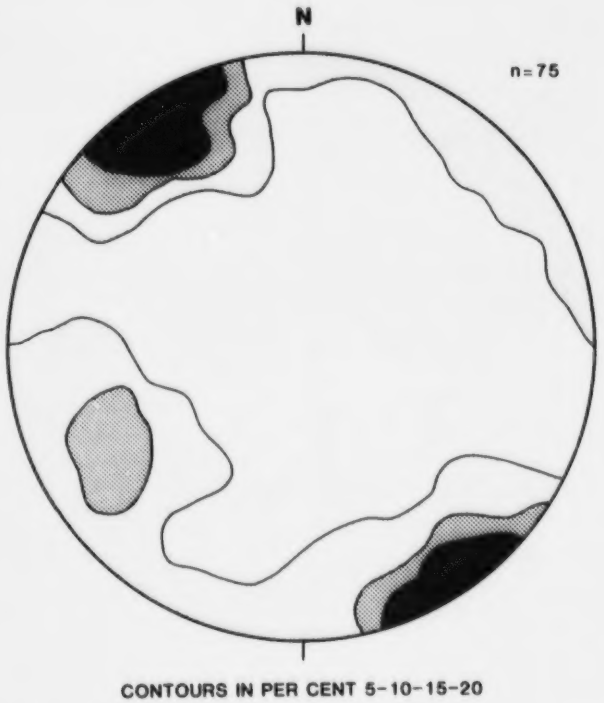

Figure 14: Pebble fabric of the Komarno till measured at sites KO 20 and KO 26 indicating southwestern ice flow.

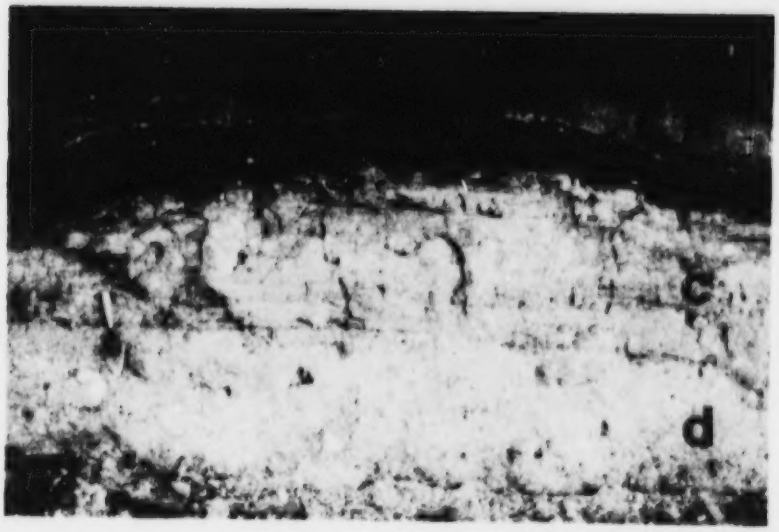

Figure 15: Stratigraphic succession indicating glacier retreat and glaciolacustrine sedimentation: (a) littoral sand, (b) poorly laminated clay, (c) poorly laminated ice rafted detritus and (d) eskerine sand and gravel. Location 7 km southeast of Balmoral.

Figure 16: Pinkish grey stony lake clay and thinly bedded olive lake clay, 3 km south of Argyle, just south of the map area.

Figure 17: Laminated stony lake clay with dropstones of t(a) and carbonate cobble (b), 3 km south of Argyl Note 25 cent piece for scale.

The drift-ice turbate is composed primarily of a mixture of Komarno till and olive grey glaciolacustrine clay (Fig. 23). The presence of furrows is used to distinguish the drift-ice turbate from the Komarno till, as both sediments are relatively soft (Fig. 24). During the scouring process, glaciolacustrine clay and the underlying till were ploughed and mixed by the impinging keels. The till in the bottom of the furrows may also have been deformed by impinging keels. The structure may have been altered such that it is no longer overconsolidated but otherwise the till shows no visible properties of turbate (Lien, 1986) (Fig. 25). The contact between the till and the drift-ice turbate can therefore be gradational or sharp. Elsewhere, the contact is marked by a thin sand layer deposited by bottom currents during the time between till deposition and drift-ice activity.

A consequence of drift-ice scouring is the general absence of eskers and other glaciofluvial sediments that were eroded by scouring keels.

Geochemistry

Histograms showing frequency distribution of copper, lead, zinc, nickel, cobalt, chromium, iron, manganese and barium in the <2 micron fraction and carbonate in the <63 micron fraction for Inwood till, Komarno till, (without clay inclusions), glaciolacustrine sediments and drift-ice turbate (including Komarno till with clay inclusions) are shown in Figure 26. Statistics summarizing geochemical data are listed in Table 2. The geochemical data is listed in Appendix I.

Tills

Frequency distributions of trace elements in Inwood and Komarno tills are similar except Komarno till has slightly higher mean trace element concentrations than the underlying Inwood till. Carbonate contents are the same. Higher trace element concentrations in Komarno till cannot easily be explained by enrichment of Precambrian material as Komarno till has less Precambrian material than Inwood till. The difference in geochemistry of the two tills may be attributed to different provenances in Paleozoic formations; Komarno till having been deposited by ice from the northwest whereas Inwood till was derived from the north as indicated by pebble composition and ice flow features.

Trace element analysis on drill core from Paleozoic bedrock of southern Manitoba (Table 3) indicates Devonian formations generally have higher trace element concentrations than Silurian and Ordovician formations, excluding the Winnipeg Formation (Gale, in prep.). Thus ice flow features and geochemistry of the tills are in agreement; Inwood till was derived by ice crossing only Silurian and Ordovician bedrock, whereas Komarno till, with higher trace element concentrations, was derived in part from Devonian bedrock to the northwest.

The frequency distribution of lead in both Inwood till and Komarno till is noteworthy because it is the highest positively skewed element and the tills have higher lead concentrations than either glaciolacustrine sedi-

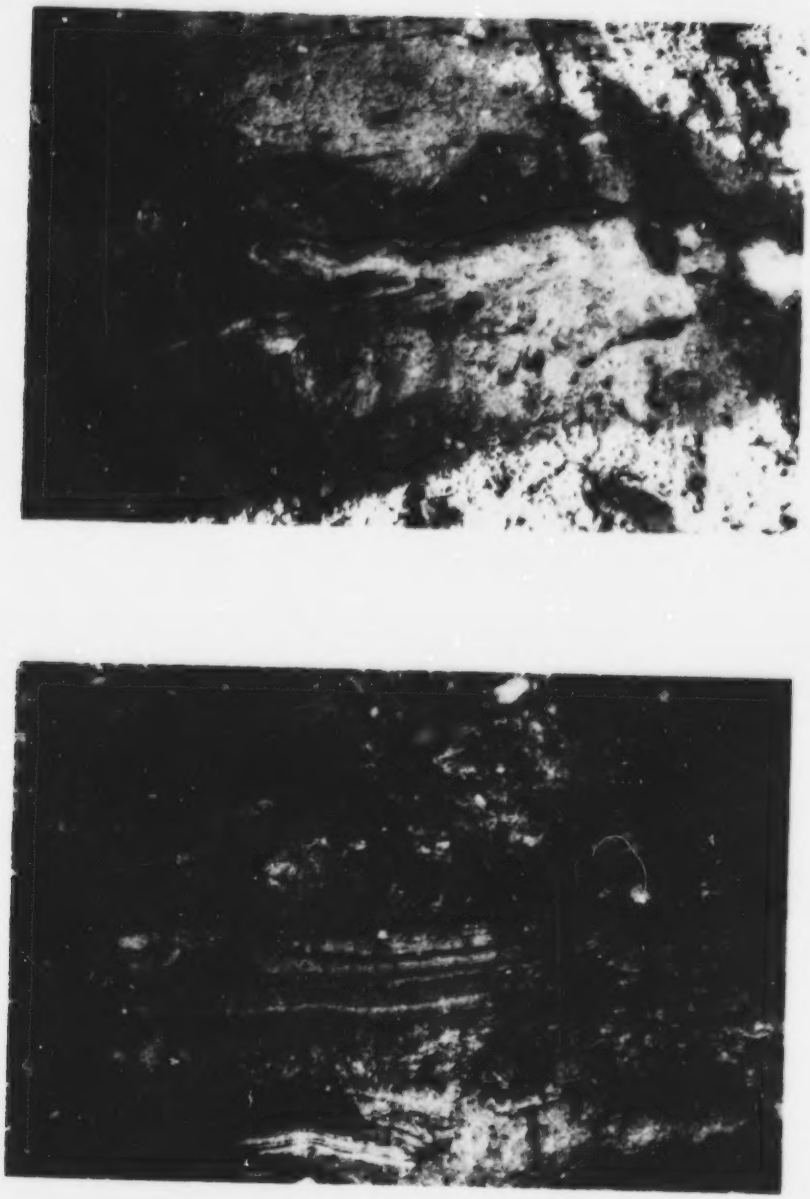

Figure 18: Flow fold (A) and disturbed bedding (B) related to slumping in the laminated stony lake clay, 3 km south of Argyle.

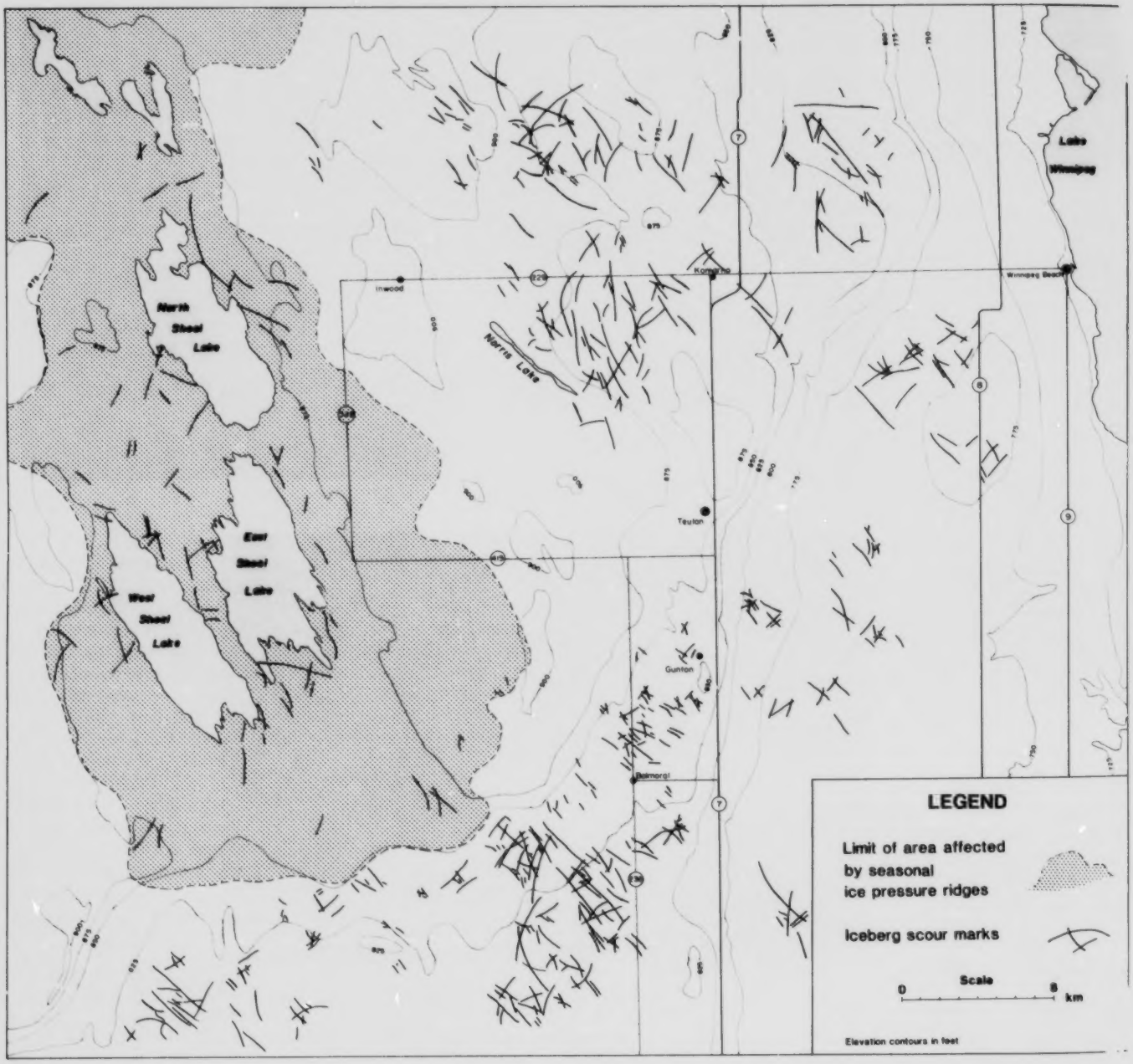

Figure 19: Distribution of iceberg furrows and inshore drift-ice furrows in the Balmoral-Komarno area.

Figure 20: Intersecting iceberg furrows (arrow) accented by standing water. Note the prominent flute (a) in the Komarno till. Sampling site KO 33 is shown for location.

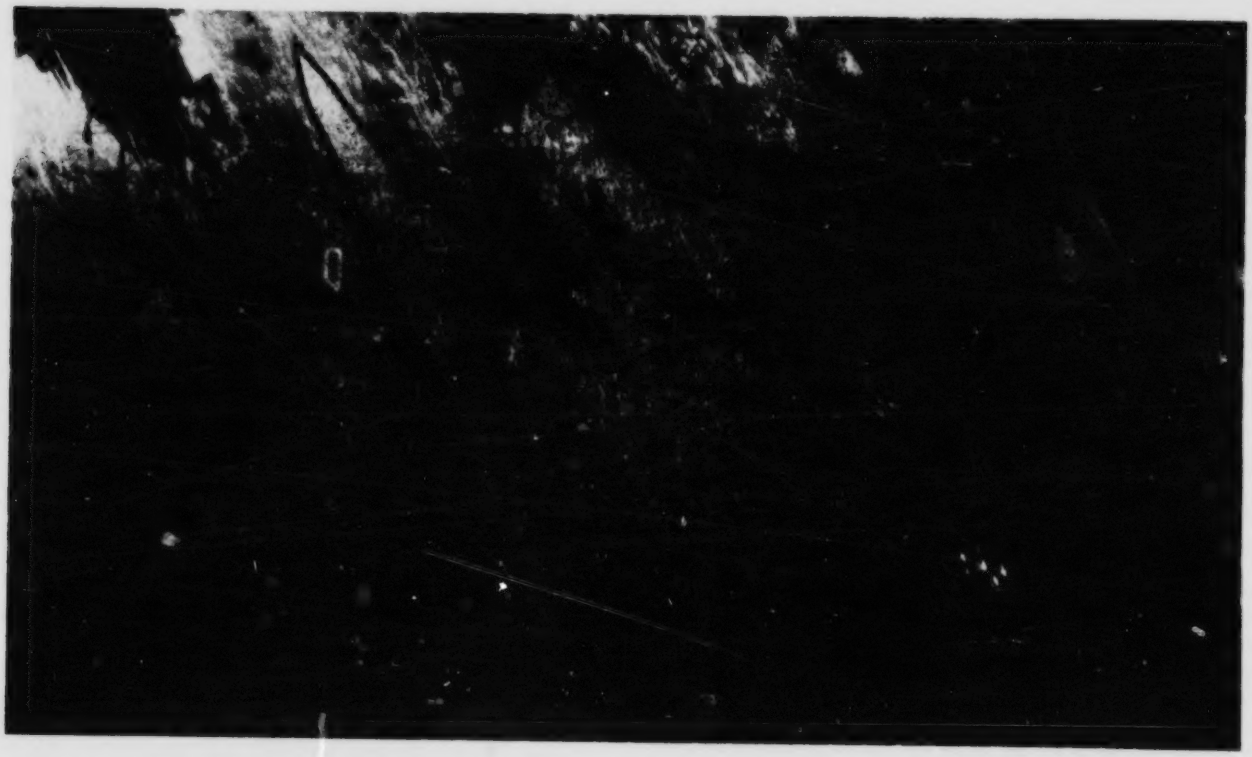

Figure 21: Intensely furrowed area southeast of South Shoal Lake. The stipppled pattern made by the trees is due to intense scouring by inshore drift-ice from several directions. Note the edge of flutes in the Komarno till highlighted by the black line.

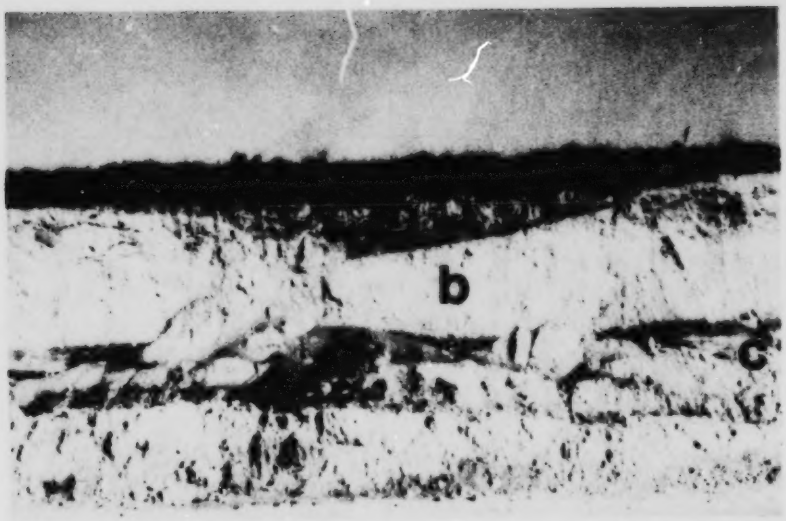

Figure 22: Cross section of an iceberg furrow filled with Lake Agassiz sediment (a). The furrow is cut into Komarno till (b) that overlies eskerine gravel (c). The iceberg furrow is 1.5 m deep. Photograph from a gravel pit 7 km southeast of Balmoral.

ments or turbate. The source of the lead in the anomalous samples (above 12 ppm - determined by inspection) is unknown as there is little or no variation in lead concentrations in the bedrock (Table 3).

Nickel, chromium, iron and manganese in Inwood till are bimodally distributed. Modes occur at 32 and 42 ppm for nickel, at 43 and 58 ppm for chromium, at 10 300 and 14 400 ppm for iron and at 260 and 370 ppm for manganese (not obvious for manganese at the scale plotted in Fig. 25). These modes are also found in Komarno till indicating incorporation of Inwood till or possibly misclassification of some samples. The origin of the bimodal distribution of these elements is believed to reflect different bedrock source areas such as the Thompson nickel belt or the Precambrian inlier near Gypsumville.

Glaciolacustrine sediments

The glaciolacustrine sediments have the highest mean trace element concentrations of all the sediments in the area reflecting the high clay content of these sediments. This is also reflected in the low carbonate content of these samples; carbonate generally reaches maximum concentrations in the silt fraction.

The Doan galena pebble was found in either olive coloured stony lake clay or in ice rafted glaciolacustrine diamicton at site IBO 55. Komarno till was not positively identified at the site but Inwood till was intersected a depth of about 5 m. Neither Inwood till nor the overlying glaciolacustrine diamictons are geochemically anomalous. The upper, thin, stony lake clay was not sampled.

Drift-ice turbate

The drift-ice turbate (including Komarno till with clay inclusions) has mean trace element and carbonate concentrations intermediate between those of the underlying till(s) and glaciolacustrine sediments.

In addition, the frequency distributions of lead, chromium and iron in the drift-ice turbate are bimodal, indicating mixing of two populations. Thus, trace element geochemistry and carbonate analyses suggest similar conditions and reinforce the field observations that the turbate was the result of drift-ice ploughing and mixing of till and glaciolacustrine sediments.

Conclusions

The succession of Inwood till, lake sediment, Komarno till, lake sediment and drift-ice turbate in the Balmoral-Komarno area records two ice advances and two glacial lakes followed by a period of drift-ice scouring. Most of the lithosomes are easily differentiated except for the turbate and Komarno till which are similar.

Of the 266 till samples analyzed geochemically, 9 Inwood till and 4 Komarno till samples may be considered marginally anomalous in lead (12 ppm) (Appendix I). The values are low but with two exceptions are restricted to the glaciolacustrine plain in the area where the Doan pebble was found.

Table 2: Summary statistics for the geochemical data from the Balmoral - Komarno area

Inwood till (n=142)	Cu (ppm)	Pb (ppm)	Zn (ppm)	Ni (ppm)	Co (ppm)	Cr (ppm)	Fe (ppm)	Mn (ppm)	Ba (ppm)	CO_3 (%)
Mean	29.6	7.9	65.0	32.3	9.9	56.3	14112.7	360.8	197.4	39.5
S.D.	4.1	2.8	7.3	5.2	1.6	10.5	2156.8	48.9	32.2	2.6
Max	42.0	22.0	106.0	51.0	15.0	134.0	20500.0	505.0	325.0	44.2
Min	20.0	5.0	49.0	22.0	7.0	40.0	9950.0	240.0	130.0	28.3

Komarno till (n=46)	Cu (ppm)	Pb (ppm)	Zn (ppm)	Ni (ppm)	Co (ppm)	Cr (ppm)	Fe (ppm)	Mn (ppm)	Ba (ppm)	CO_3 (%)
Mean	32.3	9.2	71.5	35.2	11.8	63.2	16144.6	374.7	207.7	39.4
S.D.	6.4	3.7	13.9	7.0	2.3	11.1	3658.4	49.1	29.5	2.0
Max	60.0	27.0	129.0	61.0	23.0	87.0	24000.0	478.0	273.0	43.4
Min	22.0	6.0	48.0	24.0	9.0	39.0	9200.0	245.0	145.0	34.0

Glaciolacustrine sediments (n=7)	Cu (ppm)	Pb (ppm)	Zn (ppm)	Ni (ppm)	Co (ppm)	Cr (ppm)	Fe (ppm)	Mn (ppm)	Ba (ppm)	CO_3 (%)
Mean	40.3	11.7	97.9	45.7	14.3	81.0	30434.3	431.0	266.0	30.1
S.D.	11.8	3.4	24.4	11.1	4.5	24.9	14420.7	128.2	62.0	6.5
Max	65.0	17.0	125.0	63.0	22.0	117.0	53000.0	636.0	375.0	37.5
Min	30.0	6.0	58.0	30.0	7.0	43.0	11500.0	295.0	190.0	20.7

Drift-ice turbate (n=69)	Cu (ppm)	Pb (ppm)	Zn (ppm)	Ni (ppm)	Co (ppm)	Cr (ppm)	Fe (ppm)	Mn (ppm)	Ba (ppm)	CO_3 (%)
Mean	34.3	9.2	79.1	39.8	12.2	66.9	20032.6	375.7	231.7	37.2
S.D.	5.8	2.6	16.9	8.0	2.7	13.3	7012.9	54.2	47.0	3.6
Max	46.0	21.0	123.0	58.0	19.0	106.0	39000.0	485.0	390.0	42.5
Min	21.0	5.0	47.0	26.0	7.0	41.0	9900.0	215.0	155.0	24.8

Moosehorn-Gypsumville Area

Location and topography

This sampling area is situated in the central Interlake up-ice from the Balmoral-Komarno area (Fig. 3). Elevations range from 317 m (asl) at a point 15 km northwest of Mantagao Lake down to the level of Lake St. Martin at 144 m. Local relief is about 1-2 m except for a few Lake Agassiz beach ridges which, in places, rise slightly higher (Fig. 27).

Bedrock geology

The area is underlain almost exclusively by undivided Silurian Interlake Group consisting mainly of yellowish to greyish dolomite (Fig. 28). A small outlier of Devonian Ashern Formation occurs at Spearhill. Precambrian granite and Ordovician Red River Formation inliers, as well as Permian and Jurassic infill, are associated with the Lake St. Martin meteorite impact structure situated just north of Lake St. Martin (McCabe and Bannatyne, 1970). The structure is 35 km in diameter and is centred on a Precambrian granite outcrop 8 km northeast of Gypsumville. The Permian and Jurassic rocks composing most of the central part of the structure are mainly carbonate and granite breccias, meltrock (trachyandesite composition), red siltstone, sandstone, conglomerate and evaporite.

A report of anomalous lead concentrations between 140 and 650 ppm, copper concentrations up to 490 ppm and zinc concentrations up to 1975 ppm by McCabe and Bannatyne (1970) on carbonate breccia from drill hole LSM-6 was the main reason for the overburden sampling in this area.

Quaternary geology

Drift thickness

Little is known about the overburden thickness. Small bedrock outcrops are widespread (Fig. 29) indicating the overburden is generally thin. However, none of the 42 backhoe pits dug in this area terminated on bedrock. Data from water wells indicate a deep valley filled with glacial deposits trends northeast in the area northwest of The Narrows of Lake St. Martin.

Ice flow

The glacier flow directions, as indicated by the orientation of flutes, was toward the south southeast (155°) in the Mantagao Lake area (Fig. 30). South of Fairford River, along the east side of Lake Manitoba and in the area south of Lake St. Martin, the ice flow varied from 150° in the west to 140° in the east (Fig. 31; Wardlaw *et al.*, 1969).

Striae directions vary between 100° and 225° but the most common directions are toward 170° and 130° (Fig. 32). The orientation of islands and peninsulas in Lake Manitoba (e.g. Peonan Point), as well as the orientation of flutes around Eriksdale, 45 km south of Mantagao Lake, indicate a major ice flow toward 170° affected the area although there is little morphological evidence for this in the Moosehorn-Gypsumville area.

Six lithosomes including two tills, stony lake clay, iceberg turbate, littoral sand and gravel, and recent alluvium were identified.

Inwood till

The stratigraphy in the Moosehorn-Gypsumville area is similar to that described for the Balmoral-

Figure 23: Iceberg turbate comprising Komarno till and dark coloured Lake Agassiz clay, 3 km south of Argyle.

Table 3. Summary Statistics for the trace element geochemical data for the Paleozoic bedrock formations

Formations	Cu (ppm)	Pb (ppm)	Zn (ppm)	Ni (ppm)	Fe (ppm)	Mn (ppm)
All Formations	6.3	4.9	14.5	6.0	2750	143
Amaranth	8.2	3.5	39.0	6.0	4694	603
St. Martens	9.0	5.1	19.3	5.9	4717	186
Souris River	7.6	2.4	15.3	7.6	3335	186
Dawson Bay	10.4	7.3	25.5	14.6	5613	235
Breccia Unit	8.8	3.7	13.2	-	3590	183
Winnipegosis	6.4	5.4	13.5	4.5	1466	105
Ashern	8.3	2.6	24.0	21.7	7533	199
Interlake Group	3.1	3.1	10.1	2.5	915	62
Stonewall	4.5	4.8	11.0	2.9	1201	71
Stony Mountain	5.6	3.9	13.9	4.2	3824	145
Red River	4.5	5.0	11.0	3.5	2178	150
Winnipeg	18.4	12.0	39.0	24.7	20407	208

Komarno area with a lower hard till overlain by relatively soft till. In the Mantagao Lake area the hard till is overlain by iceberg turbate.

The lower till is homogeneous and fissile with numerous striated pebbles. The till is similar to Inwood till in both colour and hardness.

Textural analysis of Inwood till from the Moosehorn-Gypsumville area indicates it is composed of a range of grain sizes but with a predominance of silt (Fig. 33). The 4-16 mm pebble fraction consists mainly of locally derived Paleozoic carbonate clasts. The mean Precambrian clast content is 15%. Some samples with relatively low concentrations of Precambrian clasts (<10%) may be unidentified till(s) older than Inwood till.

Because of its stratigraphic position, compositional and physical properties, this till is correlated with Inwood till in the Balmoral-Komarno area. This till is correlated with the 170° ice flow recorded in most of the area and with the 155° oriented flutes in the Mantagao Lake area where Inwood till forms the surface till.

Komarno till

Sample sites MS1 to MS20 in the Moosehorn area are characterized by a relatively thin, 1-2 m thick, soft diamicton overlying Inwood till. In the field, this diamicton is similar to the underlying hard till in colour and general texture. However, the diamicton is generally softer and slightly darker than the underlying Inwood till. There are no lake clay inclusions in this diamicton as is typical of the drift-ice turbate and Komarno till in the Balmoral-Komarno area and there is no evidence of scouring (Fig. 31). The 4-16 mm pebble fraction of the nine Komarno till samples from this area consists of 14.1% distantly derived Precambrian clasts and 85.9% locally derived carbonate clasts. The diamicton, forming southeasterly trending flutes, was deposited subglacially as till and is correlated with Komarno till in the Balmoral-Komarno area. The Komarno till is believed to have been deposited by an almost neutrally buoyant ice tongue that flowed into Lake Agassiz, reworked and deformed the underlying Inwood till.

Proglacial sediments

Glaciolacustrine sediments are not widespread in the Moosehorn-Gypsumville area. Only one hole in the south (MS30) intersected 2.0 m of brown clay with flow till overlying 0.5 m of dark grey varved clay. The twelve holes near St. Martin Station are located in an area of glaciolacustrine sediments and iceberg furrows (Fig. 34). The succession of sediments (Fig. 35) from Komarno till at the base up through iceberg turbate, blue clay, brown clay and brown silt indicates a retreating ice margin, followed by inundation by a deep water phase of Lake Agassiz with icebergs, the disappearance of icebergs, and finally the regression of Pineimuta Lake during late Holocene time.

Iceberg turbate

Drift-ice furrows, specifically iceberg furrows, have restricted areal distributions in the Moosehorn-Gypsumville area. Around Mantagao Lake, iceberg furrows are common at elevations below 282 m (925 ft.) (Fig. 29), whereas north, south and west of Lake St. Martin they are generally found below 251 m (825 ft.) and only rarely do they occur up to 259 m (850 ft.). There are large areas southeast and southwest of Lake St. Martin, above an elevation of 251 m, where iceberg furrows do

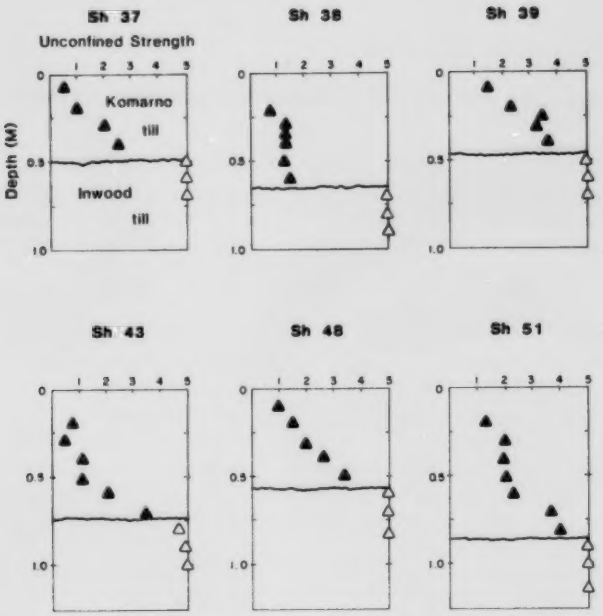

Figure 24: The relative unconfined strength in kg/cm^2 measured with a pocket penetrometer in turbate and Inwood till in the Shoal Lake area.

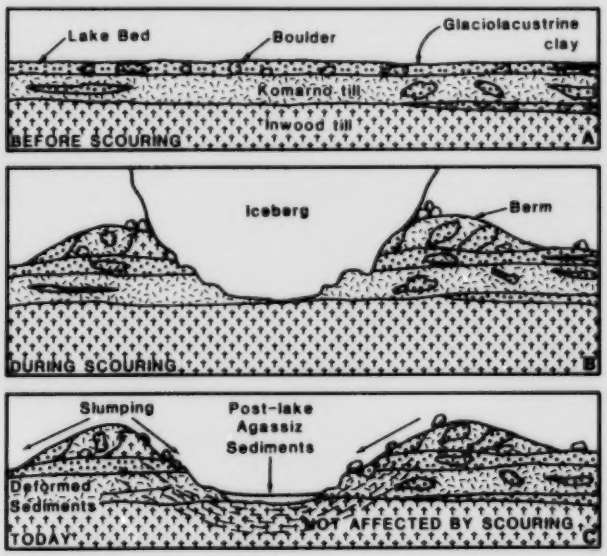

Figure 25: Different phases of iceberg furrow and iceberg turbate formation. Modified from Lien (1986).

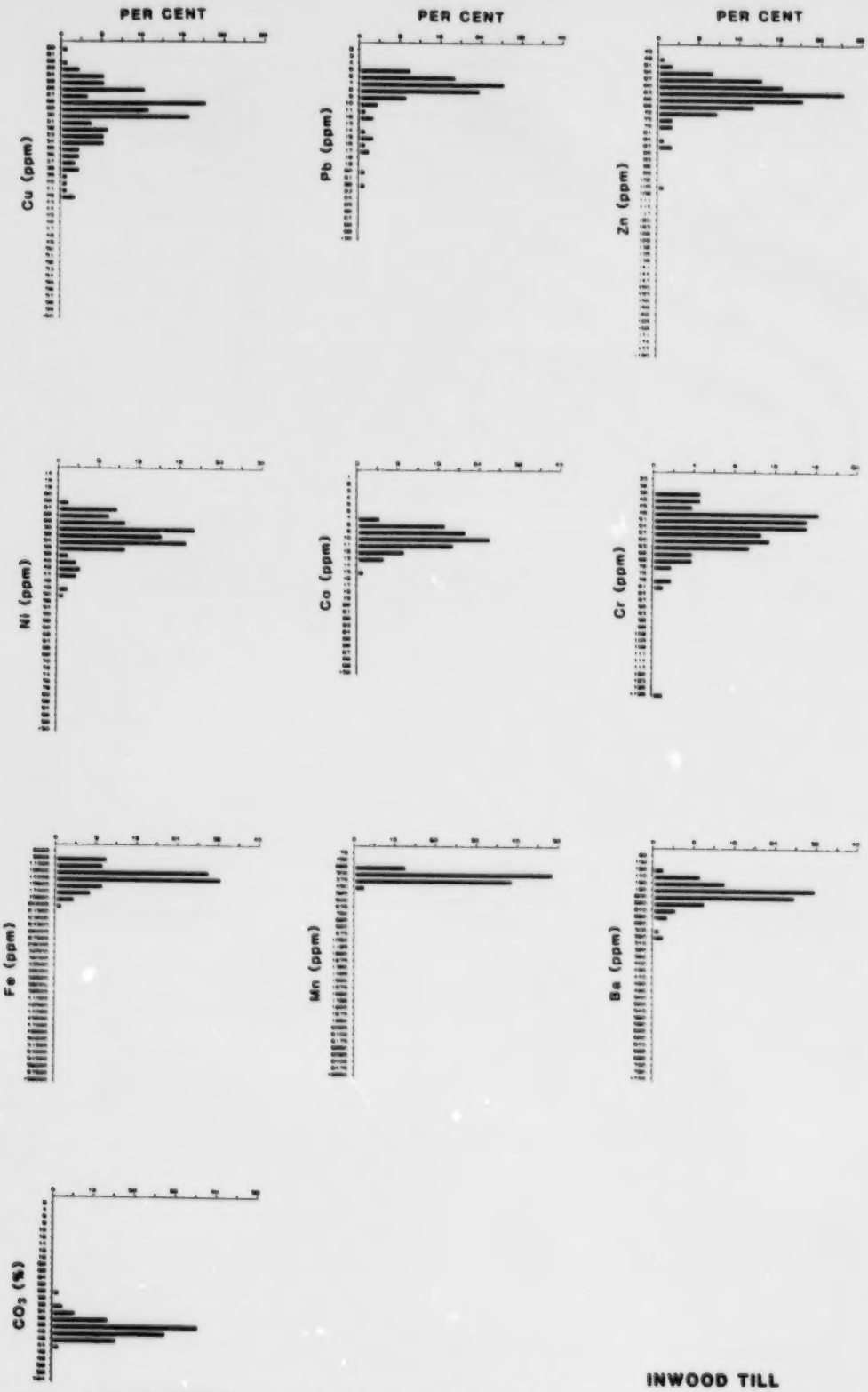

Figure 26: Histograms showing the frequency distribution of trace elements in the less than 2 micron fraction and CO_3 content of the less than 63 micron fraction of the Inwood till, Komarno till, glaciolacustrine sediment and iceberg turbate in the Balmoral-Komarno area.

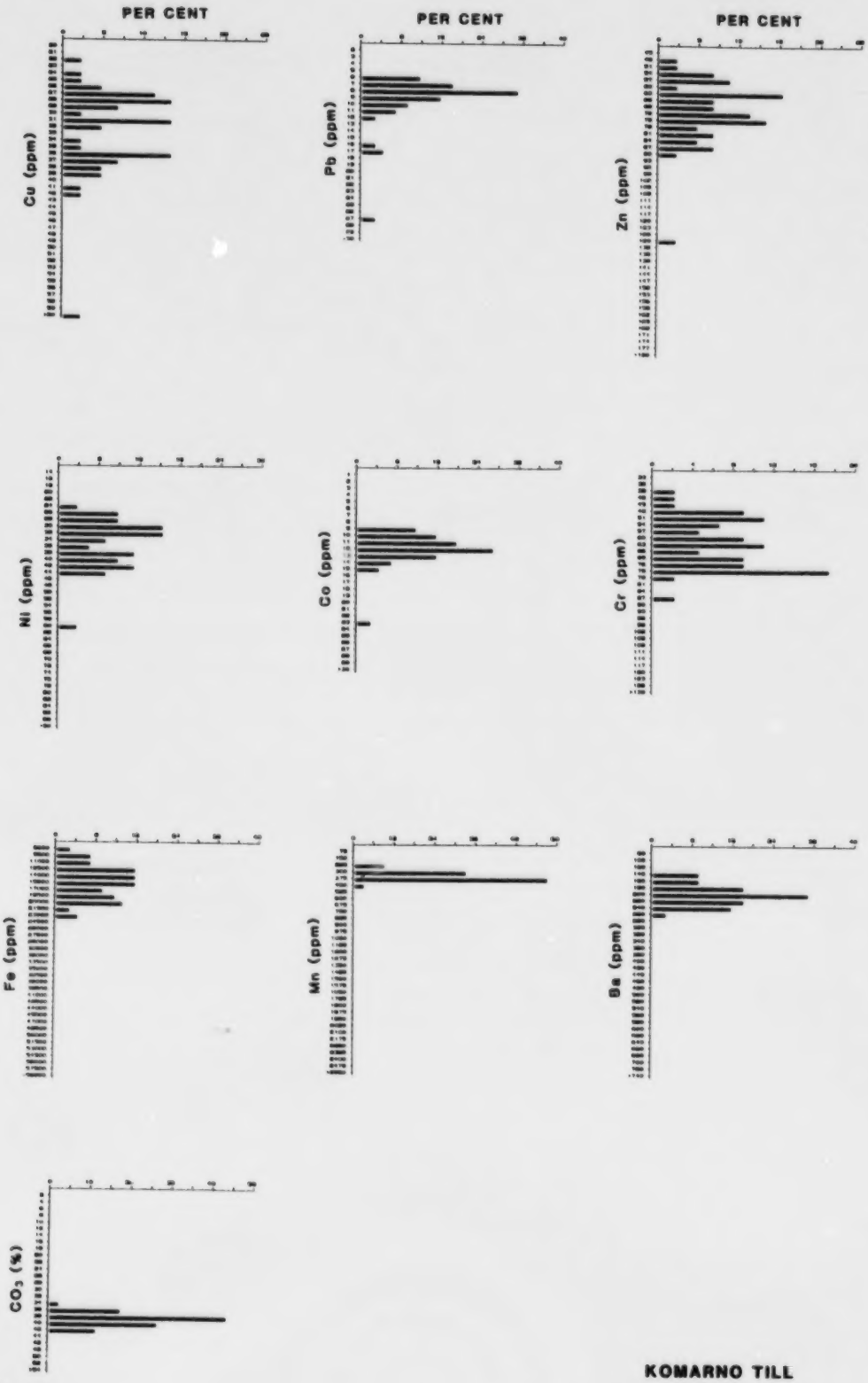

Figure 26: Continued.

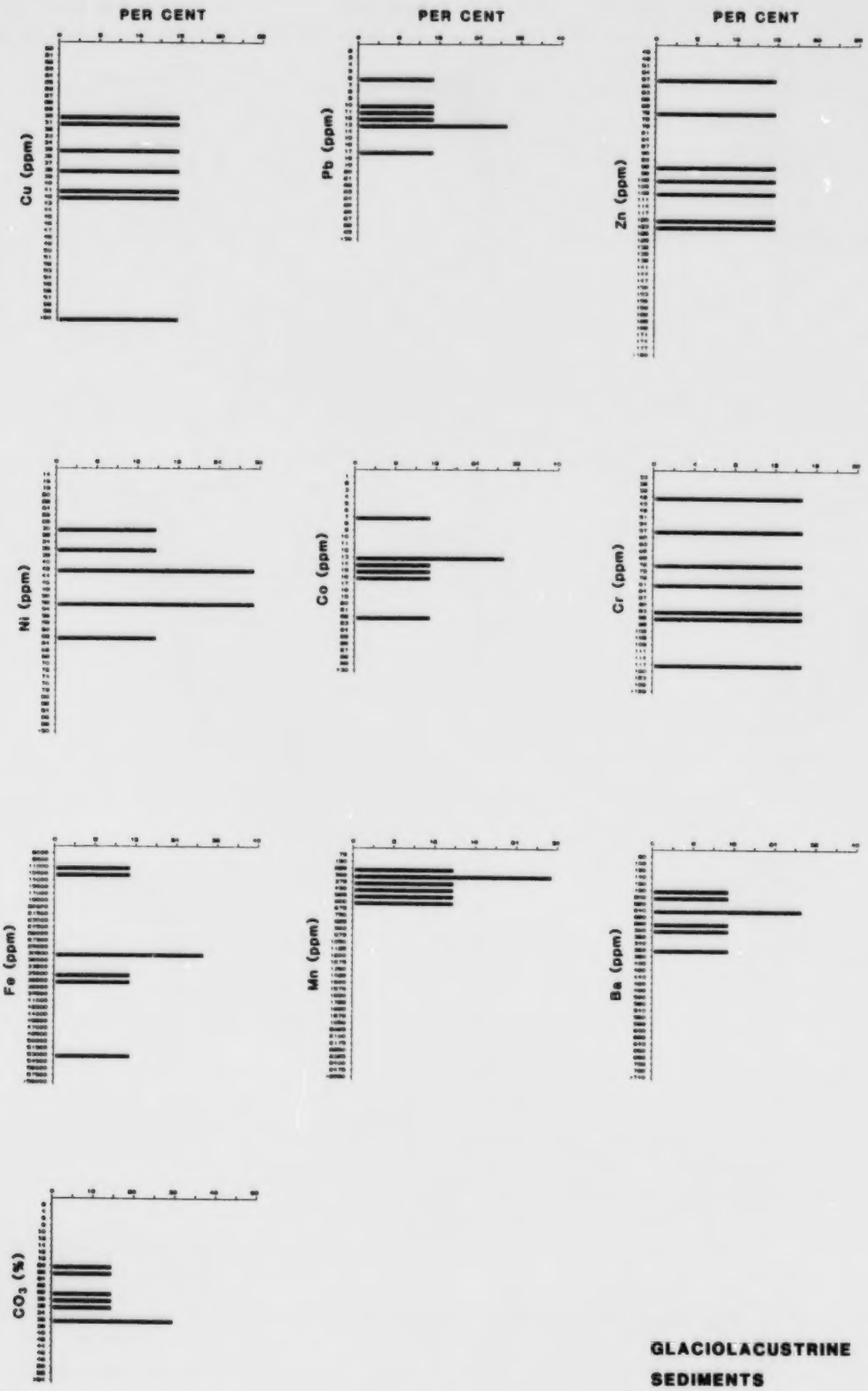

Figure 26: Continued.

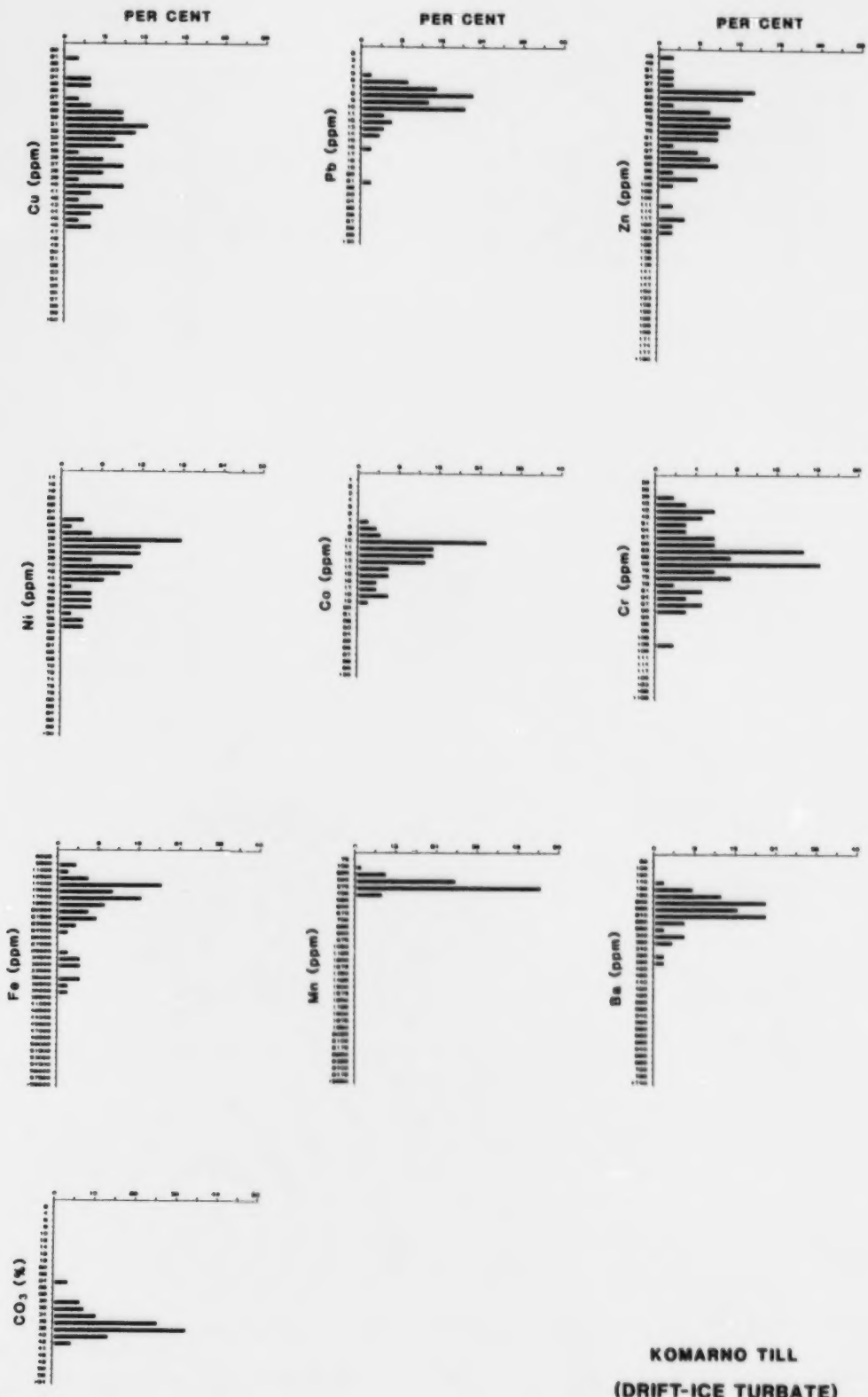

Figure 26: Continued.

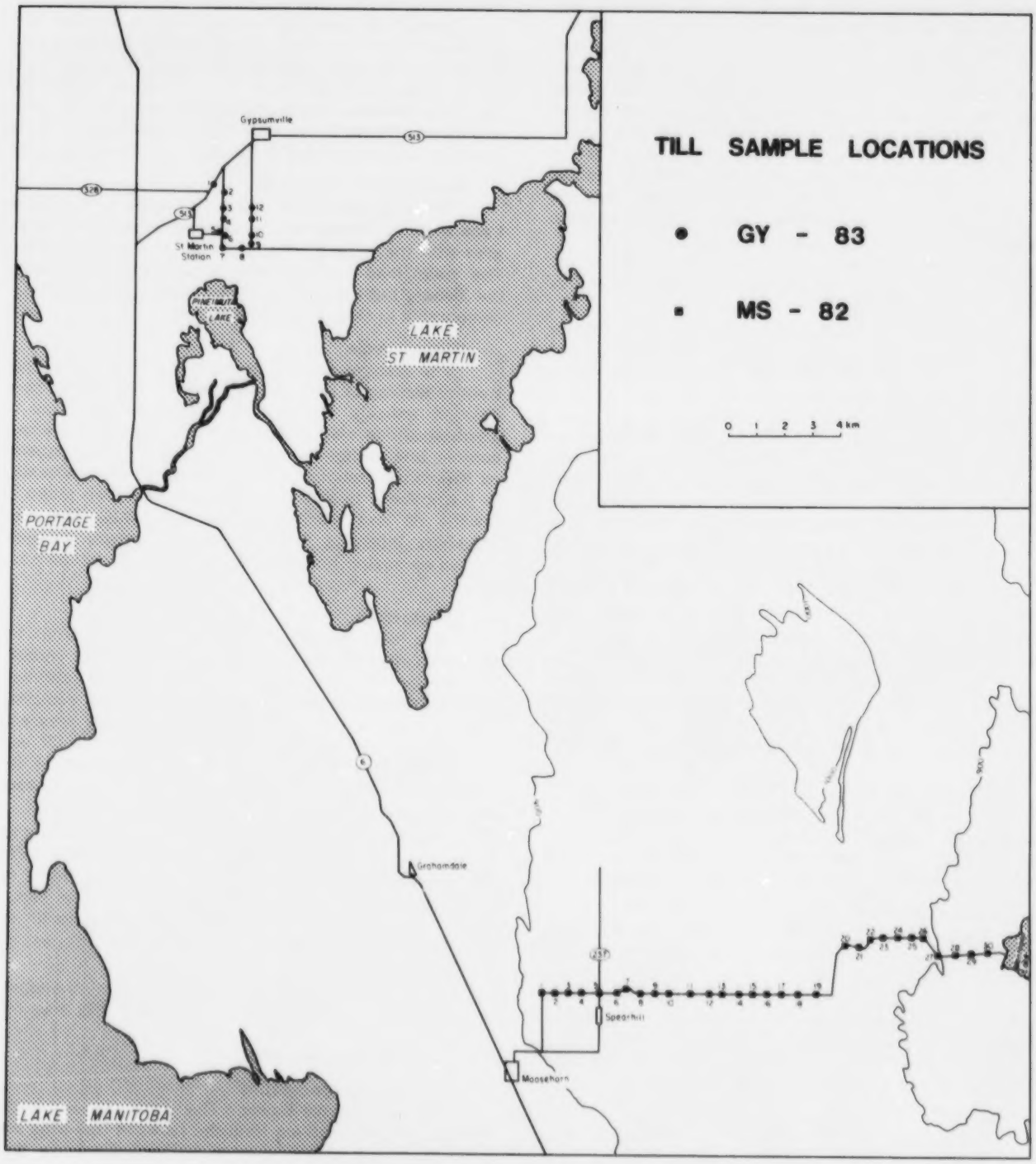

Figure 27: Till sample locations in the Moosehorn-Gypsumville area. Contours in feet.

not occur. This distribution of iceberg furrows appears to relate to different water depths of Lake Agassiz. The scour marks around Mantagao Lake formed early, possibly when the area to the east (including the southern part of Lake Winnipeg) was covered by an early deep water embayment of Lake Agassiz while the area to the west was still ice covered. The ice margin probably lay along the drainage divide 10 km east of Mantagao Lake as indicated by the change in flute orientation. The ice cover protected the western part of the area from scouring. Later, the ice margin receded an unknown distance to the north and west and the level of Lake Agassiz dropped resulting in icebergs grounding below 251 m. The high areas southeast and southwest of Lake St. Martin were left unscoured possibly because the drop in water level was very rapid.

The pattern of iceberg scour marks is reflected in the distribution of iceberg turbate. East of sample MS20, below an elevation of 282 m, the overconsolidated Inwood till is overlain by mottled diamicton similar to the turbate described in the Southern Interlake, but with a pebble composition similar to the underlying Inwood till (Table 1). As iceberg furrows are common in this area (Fig. 30), this diamicton is interpreted as having originated by the mixing of previously deposited Inwood till and glaciolacustrine clay. West of sample MS20 Inwood till is overlain by Komarno till with no glaciolacustrine clay inclusions (mottling). Therefore, in the Moosehorn-Mantagao Lake region there is a direct correlation between the presence of iceberg furrows and mottled iceberg turbate, a relationship that is unclear in the Balmoral-Komarno area.

The iceberg furrows are similar to those described from the till plain in the Balmoral-Komarno area. They are generally less than a metre deep and in places show low, but well developed berms on either side (Fig. 36).

The iceberg turbate is similar to that found on the till plain in the southern Interlake comprising variable mixtures of till and glaciolacustrine clay. Highly deformed mixtures of light coloured till and dark clay are exposed in ditch sections south of Gypsumville (Fig. 37)

Geochemistry

Histograms showing the frequency distribution of copper, lead, zinc, nickel, cobalt, chromium, iron, manganese and barium in the <2 micron fraction and carbonate in the <63 micron fraction for the Inwood till, Komarno till, glaciolacustrine sediments and iceberg turbate are shown in Figure 38. Statistics summarizing the geochemical data are listed in Table 4. The geochemical data is listed in Appendix II.

Tills

Comparison of trace element concentrations indicates Inwood till has lower mean concentrations than Komarno till, which is similar to tills in the Balmoral-Komarno area. The mean concentrations of trace elements in both tills are, however, significantly higher than in the Balmoral-Komarno area, possibly due to proximity of Devonian bedrock to the northwest and Permian and Jurassic outliers north of Lake St. Martin.

Inwood till generally shows a wider range of concentrations than Komarno till and several elements have bimodal distributions. The double peaks of copper, zinc, nickel, cobalt and chromium concentrations reflect the low trace element concentrations of the Silurian Interlake Group (Table 3), and the high concentrations of the Devonian, and possibly the Permian and Jurassic rocks.

Glaciolacustrine sediments

The glaciolacustrine sediments have higher mean trace element concentrations than other sediment in the area with the noticeable exceptions of lead and nickel. The mean lead concentration is comparable to that of the iceberg turbate and the mean nickel concentration is comparable to that of the Komarno till.

Iceberg turbate

The iceberg turbate is restricted to the area just west of Mantagao Lake. Field relations and pebble composition indicate the turbate comprises mixtures of glaciolacustrine clay and Inwood till. The trace element content and carbonate content support this conclusion as the concentrations of trace elements and carbonate in the iceberg turbate are generally between those of Inwood till and glaciolacustrine sediments. The geochemistry indicates that the iceberg turbate was not formed by mixing Komarno till and glaciolacustrine sediment.

Conclusions

The succession of Inwood till, Komarno till, glaciolacustrine sediment, and iceberg turbate records two glacier advances towards the south and southeast followed by glacial lake incursion and iceberg scouring. The area below 282 m in the Mantagao Lake area was affected by iceberg scouring while Komarno till was being deposited to the west. After the retreat of the Komarno ice the level of Lake Agassiz dropped such that icebergs scoured only to elevations of 251 m.

The geochemistry of the four lithosomes clearly reflects the different provenances of the sediments. The low mean trace element concentrations of Inwood till reflect the generally local origin of this till. The higher mean trace element concentrations of Komarno till reflect the Devonian bedrock source to the northwest for much of this till.

None of the overburden samples collected suggest any evidence of lead-zinc mineralization in this area.

Swan Lake-Dawson Bay Area

Location and topography

The Swan Lake-Dawson Bay area, situated in the Westlake Plain down-ice from the Dawson Bay area has been the focus of lead-zinc exploration for some time (Stevenson, 1973; Fig. 39).

The Westlake Plain and the adjoining Swan River Plain are relatively low areas with elevations ranging from 366 m along the base of the Manitoba escarpment,

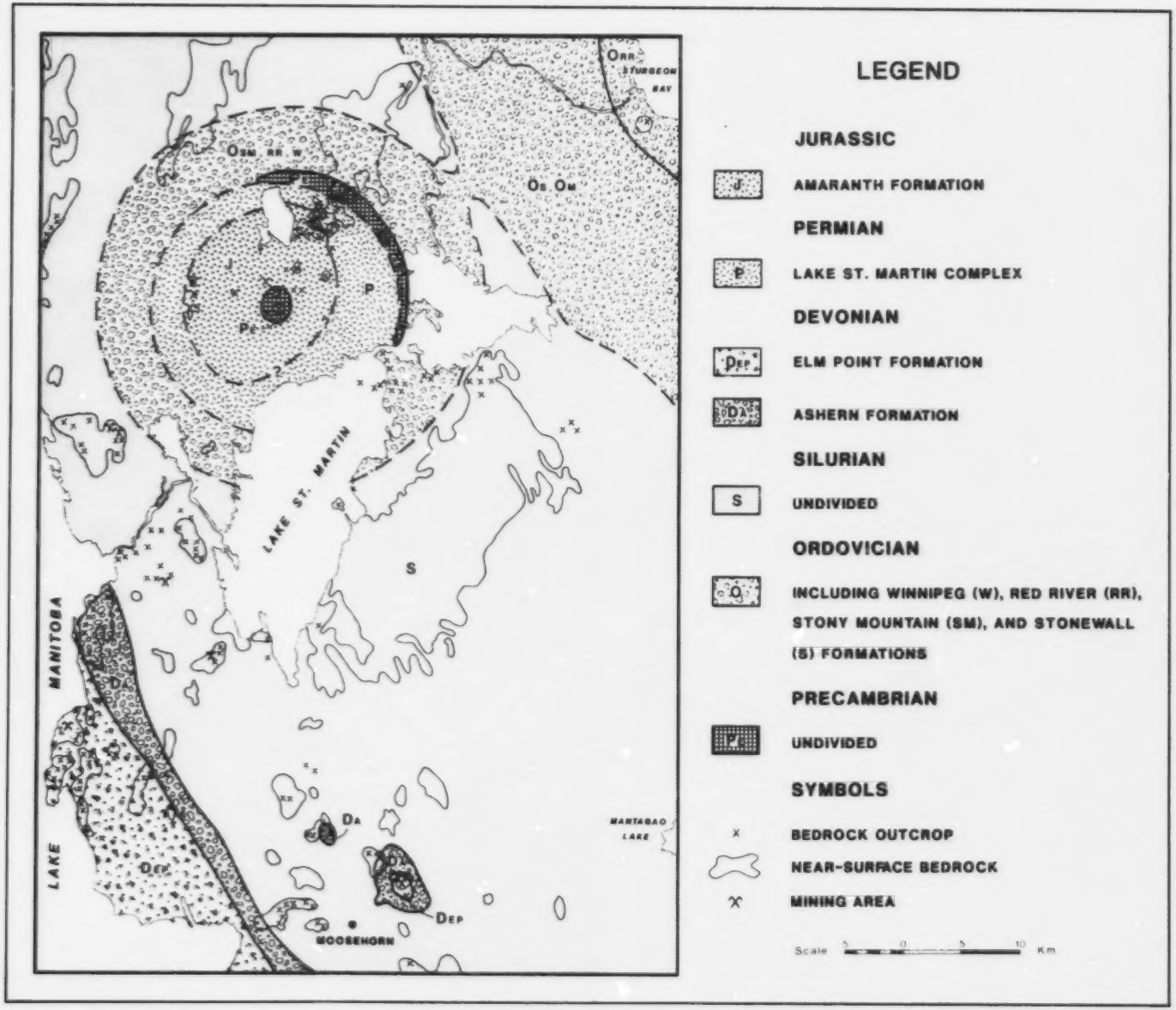

Figure 28: Bedrock geology of the Moosehorn-Gypsumville area (Manitoba Mineral Resources Division, 1979).

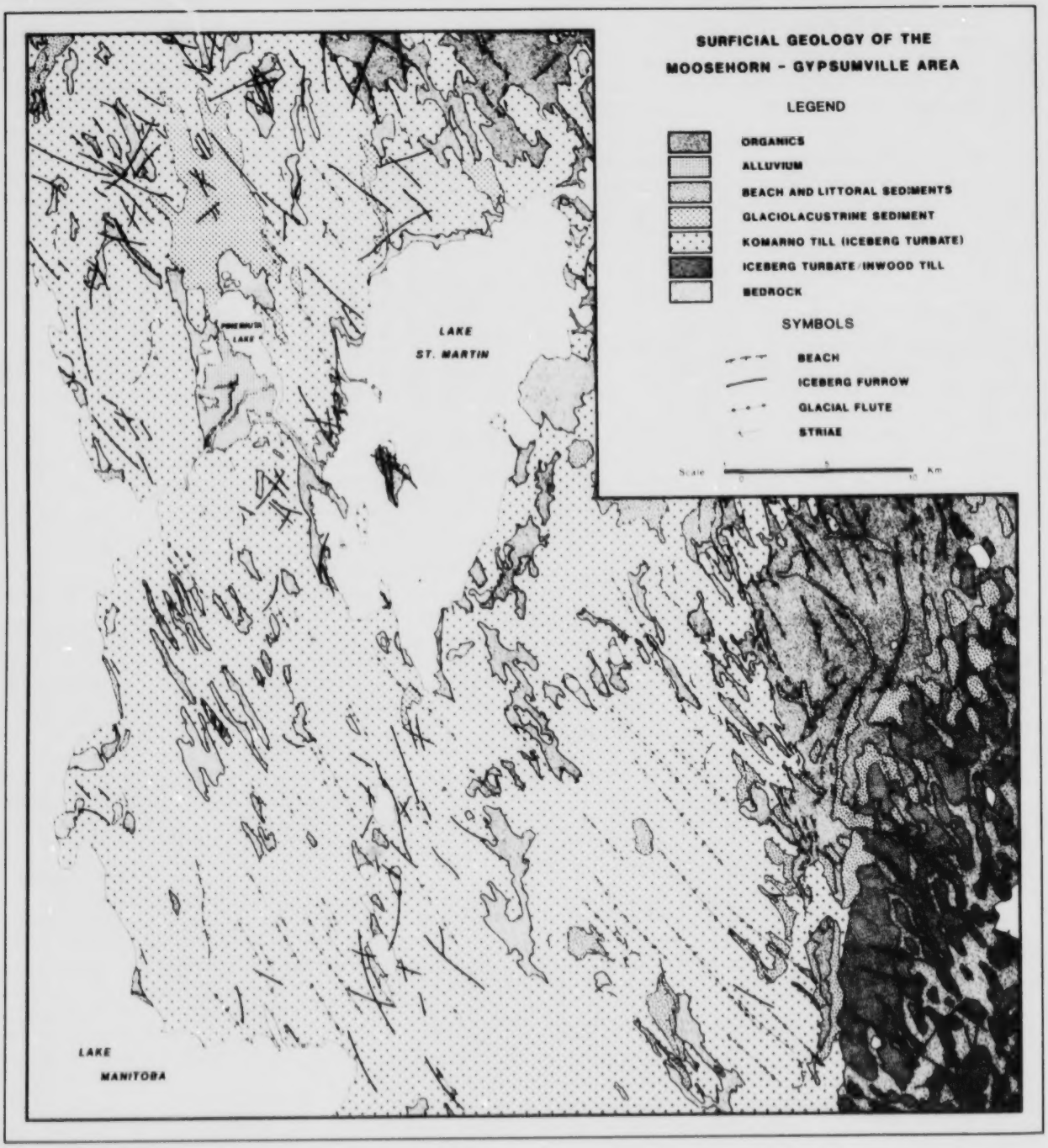

Figure 29: Surficial geology of the Moosehorn-Gypsumville area (modified from Nielsen and Matile, 1982b).

Figure 30: Drumlinoid ridges oriented toward 155° in the area around Mantagao Lake. Iceberg furrows are indicated by arrows.

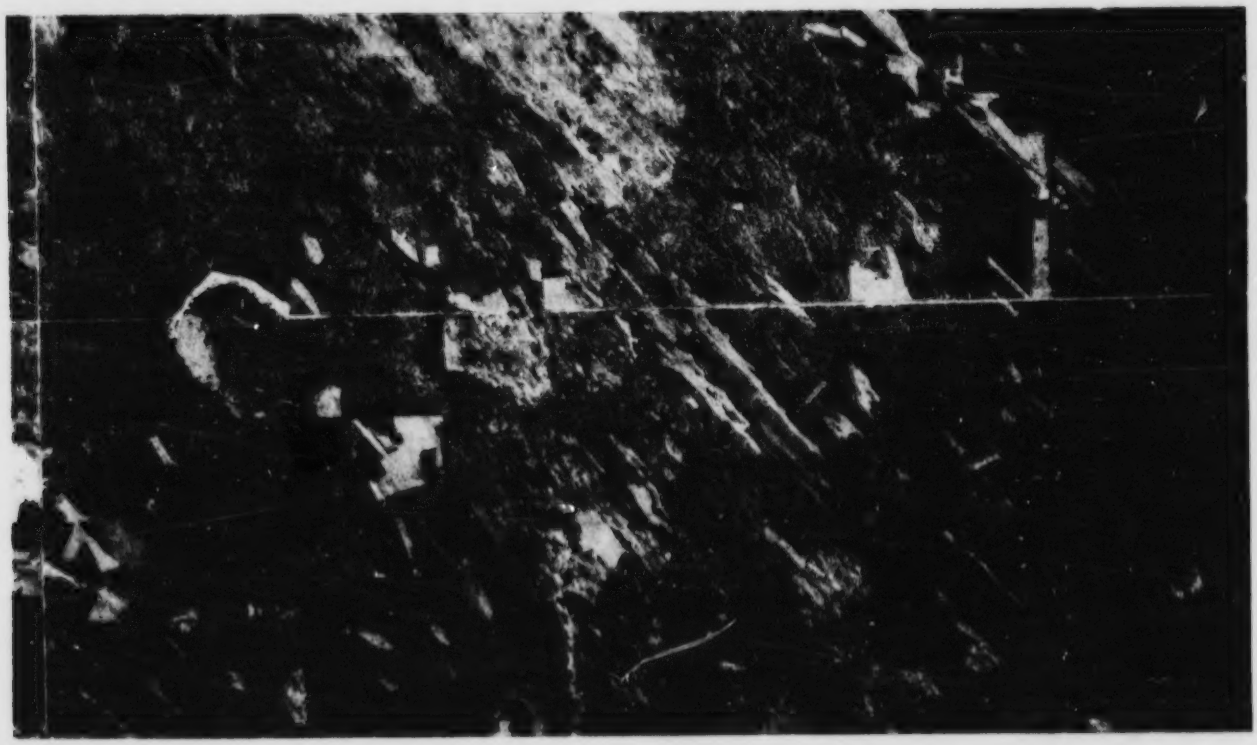

Figure 31: Flutes oriented toward 140° in the Spearhill area.

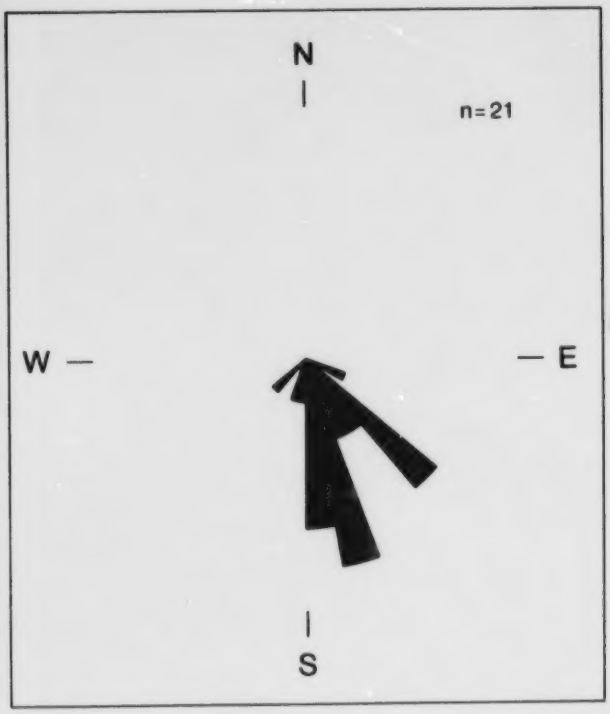

Figure 32: Striae directions in the Moosehorn-Gypsumville area.

down to the level of Lake Winnipegosis at 253 m. In the area of Winnipegosis reefs, along the south shore of Dawson Bay, local relief is in places up to 15 m.

Porcupine Hills in the western part of the area are separated from the Westlake Plain by the Manitoba escarpment (Fig. 40). This prominent escarpment rises from 366 m to over 670 m in a distance of about 6 km. Local relief on the escarpment is up to 30 m. The top of Porcupine Hills is relatively flat with elevations between 670 and 795 m. Local relief is over 30 m in many areas.

Bedrock geology

Unlike the Balmoral-Komarno and Moosehorn-Gypsumville areas, this area is underlain by a variety of lithologies including Devonian carbonate and Cretaceous sandstone and shale (Fig. 41). The oldest Paleozoic formation in the area is the Winnipegosis Formation outcropping on Salt Point. It consists mainly of carbonate mounds of massive, light yellowish grey, vuggy dolomite (Fig. 42). Interreef areas consist of thinly bedded bituminous dolomite and evaporite. The evaporite consists of halite with thin potash beds and anhydrite; it originally extended throughout the Devonian outcrop belt but was removed from the region by subsurface salt solution (McCabe and Barchyn, 1982). The solution of the evaporite has given rise to the almost 50 brine springs found in the Devonian outcrop belt (Fig. 43).

The eastern part of the area, including most of Dawson Bay and Swan Lake, is underlain by the Dawson Bay and Souris River formations. The Dawson Bay Formation comprises white to pale yellowish fossiliferous limestone, calcareous and fossiliferous shale, laminated and bituminous dolomite, and red to greenish grey dolomitic shale (McCabe and Barchyn, 1982). The Dawson Bay Formation is draped over reefs of the underlying Winnipegosis Formation and reflects the topography of the Winnipegosis depositional surface (Fig. 42).

The Souris River Formation consists mainly of fine grained, sparsely fossiliferous micritic limestone. The upper part of the formation is dolomitized in places. The base of the formation is characterized by shale and reddish grey and dark brown argillaceous dolomite (McCabe and Barchyn, 1982).

The lower Cretaceous Swan River Formation, comprising lithified and unlithified sandstone, overlies the Devonian carbonate in the Westlake Plain almost to the base of the Manitoba escarpment (Fig. 44).

The Manitoba escarpment and Porcupine Hills are underlain by Cretaceous shale of the Ashville, Favel (Fig. 45), Morden Shale, Niobrara and Pierre Shale formations (McNeil and Caldwell, 1981).

Quaternary geology

Drift thickness

The drift thickness varies considerably. Bedrock outcrops are common in the Dawson Bay area (Fig. 46) and many of the backhoe pits in the Mudlen Creek area of the Manitoba escarpment terminated in shale, indicating the bedrock is relatively shallow. On Porcu-

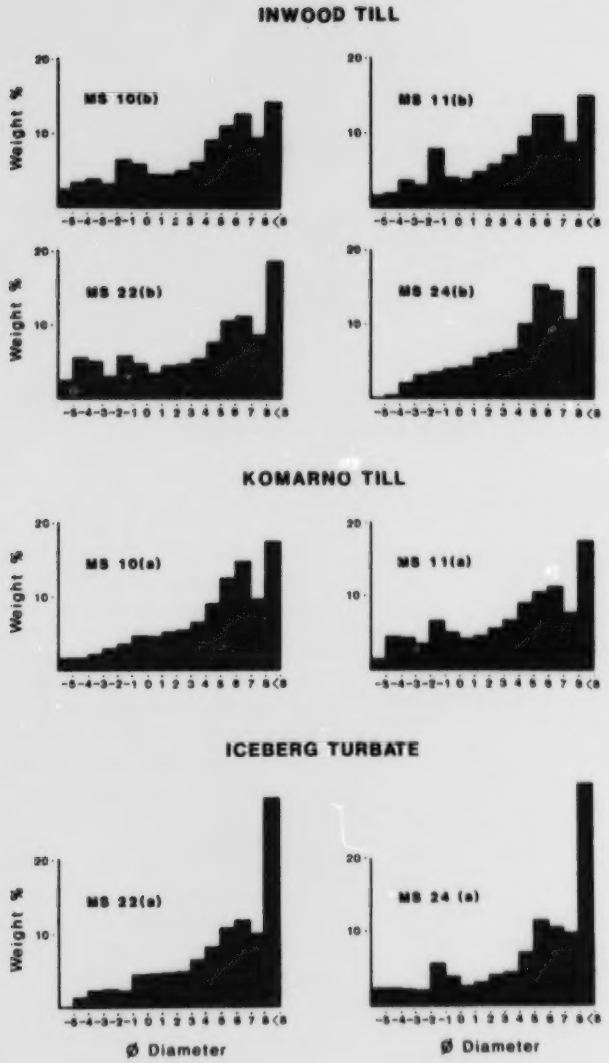

Figure 33: Histograms showing the grain size distribution of Inwood till, Komarno till and iceberg turbate from the Moosehorn-Gypsumville area.

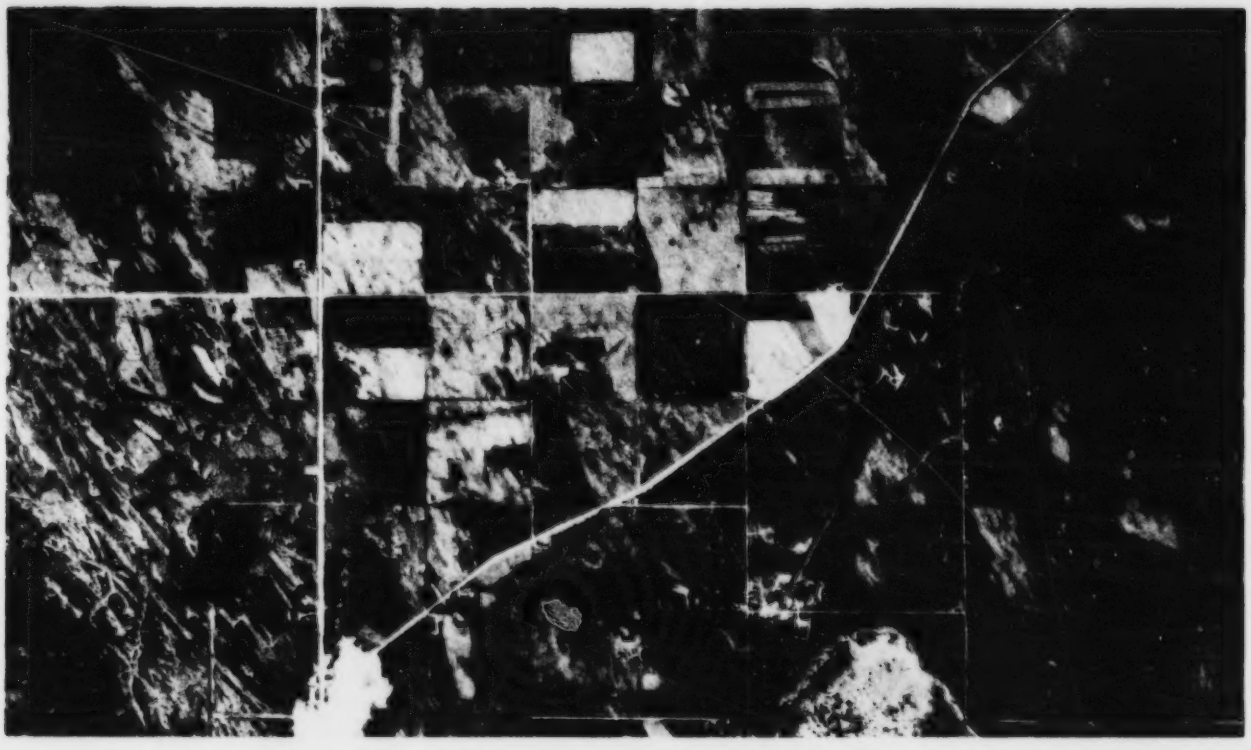

Figure 34: Iceberg furrows on the clay plain near St. Martin Station.

pine Hills the overburden thickness may be up to 300 m thick (Nielsen, 1988).

Ice flow

Two main ice flow regimes are recognized. On Porcupine Hills, a southerly ice flow is inferred for the Zelena Till on the basis of the pebble composition and the orientation of drumlins in the adjacent part of Saskatchewan (Moran, 1969). A southwesterly (250°) ice flow is associated with the Arran Till on the Westlake plain as recorded by striae in the Dawson Bay area (Fig. 47), and by the orientation of fluted till east of Swan Lake (Fig. 46; Nielsen 1988).

Six major lithosomes, including three tills, glaciolacustrine sediments, iceberg turbate, and alluvial sediments were recognized in the area.

Older till

The oldest till encountered is an oxidized sandy till underlying the Arran Till in 5 backhoe pits on the southeast side of Porcupine Hills. The till, which is of unknown age, is termed the older till; it is chocolate brown, oxidized and sandy (Fig. 48). Because of the oxidation and sandy texture this till is tentatively correlated with the Minnedosa Till described by Klassen (1979) on Duck and Riding mountains.

Zelena till

The Porcupine Hills are covered with hummocky stagnation moraine composed primarily of Zelena Till (Fig. 49; Nielsen, 1988). Zelena Till is relatively soft as it was not overridden by glacier ice but was deposited supraglacially (Fig. 50). Zelena Till is chocolate brown and has a clayey texture (Fig. 48). Pebbles derived from the shield constitute 26.4% of the 4-16 mm size fraction, whereas the locally derived shale constitutes only 7.1% (Table 1). The remaining 60-65% of the pebbles are carbonates derived from the Paleozoic bedrock. Sandstone pebbles from the Cretaceous Swan River Formation make up approximately 1% of the pebbles. The low concentrations of sandstone and shale are due to the inability of these lithologies to withstand extended glacial transport. The presence of erratics from the Missi Group, outcropping in the Flin Flon area, and the relatively low concentration of carbonate clasts indicate a northern provenance for the Zelena Till.

Arran till

Along the Manitoba escarpment Zelena Till is overlain by the light buff coloured calcareous Arran Till. It occurs only sporadically along the escarpment where it is generally less than a metre thick. In the Westlake Plain, Arran Till is widespread forming the surface till over most of the area.

Arran Till is generally fissile and compact with an abundance of carbonate clasts (Fig. 51). Along the Manitoba escarpment reverse grading, lack of fissility and inverted stratigraphies indicates redeposition of Arran Till as gravity flows (Fig. 52).

Table 4: Summary statistics for the geochemical data from the Moosehorn - Gypsumville area

Inwood till (n=25)	Cu (ppm)	Pb (ppm)	Zn (ppm)	Ni (ppm)	Co (ppm)	Cr (ppm)	Fe (ppm)	Mn (ppm)	Ba (ppm)	CO_3 (%)
Mean	36.2	7.3	75.1	47.4	14.6	74.4	13194.0	312.0	216.4	40.2
S.D.	7.3	1.6	16.5	11.5	2.8	17.7	5382.1	48.9	33.7	2.5
Max.	50.0	10.0	127.0	68.0	22.0	100.0	35000.0	435.0	285.0	43.8
Min.	23.0	5.0	57.0	26.0	9.0	38.0	8600.0	250.0	160.0	32.3

Komarno till (n=12)	Cu (ppm)	Pb (ppm)	Zn (ppm)	Ni (ppm)	Co (ppm)	Cr (ppm)	Fe (ppm)	Mn (ppm)	Ba (ppm)	CO_3 (%)
Mean	39.2	8.4	82.3	52.8	15.7	85.6	14929.2	346.1	240.3	39.0
S.D.	5.5	1.6	15.8	5.0	1.9	12.4	3645.8	63.1	29.4	4.1
Max.	49.0	11.0	113.0	60.0	18.0	105.0	21900.0	450.0	300.0	44.0
Min.	29.0	6.0	67.0	44.0	13.0	67.0	11400.0	270.0	204.0	30.7

Glaciolacustrine sediments (n=16)	Cu (ppm)	Pb (ppm)	Zn (ppm)	Ni (ppm)	Co (ppm)	Cr (ppm)	Fe (ppm)	Mn (ppm)	Ba (ppm)	CO_3 (%)
Mean	45.2	10.8	115.3	53.0	18.6	86.8	30934.4	499.1	291.4	27.0
S.D.	7.5	3.9	17.1	9.7	3.9	23.6	8277.6	100.8	80.9	11.3
Max.	58.0	18.0	139.0	63.0	26.0	121.0	40400.0	637.0	460.0	42.8
Min.	31.0	5.0	74.0	28.0	9.0	36.0	13850.0	268.0	194.0	11.3

Iceberg turbate (n=13)	Cu (ppm)	Pb (ppm)	Zn (ppm)	Ni (ppm)	Co (ppm)	Cr (ppm)	Fe (ppm)	Mn (ppm)	Ba (ppm)	CO_3 (%)
Mean	39.4	10.4	95.1	49.8	15.9	76.8	18315.4	382.0	250.2	34.3
S.D.	5.1	1.3	14.1	6.9	1.8	15.2	5634.0	56.7	41.6	4.6
Max.	46.0	14.0	119.0	59.0	19.0	105.0	31500.0	480.0	305.0	40.6
Min.	29.0	9.0	65.0	35.0	13.0	46.0	11300.0	245.0	163.0	26.3

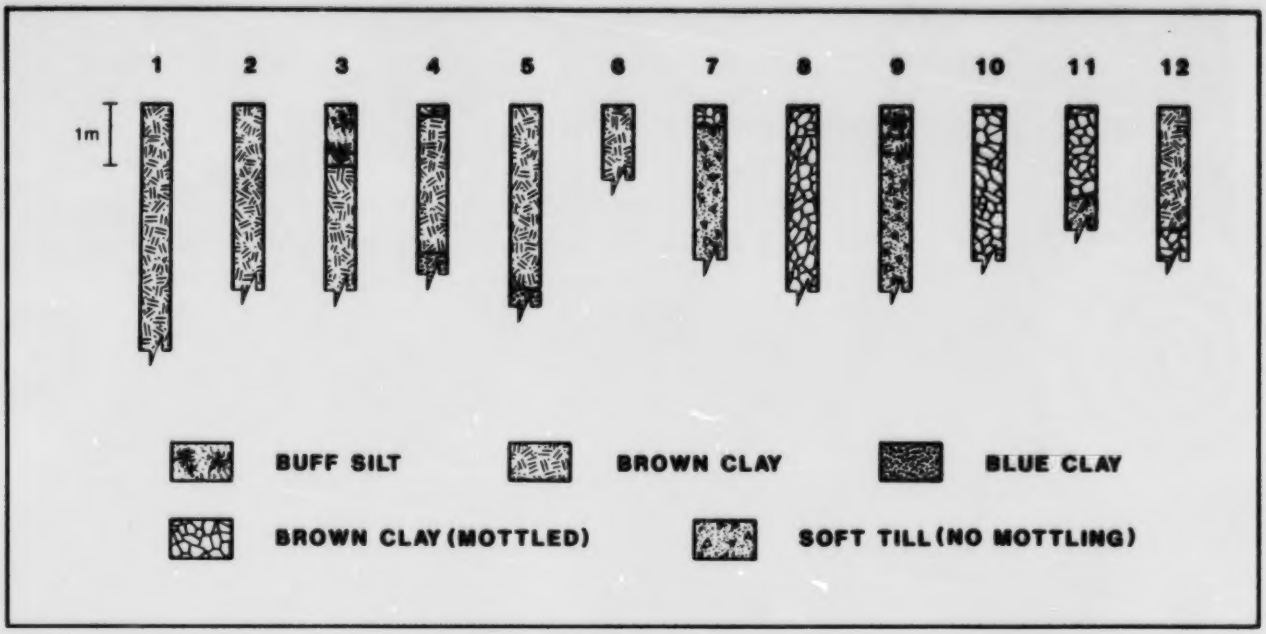

Figure 35: Stratigraphy of the surficial sediments near St. Martin Station. See Figure 27 for the location of the holes.

Figure 36: Ditch section across an iceberg furrow at a low angle, 1 km east of sampling site GY1.

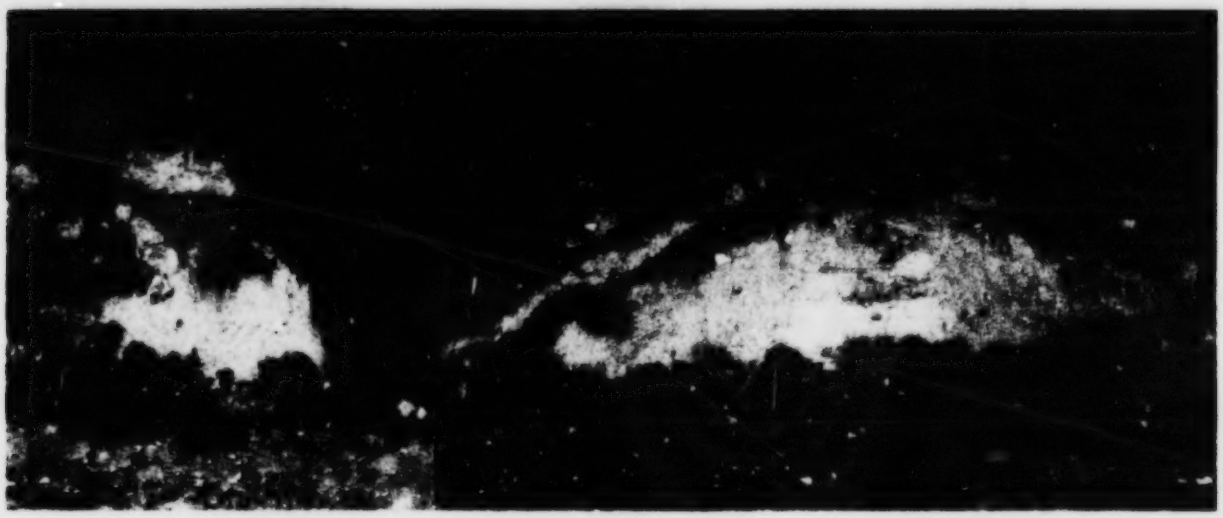

Figure 37: Details of the iceberg turbate exposed in the section shown in Figure 36 showing the mixed till and glaciolacustrine clay.

The pebble fraction of Arran Till in the Dawson Bay-Swan Lake area is generally <10% Precambrian clasts and 90% locally derived carbonate clasts (Table 1). Along the escarpment, Arran Till contains more Precambrian clasts, possibly due to incorporation of the underlying Zelena Till.

The texture of the Arran Till is also variable. Over the Paleozoic carbonate bedrock in the Dawson Bay area and west of Swan Lake, Arran Till is relatively silty (Fig. 48), whereas over the Swan River sandstone, between the escarpment and Swan Lake, it is sandy. The texture of the Arran Till reflects the terminal grain sizes of the underlying carbonate and sandstone bedrock.

Iceberg turbate

Iceberg turbate was encountered in only 12 backhoe pits in the Dawson Bay area. The iceberg turbate is recognized by the presence of lake clay inclusions in "till-like" diamicton or in some cases "till-like" diamicton inclusions in glaciolacustrine clay. The general absence of iceberg furrows may be due to the water in Lake Agassiz being either too shallow or too deep for furrows to form. Alternatively, the furrows may have been eroded or filled in during subsequent stages of Lake Agassiz. Regardless, iceberg turbate is not widespread in the area.

Postglacial sediments

A variety of fine textured sediments including sand, silt and clay deposits are widespread. These sediments include proglacial deposits on Porcupine Hills, and deep and shallow water Lake Agassiz and post-Lake Agassiz off-lap deposits along the Manitoba escarpment and on the Westlake plain. Alluvial fan deposits are common along the base of the escarpment (Fig. 46).

Geochemistry

Histograms showing the frequency distribution of copper, lead, zinc, nickel, cobalt, chromium, iron, manganese and barium in the <2 micron fraction and carbonate in the <63 micron fraction for the older till, Zelena Till, Arran Till, iceberg turbate and postglacial sediments are shown in Figure 53. Statistics summarizing the geochemical data are listed in Table 5. The geochemical data is listed in Appendix III.

Older till

The 5 samples of older till are recognized by their low carbonate content and high trace element concentrations. The mean carbonate content of 11.5% is lower than for any of the other sediments. Copper, zinc, chromium, iron and barium concentrations are higher than those of both the Zelena and Arran tills. The copper, lead, zinc, nickel and iron concentrations are close to

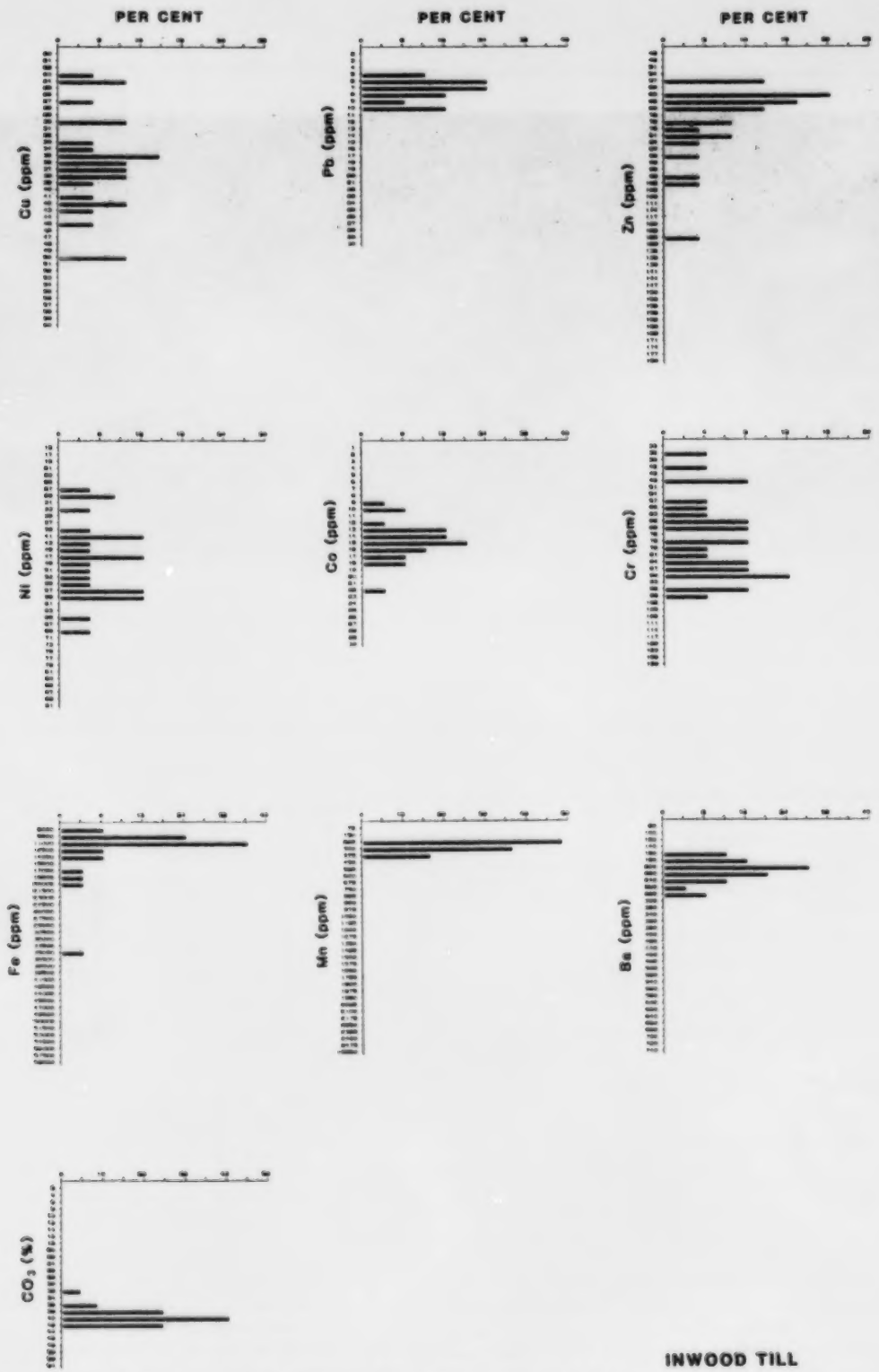

Figure 38: Histograms showing the frequency distribution of trace elements in the less than 2 micron fraction and CO_3 content of the less than 63 micron fraction of Inwood till, Komarno till, glaciolacustrine sediments and iceberg turbate in the Moosehorn-Gypsumville area.

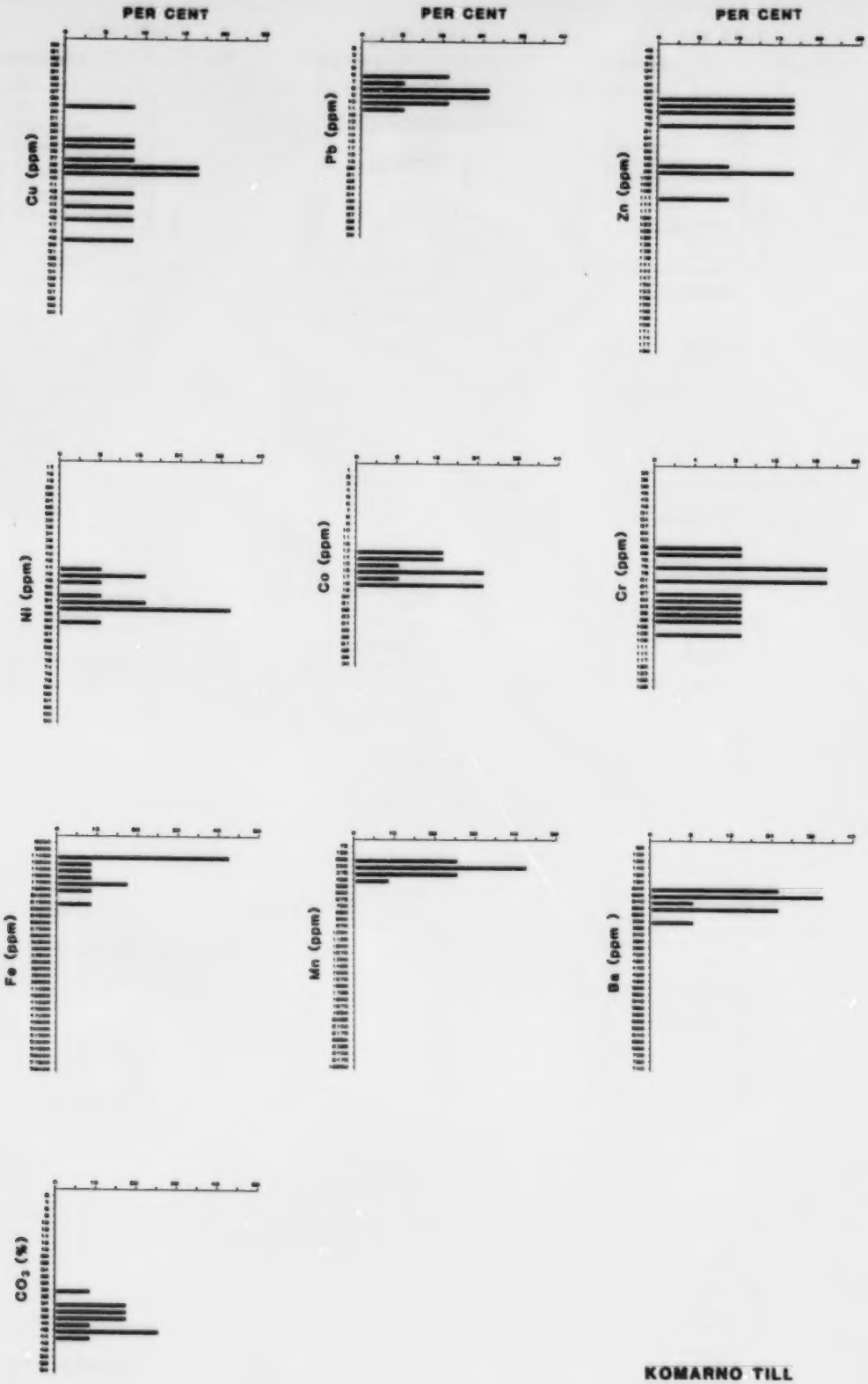

Figure 38: Continued.

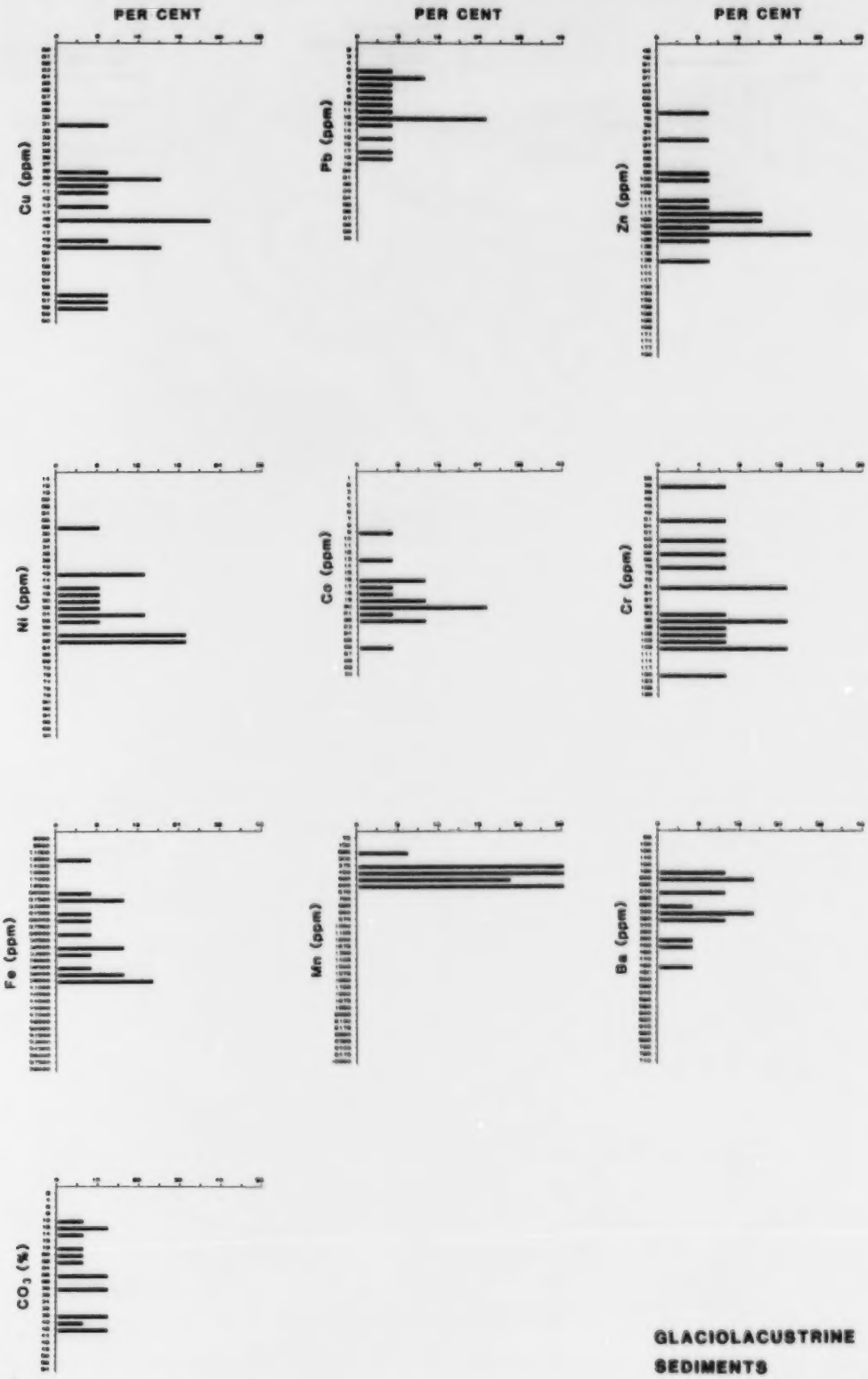

Figure 38: Continued.

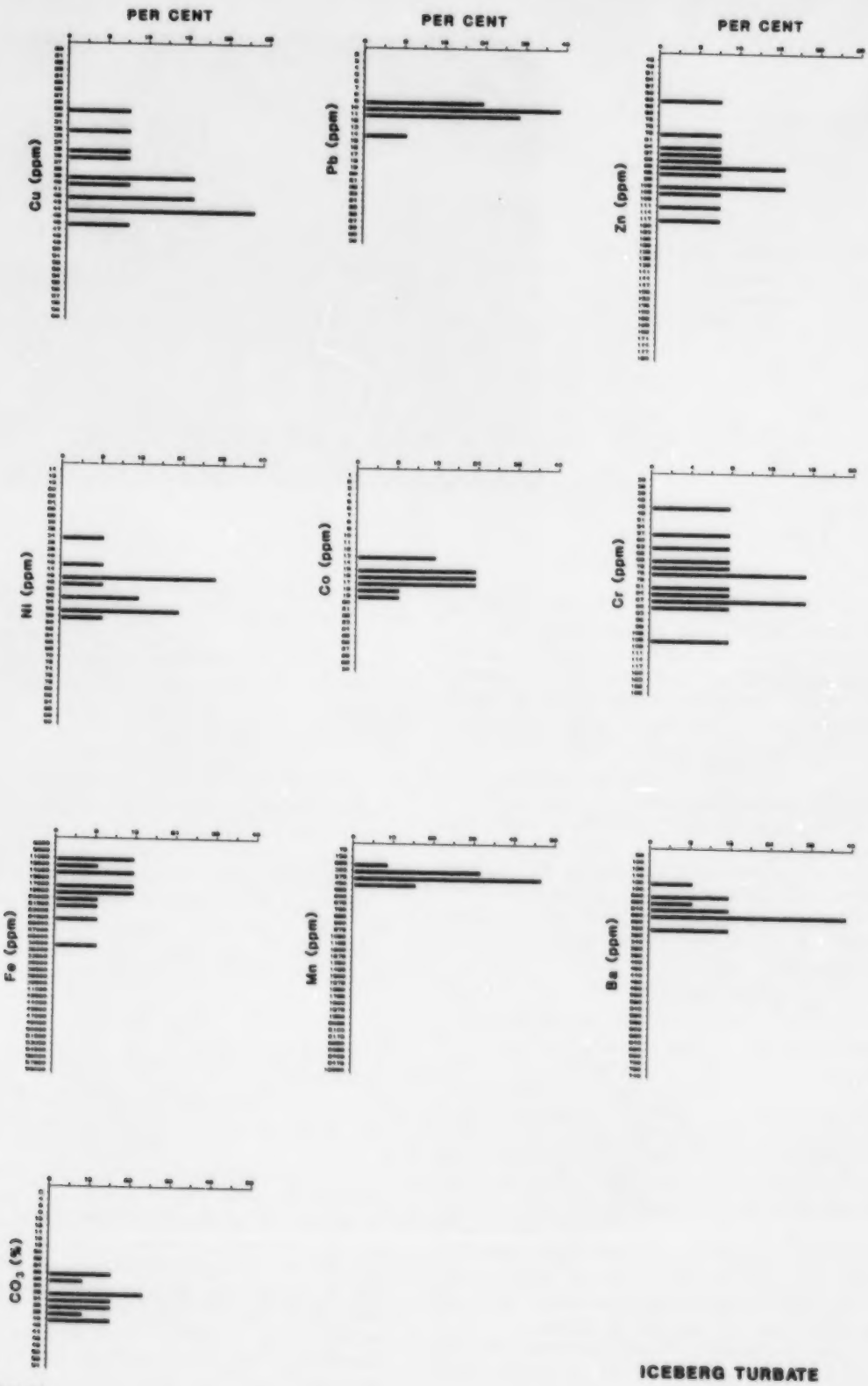

Figure 38: Continued.

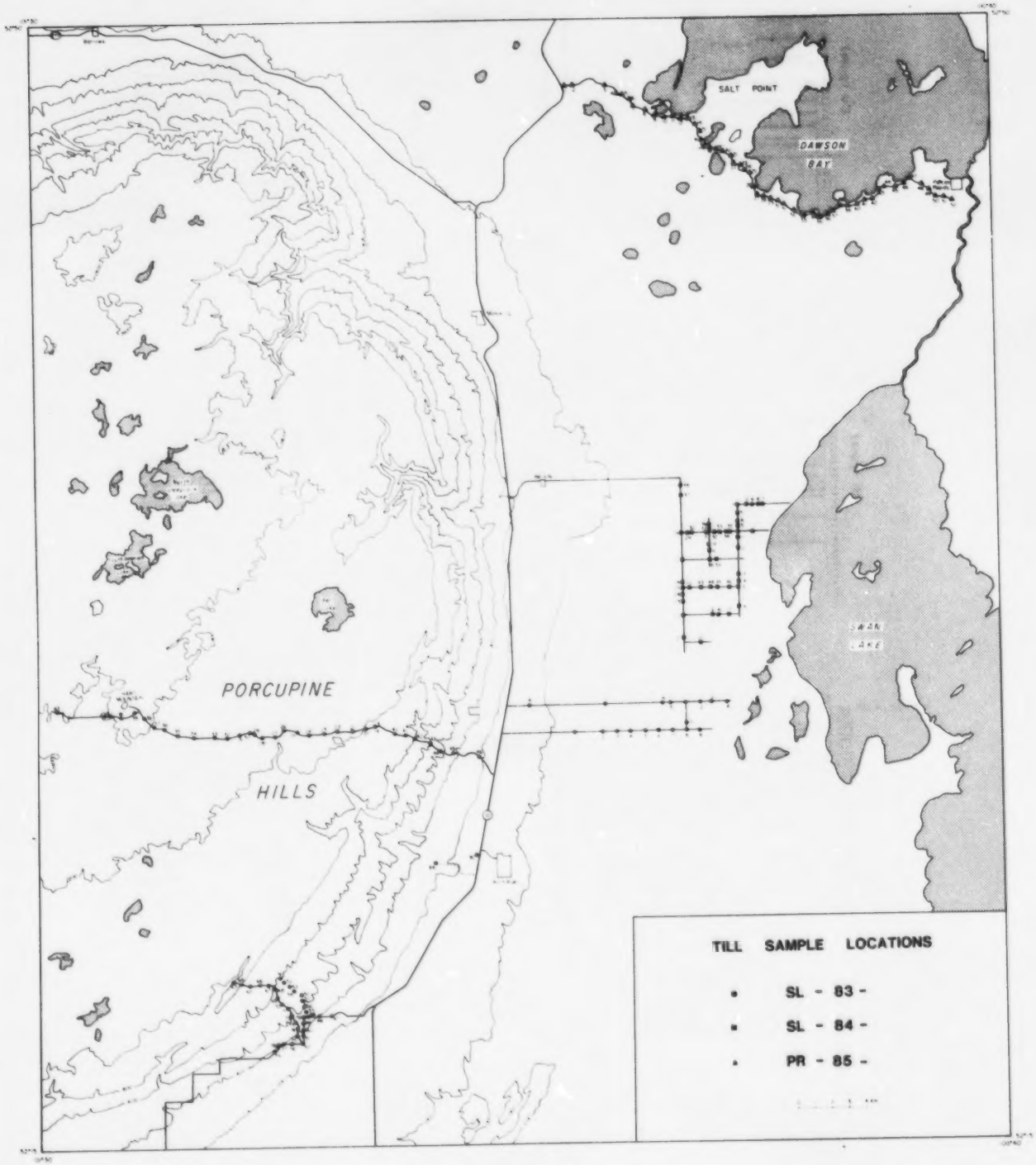

Figure 39: Sampling sites in the Swan Lake-Dawson Bay area. Contours in feet.

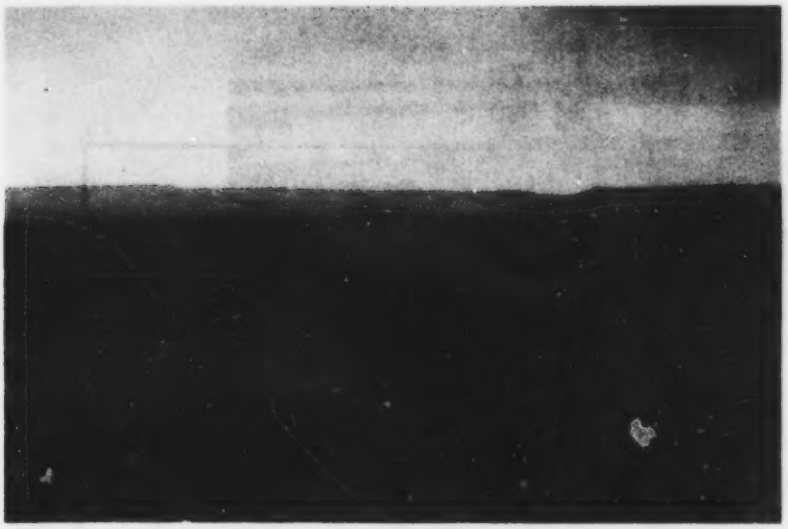

Figure 40: The Manitoba escarpment and Porcupine Hills as seen from the Westlake plain near Swan Lake.

those of the Zelena Till whereas the chromium and manganese concentrations are closer to those of the Arran Till. The trace element concentrations therefore suggest a provenance intermediate between Zelena Till derived from the north and Arran Till derived from the northeast. Alternatively, the low carbonate content may be the result of weathering that may be responsible for the trace element characteristics of this till.

Zelena Till

The mean carbonate content of Zelena Till on Porcupine Hills is 20.6%. This concentration is intermediate between the old till and the Arran Till and reflects the relatively narrow Silurian and Ordovician outcrop belt south of Flin Flon that was the source of the carbonate.

The relatively high copper, lead, zinc, iron and manganese concentrations reflects the Precambrian source for this till; a conclusion supported by the pebble composition.

Arran Till

The mean carbonate content of the 126 Arran Till samples is 39.5%, which is similar to the concentrations reported for the till in The Pas area by Nielsen and Groom (1989) and the Inwood and Komarno tills in the Interlake.

Copper, lead, zinc, iron and manganese concentrations are lower than those of the older till and the Zelena Till. This is the result of the Arran Till being derived primarily by the comminution of Paleozoic carbonate bedrock along its southwestern ice flow. Nickel, cobalt and chromium concentrations are higher in the Arran Till than in any of the other tills and reflect the incorporation of material from Thompson Nickel Belt to the composition of this till. This conclusion is substantiated by the discovery of erratics from the Thompson Nickel Belt along the south side of Swan Lake.

Iceberg turbate

The geochemistry and carbonate content of the iceberg turbate are similar to those of the Arran Till reflecting the mixing of the till with glaciolacustrine sediments. Glaciolacustrine sediments are not common on the Westlake Plain, and data are not available for comparison with the iceberg turbate geochemistry.

Postglacial sediments

Fine textured sediments related to Lake Agassiz and the post-Lake Agassiz regression of Lake Winnipegosis have a mean carbonate concentration of 22.6%. The geochemistry of these fine textured sediments is similar to that of the Arran Till, which generally underlies the clays. Copper, lead and zinc concentrations are slightly higher than in the underlying iceberg turbate and Arran Till, but the difference is not high enough to be considered significant.

Conclusions

The first glacial event in the Swan Lake-Dawson Bay area is recorded by the older till deposited by ice flowing into the area possibly from the north northeast. The classification of the 5 till samples assigned to the older till is however problematic and these till samples may represent anomalous samples of Zelena Till. This interpretation is supported by the presence of Arran Till overlying the older till in all 5 back-hoe pits where older till was identified.

The most extensive glacial event to affect the Porcupine Hills was the Late Wisconsinan advance from the north depositing Zelena Till over the entire highland area. Deposition of Zelena Till was followed by Lake Agassiz incursion into the Westlake Plain and Swan River Valley as the ice receded to the north. Renewed activity of the ice margin resulted in the Arran readvance depositing Arran Till throughout the Westlake Plain

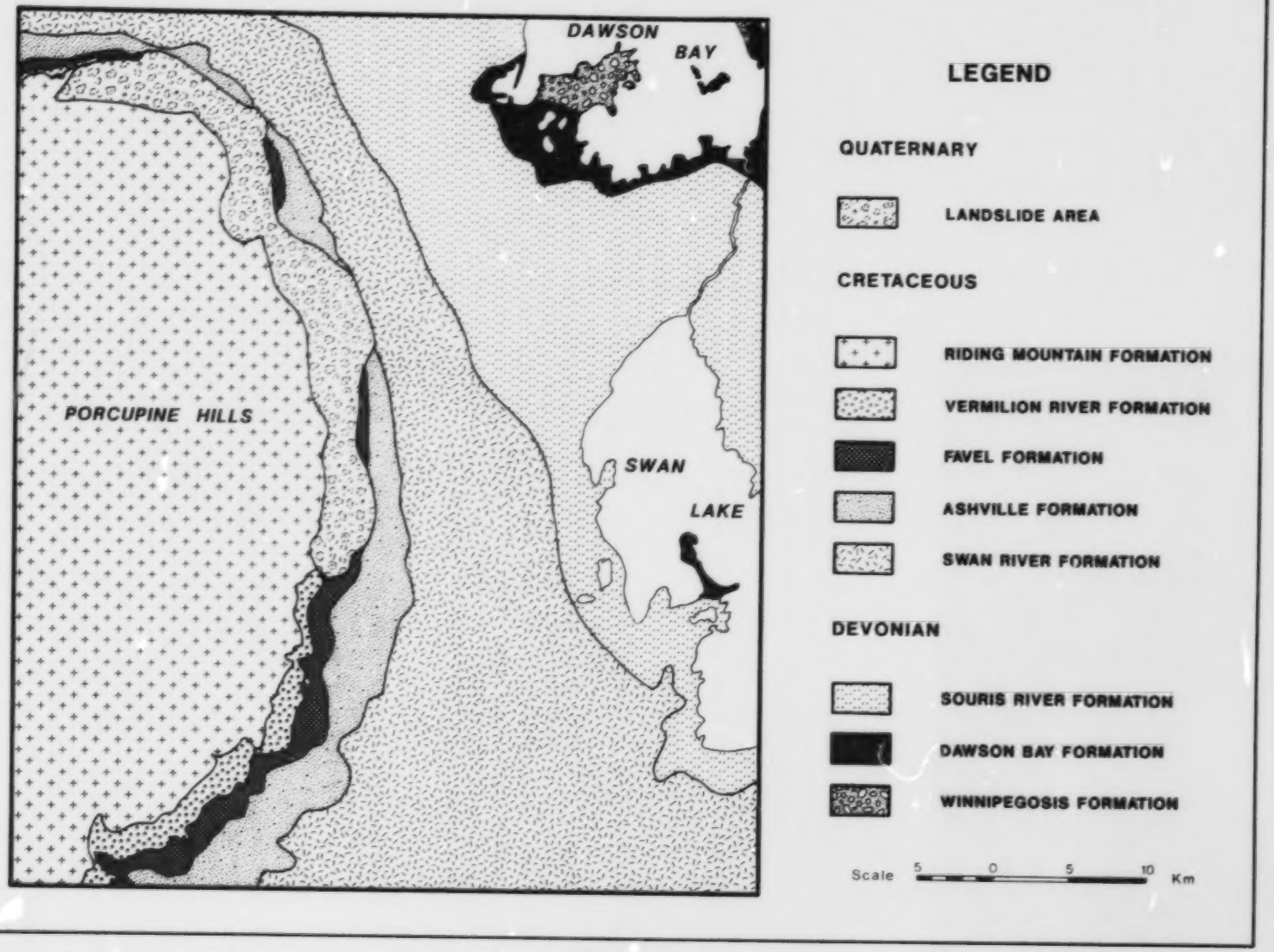

Figure 41: Bedrock geology of the Swan Lake-Dawson Bay area (from Wickenden, 1945 and Norris et al., 1982).

Figure 42: Lower Dawson Bay strata draped over an underlying Winnipegosis reef at the mouth of Steeprock River.

Figure 43: Brine spring 1 km east of German Lake south of Dawson Bay.

Figure 44: Concretion of Swan River sandstone on the Kettles Hills, south shore Swan Lake.

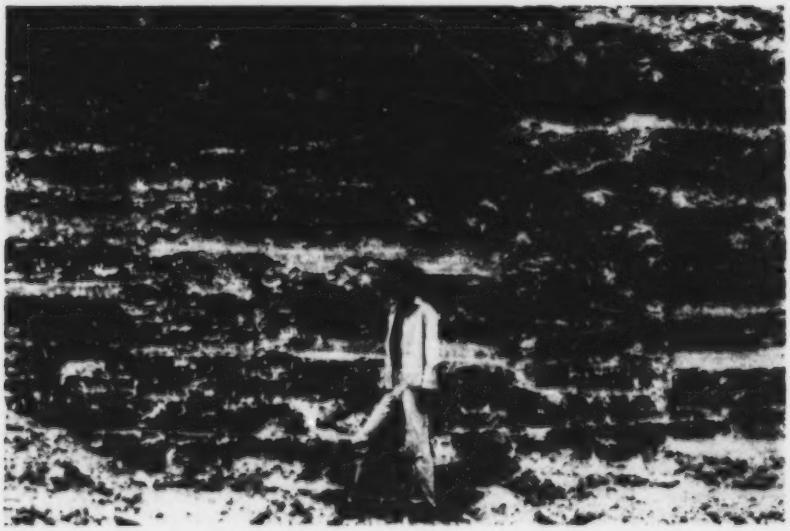

Figure 45: Black bentonitic shale of the Favel Formation outcropping along the Manitoba escarpment at site SL-83-84.

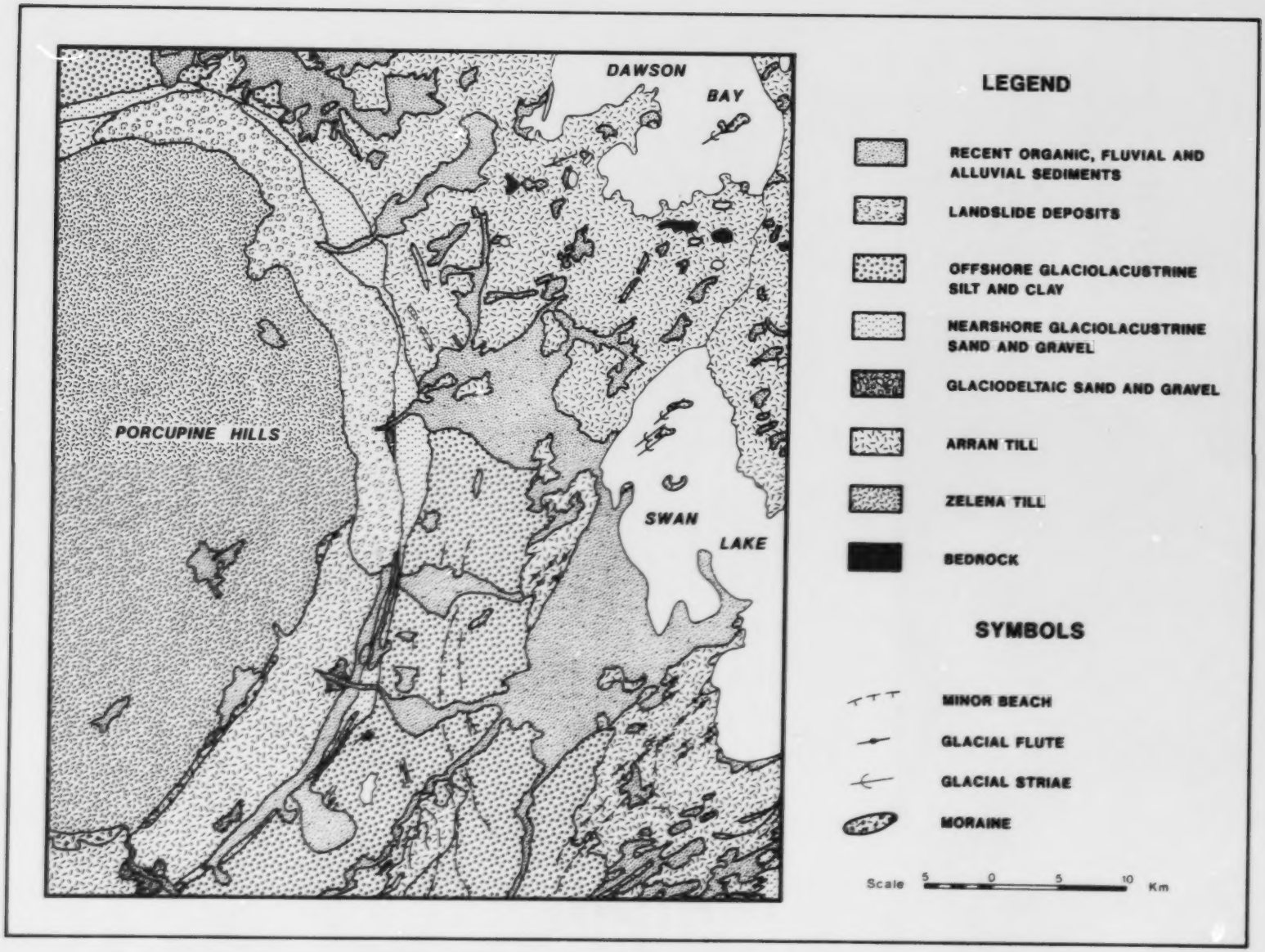

Figure 46: Surficial geology of the Swan Lake-Dawson Bay area. Modified from Nielsen, 1988 and unpublished information by M. Clarke.

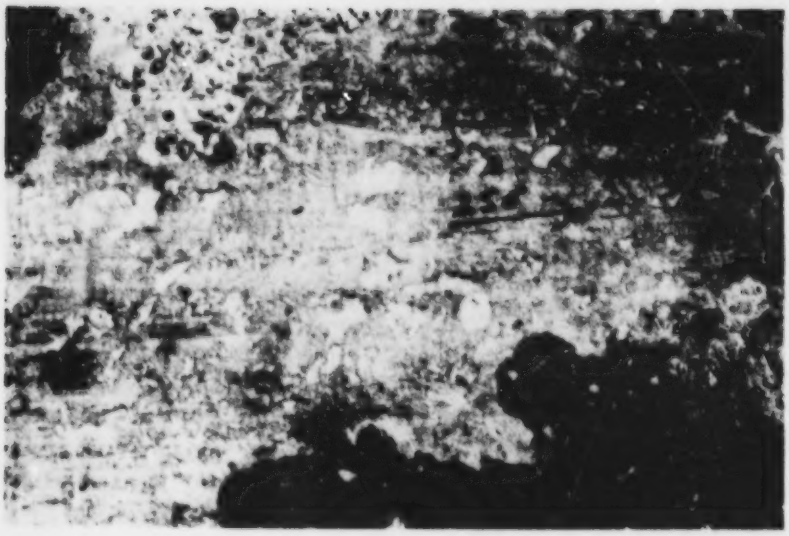

Figure 47: Striae associated with the Arran Till indicating ice flow toward 250° at site PR-85-15.

and on the flanks of Porcupine Hills. Arran Till overlies Zelena Till extensively along the escarpment. The final retreat of ice from the area was followed by incursion of Lake Agassiz and the deposition of extensive glaciolacustrine beach deposits along the escarpment and some finer textured sediments overlying the Arran Till in the Swan River Valley and west of Swan Lake. There is some evidence for iceberg activity in late glacial times. Landslides and fluvial and alluvial sedimentation continue in the area today.

The older till, Zelena Till and Arran Till are easily differentiated by their grain size, carbonate content and geochemistry which reflect the different source areas and ice flow histories. Late glacial and postglacial sediments have chemistries similar to the underlying tills. The chemistry of the sediments in this area do not suggest the presence of lead-zinc mineralization.

Table 5: Summary statistics for the geochemical data from the Swan Lake - Dawson Bay area.

Older till (n=5)	Cu (ppm)	Pb (ppm)	Zn (ppm)	Ni (ppm)	Co (ppm)	Cr (ppm)	Fe (ppm)	Mn (ppm)	Ba (ppm)	CO_3 (%)
Mean	48.8	14.0	154.0	37.0	11.0	63.2	39350.0	442.0	330.2	11.5
S.D.	6.3	3.4	10.8	7.0	4.4	6.6	5623.5	39.5	238.3	1.3
Max.	59.0	18.0	171.0	49.0	16.0	70.0	48500.0	482.0	726.0	13.4
Min.	43.0	9.0	143.0	32.0	6.0	54.0	33150.0	388.0	119.0	10.1

Zelena till (n=60)	Cu (ppm)	Pb (ppm)	Zn (ppm)	Ni (ppm)	Co (ppm)	Cr (ppm)	Fe (ppm)	Mn (ppm)	Ba (ppm)	CO_3 (%)
Mean	45.5	15.4	144.9	34.9	12.8	49.8	35545.0	621.6	258.4	20.6
S.D.	5.8	3.5	19.7	11.8	4.7	8.8	5736.8	366.9	75.2	2.7
Max.	68.0	22.0	225.0	77.0	23.0	82.0	57000.0	1930.0	561.0	27.1
Min.	36.0	9.0	100.0	20.0	2.0	34.0	27000.0	267.0	103.0	16.5

Arran till (n=127)	Cu (ppm)	Pb (ppm)	Zn (ppm)	Ni (ppm)	Co (ppm)	Cr (ppm)	Fe (ppm)	Mn (ppm)	Ba (ppm)	CO_3 (%)
Mean	37.4	7.5	96.2	49.2	13.7	62.9	22874.0	389.5	276.7	39.5
S.D.	6.1	4.6	18.0	8.5	3.3	11.5	7695.4	208.9	73.4	4.2
Max.	56.0	19.0	166.0	86.0	24.0	119.0	59500.0	2560.0	450.0	45.5
Min.	27.0	2.0	68.0	27.0	4.0	43.0	14000.0	250.0	132.0	23.1

Iceberg turbate (n=12)	Cu (ppm)	Pb (ppm)	Zn (ppm)	Ni (ppm)	Co (ppm)	Cr (ppm)	Fe (ppm)	Mn (ppm)	Ba (ppm)	CO_3 (%)
Mean	37.9	7.3	89.8	48.3	12.2	74.3	22391.7	339.5	338.6	35.8
S.D.	5.9	3.9	15.7	9.4	3.5	15.8	7061.3	94.1	75.5	6.6
Max.	46.0	13.0	133.0	71.0	20.0	104.0	39000.0	546.0	463.0	42.7
Min.	29.0	2.0	72.0	34.0	8.0	53.0	15100.0	248.0	205.0	22.0

Postglacial sediments (n=34)	Cu (ppm)	Pb (ppm)	Zn (ppm)	Ni (ppm)	Co (ppm)	Cr (ppm)	Fe (ppm)	Mn (ppm)	Ba (ppm)	CO_3 (%)
Mean	40.5	13.5	116.7	41.5	12.1	63.6	26933.8	394.1	309.8	22.6
S.D.	7.4	6.2	29.6	9.7	5.0	18.1	8565.7	174.8	150.4	11.0
Max.	61.0	26.0	165.0	61.0	31.0	98.0	55000.0	889.0	742.0	43.0
Min.	23.0	2.0	64.0	23.0	4.0	34.0	10550.0	167.0	104.0	4.0

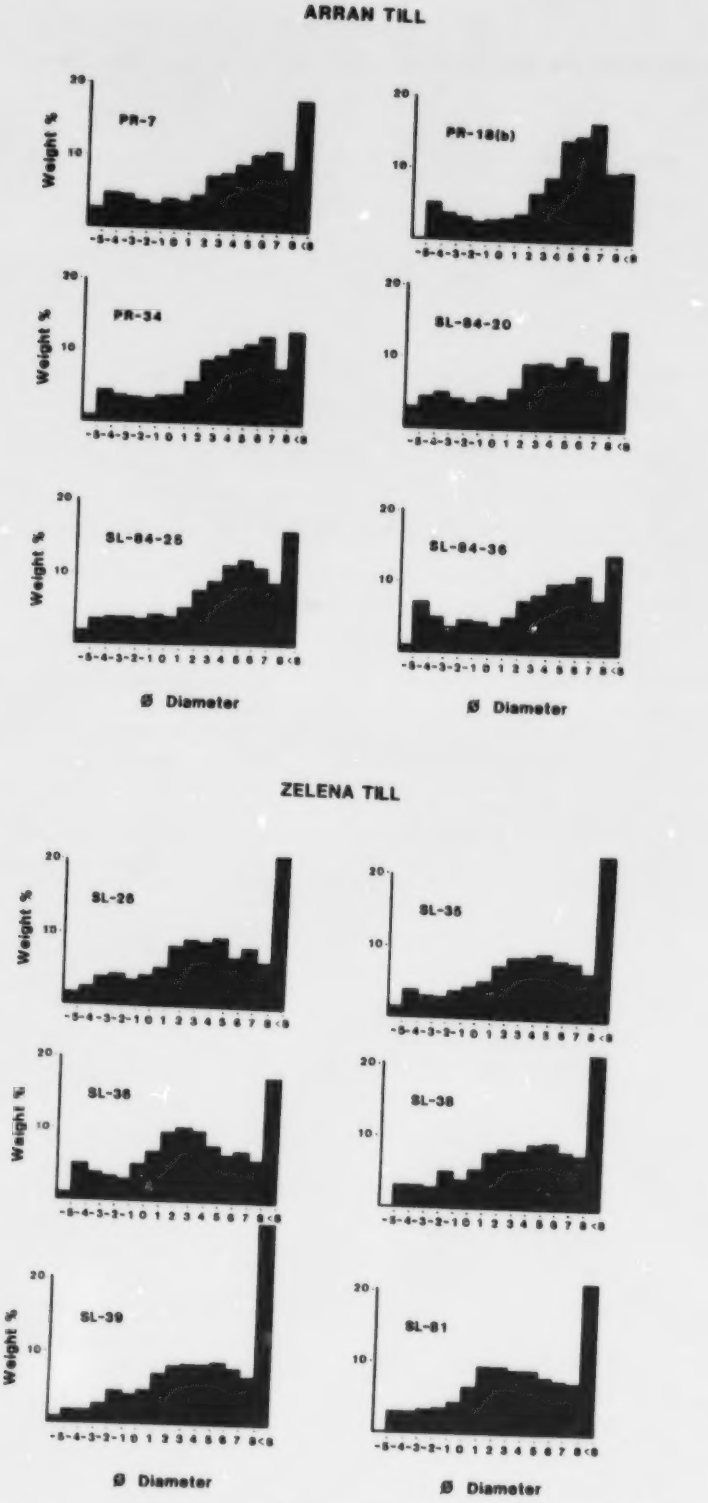

Figure 48: Histograms showing the grain size distribution of Zelena Till and Arran Till from the Swan Lake-Dawson Bay area.

Figure 49: Hummocky stagnation moraine composed of Zelena Till, 2 km west of Hart Mountain, Porcupine Hills.

Figure 50: Zelena Till (a) overlying deformed sand (b) in the hummocky stagnation moraine at site SL-83-33 on Porcupine Hills.

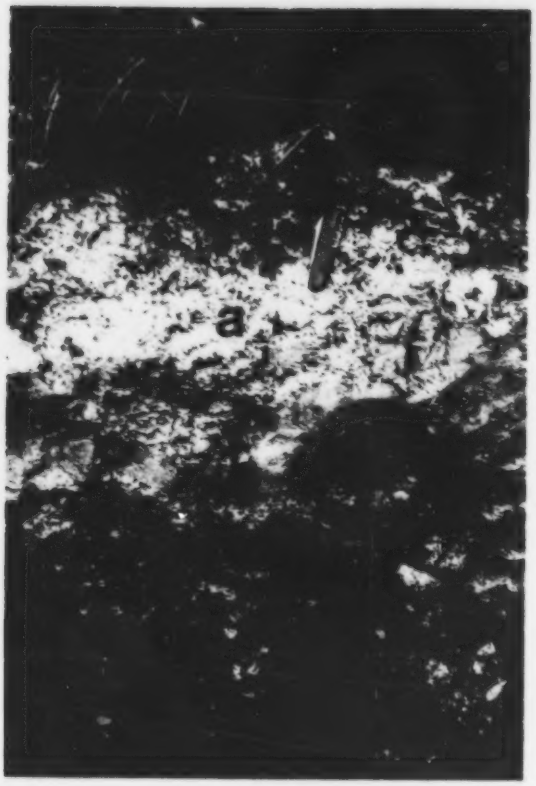

Figure 51: Fossiliferous sand and gravel (a) overlying Arran Till (b) at site PR-85-46.

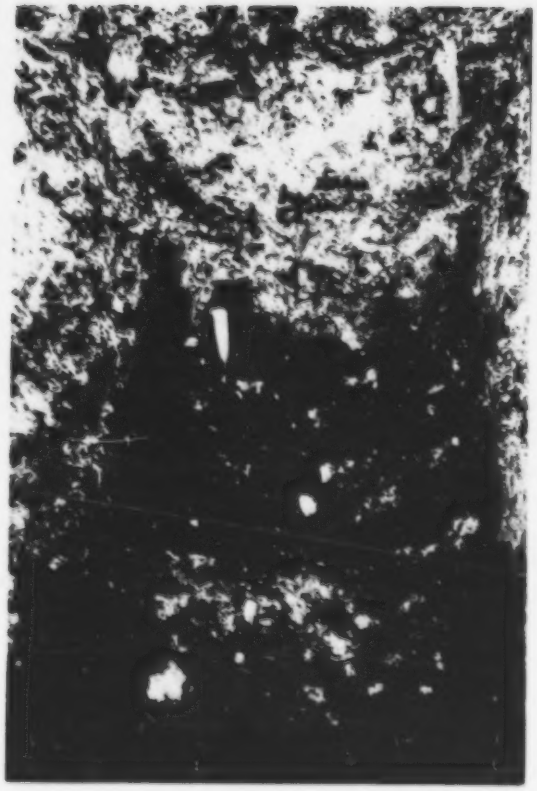

Figure 52: Slumped Arran Till (a) overlying glaciolacustrine clay (b) and Arran Till (c) at site SL-83-72.

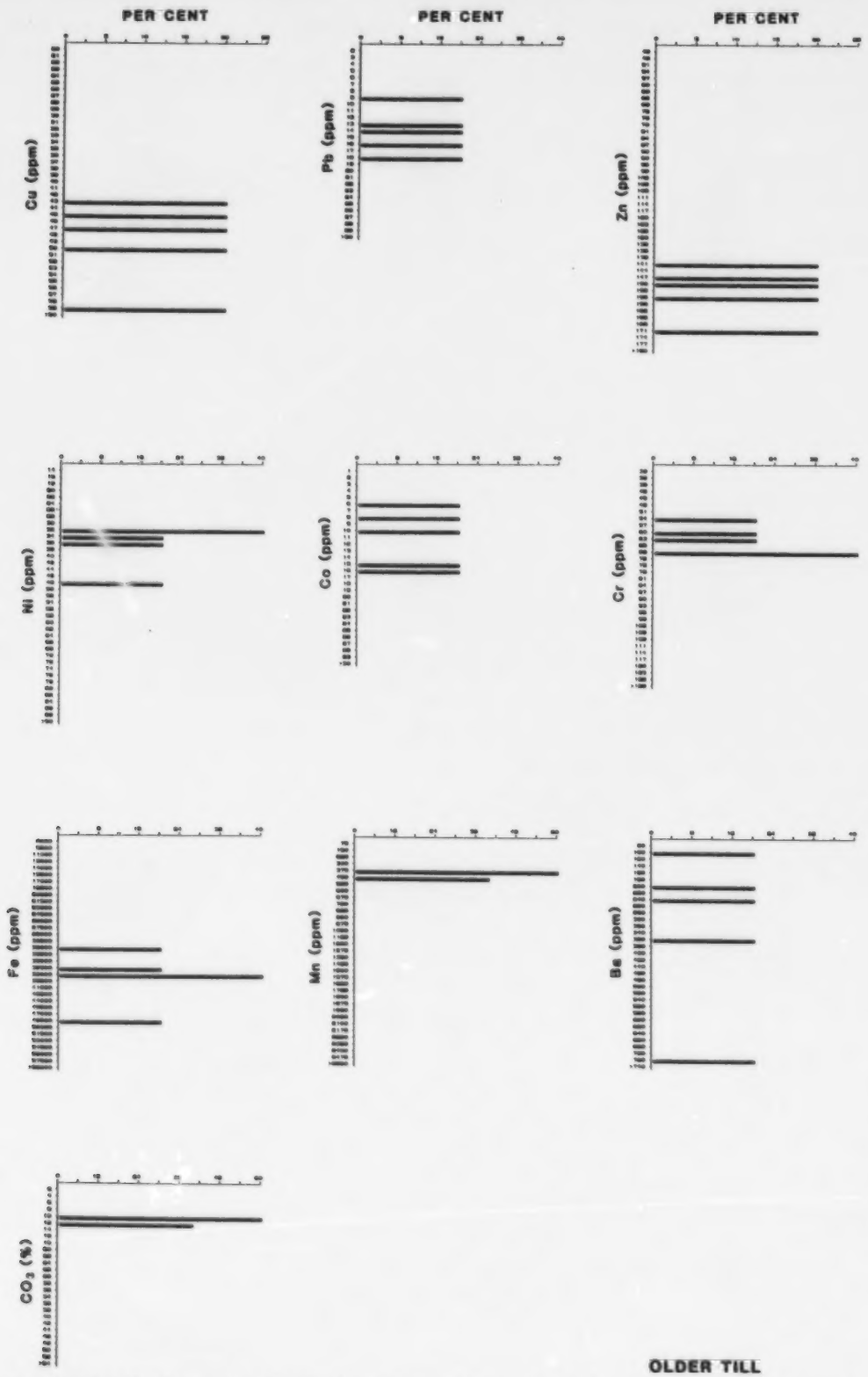

Figure 53: Histograms showing the frequency distribution of trace elements in the less than 2 micron fraction and CO_3 content of the less than 63 micron fraction of the Older till, Zelena Till, Arran Till, iceberg turbate and postglacial sediments.

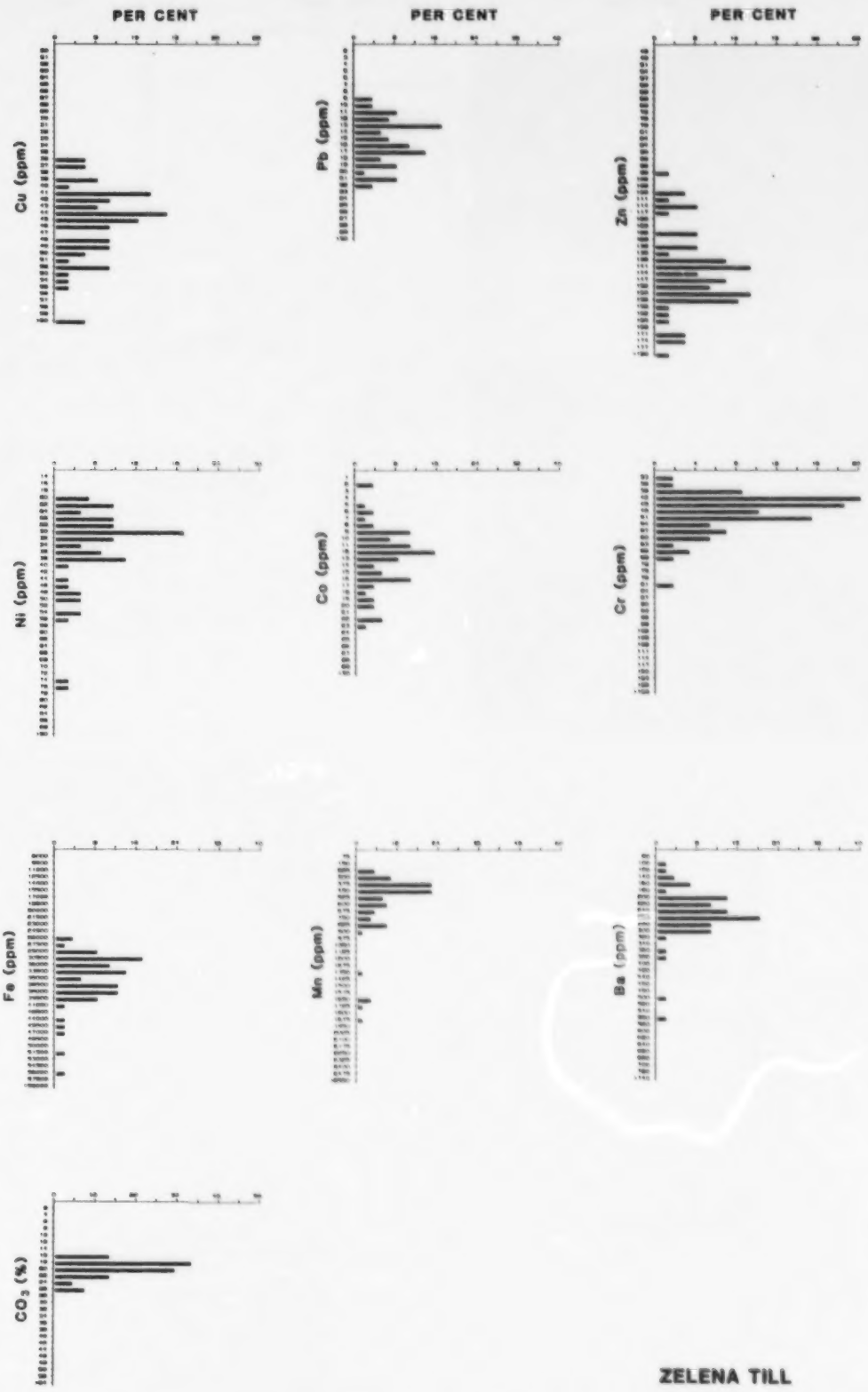

Figure 53: Continued.

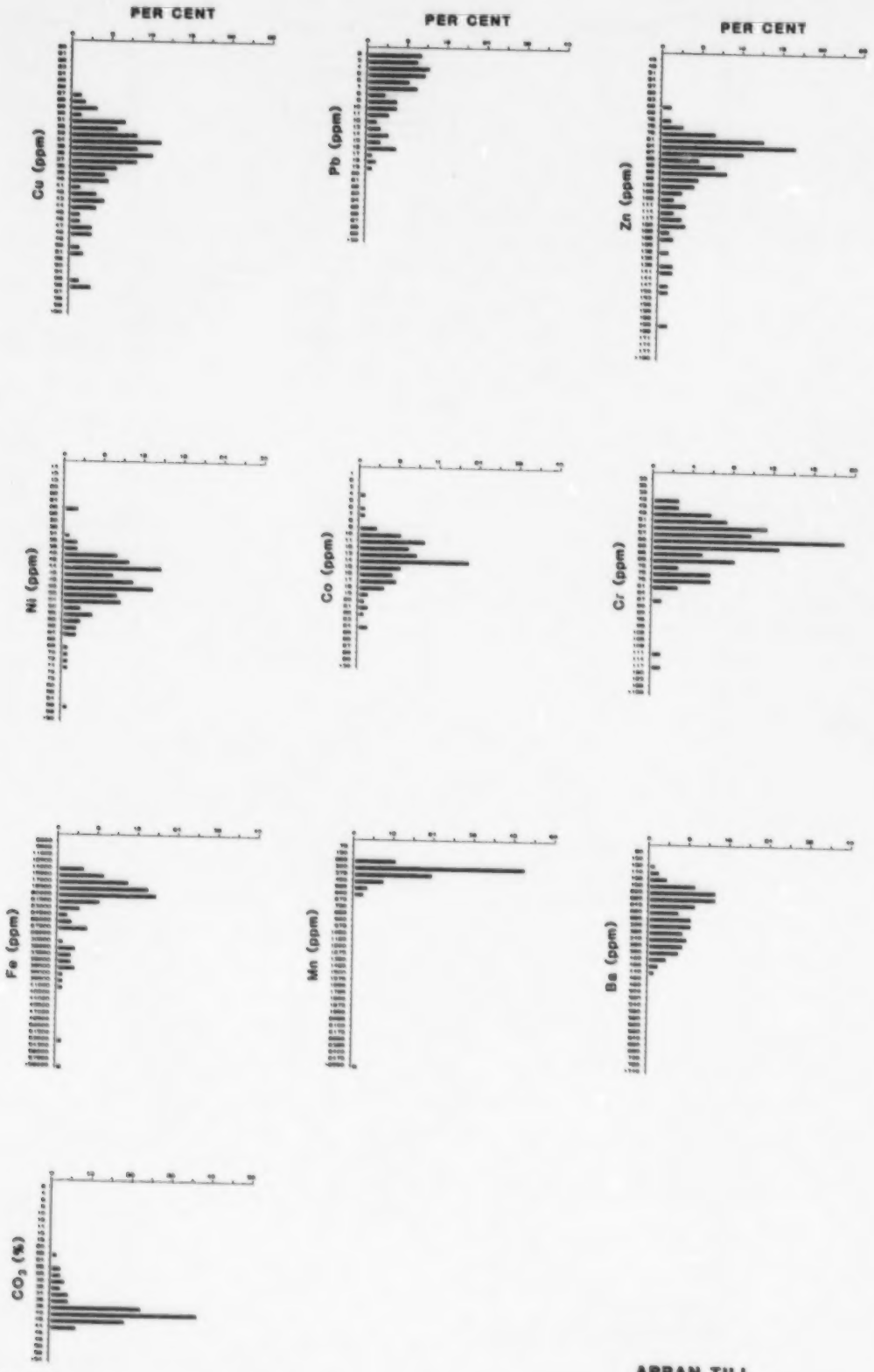

Figure 53: Continued.

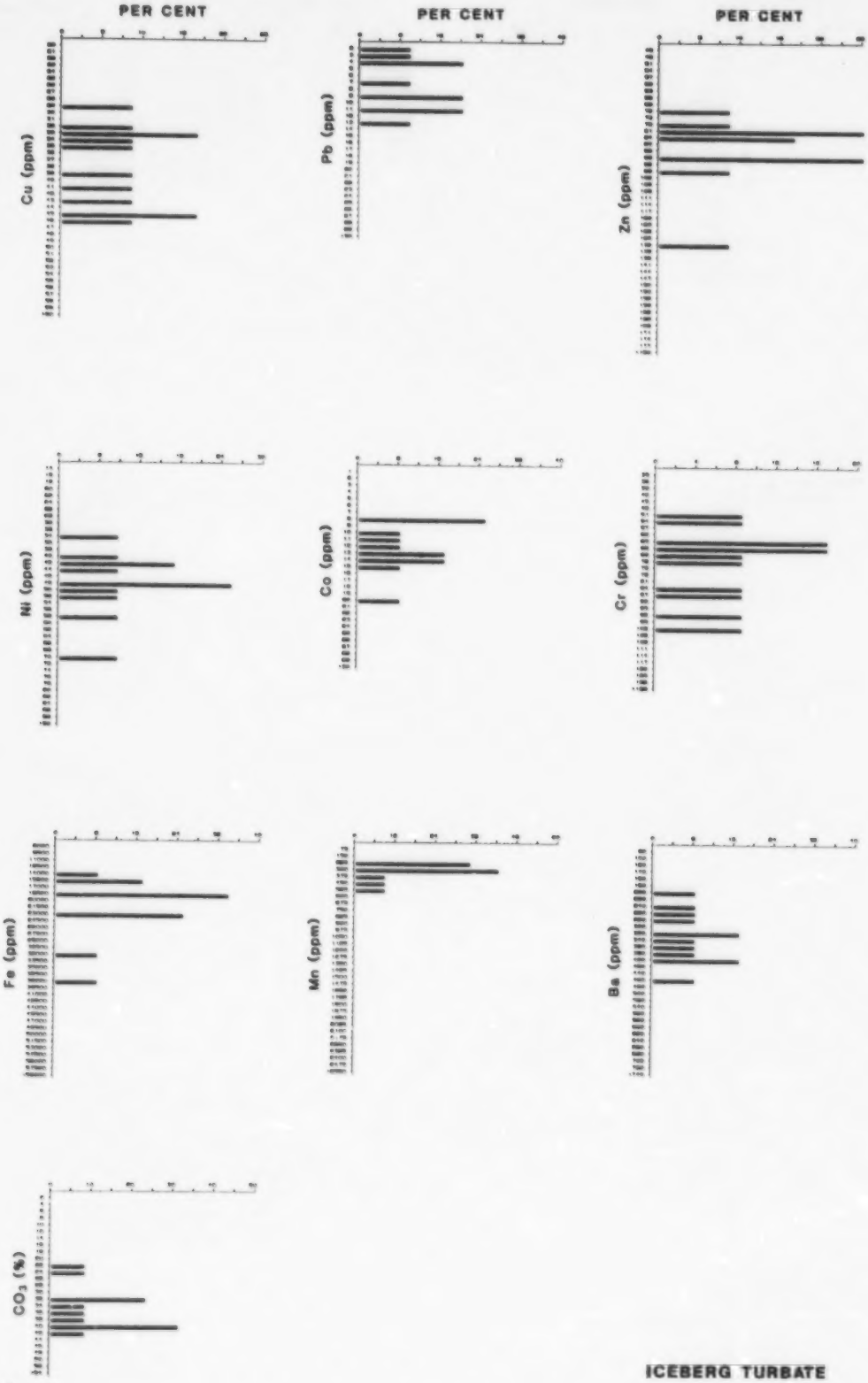

Figure 53: Continued.

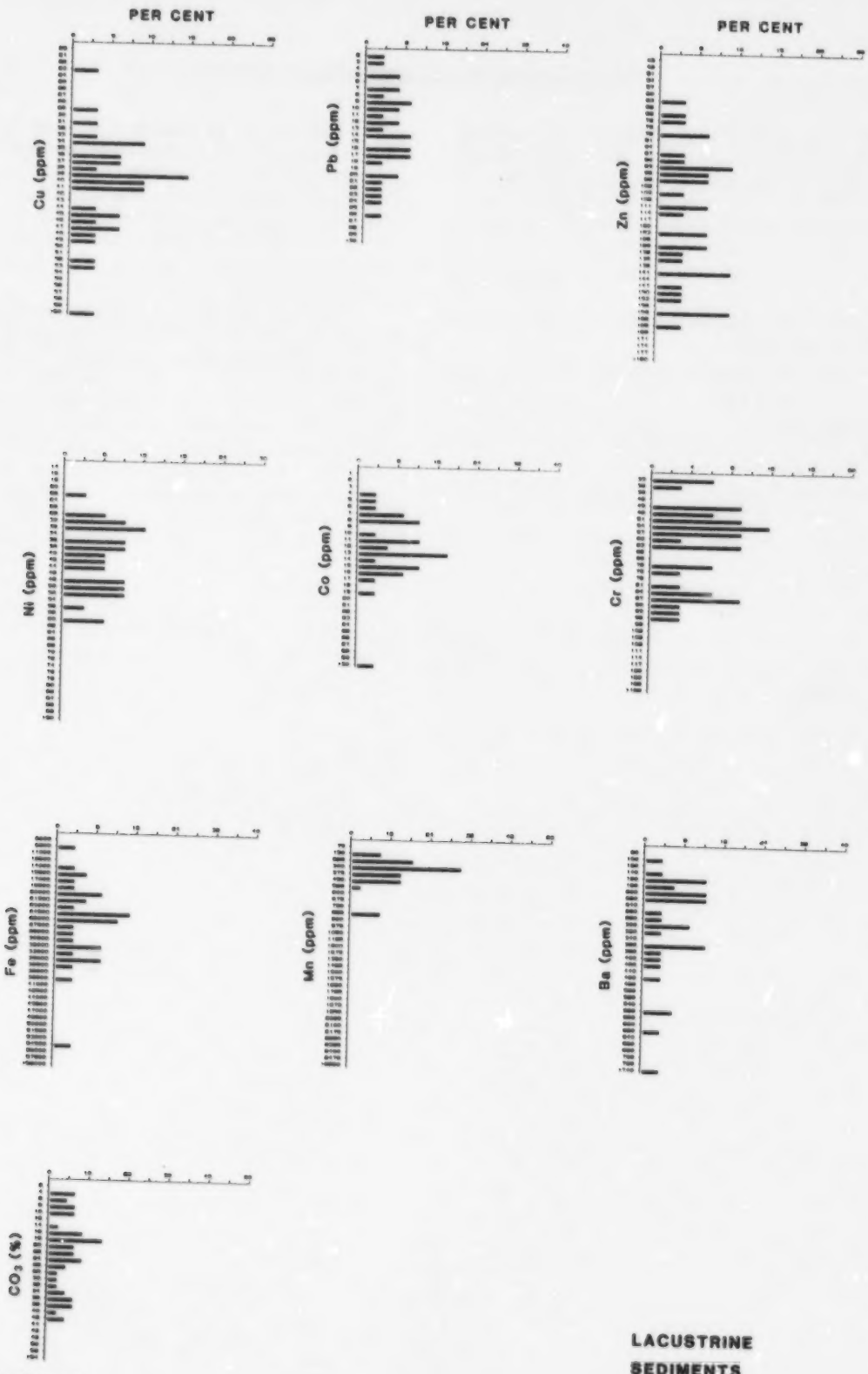

Figure 53: Continued.

CONCLUSIONS AND RECOMMENDATIONS

Detailed stratigraphic and geochemical investigations of the overburden in the Balmoral-Komarno, Moosehorn-Gypsumville and Swan Lake-Dawson Bay areas reveal evidence of a series of complex ice advances and retreats and glaciolacustrine sedimentation. The results can be summarized as follows:

1. Deposition of Zelena Till and Inwood till by southerly ice flow.
2. Glacier retreat and glaciolacustrine deposition in the Balmoral-Komarno area.
3. Surging of the ice margin toward the southeast and deposition of Komarno till.
4. Glacier retreat and incursion of Lake Agassiz accompanied by iceberg scouring to an elevation of at least 275 m in the southern Interlake.
5. Retreat of Komarno ice from the central Interlake and a drop in the level of Lake Agassiz.
6. Readvance of Arran lobe in the Swan Lake-Dawson Bay area to an unknown position in the Interlake.
7. Final glacier retreat from southern Manitoba and the incursion of Lake Agassiz.
8. The final regression of Lake Agassiz from southern Manitoba accompanied by deposition of beach and near shore deposits.

The major lithosomes identified in each of the three areas investigated may be characterized by their compaction, texture, pebble composition, structure and geochemical composition. The characteristics of the five tills, (older till, Zelena Till, Inwood till, Komarno till and Arran Till), can be related to provenance, ice flow direction, glacial transport and mode of deposition. Interregional correlations remain tenuous.

The geochemistry of the tills can in most cases be related to specific bedrock source areas. Precambrian bedrock generally gives the highest trace element concentrations followed by Devonian bedrock. Silurian carbonates have low trace element concentrations whereas Ordovician carbonates and shales have intermediate trace element concentrations. Contribution from the impact structure at Gypsumville and the Thompson nickel belt can also be recognized in the tills. No radically anomalous till samples were encountered during the study. A number of samples from the Balmoral-Komarno area may be considered marginally anomalous in lead concentrations. This is the general area of the Doan pebble discovery and although the source of the lead anomalies in the tills is unknown this remains the most lucrative area for further investigation.

ACKNOWLEDGEMENTS

I wish to thank Ron DiLabio of the Geological Survey of Canada for concentrating the clay-sized fraction of the Balmoral-Komarno samples and for the SEM photographs of the Inwood till. I am also indebted to George Gale of Manitoba Energy and Mines who suggested the project and with whom I have had many fruitful discussions. Martin Clark of the Geological Survey of Canada supplied the unpublished surficial geology map of the Dawson Bay area.

REFERENCES

Betcher, R.N.

1986: Groundwater availability map series, Selkirk area(62 I); Manitoba Natural Resources, Water Resources.

Clayton, L., Teller, J.T., and Attig, J.W.

1985: Surging of the southwestern part of the Laurentide Ice Sheet; Boreas, v. 14, p. 235-241.

DiLabio, R.N.W., Rencz, A.N., and Egginton, P.A.

1982: Biogeochemical expression of a classic dispersal train of metalliferous till near Hopetown, Ontario; Canadian Journal of Earth Sciences, v. 19, p 2297-2305.

Evans, D.S.

1976: Dawson Bay (63C/13, 14, 15); In Manitoba Mines Resources and Environmental Management, Mineral Resources Division, Report of Field Activities, 1976, p. 56-57.

Folk, R.M.

1968: Petrology of sedimentary rocks; Hemphill's University of Texas, Austin, Texas, 170 p.

Gale, G.H.

in prep: Trace element geochemistry of Cambro-Devonian rocks as a guide in the evaluation of base metal potential of the platform sequences in southern Manitoba.

Hughes, O.L.

1965: Surficial geology of part of the Cochrane district, Ontario, Canada; In International Studies on the Quaternary (H.E. Wright Jr. and D.G. Frey ed.), Geological Society of America, Special Paper 84, p. 535-565.

Hochheim, K.P.

1982: Iceberg gouging in the Lake Agassiz basin;University of Winnipeg, B.A. Thesis (unpublished), 91 p.

Klassen, R.W.

1979: Pleistocene geology and geomorphology of the Riding Mountain and Duck Mountain areas, Manitoba-Saskatchewan; Geological Survey of Canada, Memoir 396, 52 p.

Klassen, R.A. and Shilts, W.W.

1977: Glacial dispersal of uranium: District of Keewatin, Canada; in Prospecting in areas of glaciated terrain, 1977; Institution of Mining and Metallurgy, London, England, p. 80-88.

Lien, R.

1986: An iceberg scouring model; a remedy for survey planning, data interpretation and technical evaluations; Proceedings of the Fifth International Offshore Mechanics and Arctic Engineering Symposium, vol. IV, p. 113-119.

Manitoba Mineral Resources Division

1979: Geological Map of Manitoba; Manitoba Mines, Natural Resources and Environment, Geological Map 79-2, 1:1 000 000.

McCabe, H.R.

1969: An occurrence of galena in float - Winnipeg area; In Manitoba Mines and Natural Resources, Summary of Geological Fieldwork, 1969, Geological Paper 4/69, p. 125.

McCabe, H.R., and Bannatyne, B.B.

1970: Lake St. Martin crypto-explosion crater and geology of the surrounding area; Manitoba Mines and Natural Resources, Mines Branch, Geological Paper 3/70, 70 p.

McCabe, H.R., and Barchyn, D.

1982: Paleozoic stratigraphy of southwestern Manitoba; Geological Association of Canada-Mineralogical Association of Canada, Field Trip Guidebook, Trip 10, 47 p.

McNeil, D.H., and Caldwell, W.G.E.

1981: Cretaceous rocks and their foraminifera in the Manitoba escarpment; Geological Association of Canada, Special Paper Number 21, 439 p.

Moran, S.R.

1969: Geology of the Hudson Bay area, Saskatchewan; University of Illinois, Ph.D. Thesis (unpublished), 190 p.

Nielsen, E.

1988: Surficial geology of the Swan River area; Manitoba Energy and Mines, Geological Report GR80-7, 51 p.

Nielsen, E., and Groom, H.D.

1989: Trace element geochemistry and till provenance in The Pas-Flin Flon area, Manitoba; Manitoba Energy and Mines, Geological Services Open File Report OF89-3, 20 p.

Nielsen, E. and Matile, G.

1982a: Till stratigraphy and proglacial lacustrine deposits in the Winnipeg area; Geological Association of Canada-Mineralogical Association of Canada, Field Trip Guidebook, Trip 1, 22 p.

1982b: Quaternary geology of the Gypsumville area; Manitoba Energy and Mines, Aggregate Resource Map AR84-3, 1:100 000.

Norris, A.W., Uyeno, T.T. and McCabe, H.R.

1982: Devonian rocks of the Lake Winnipegosis-Lake Manitoba outcrop belt, Manitoba; Geological Survey of Canada, Memoir 392, 280 p., and Manitoba Energy and Mines, Mineral Resources Division, Publication 77-1, 280 p.

Pratt, L.E., Ehrlich, W.A., Leclaire, F.P. and Barr, J.A.

1961: Report of the Detailed Reconnaissance Soil Survey of Fisher and Teulon map sheet areas; Manitoba Soil Survey, Report #12, 80 p.

Shilts, W.W.

1975: Principles of geochemical exploration for sulphide deposits using shallow samples of glacial drift; Canadian Institute of Mining and Metallurgy Bulletin, v. 68, p. 73-80.

1976: Mineral exploration and till; In Glacial till (R. F. Legget, ed.), Royal Society of Canada, Special Publication 12, p. 205-224.

1977: Geochemistry of till in perennially frozen terrain of the Canadian Shield, application to prospecting; Boreas, v. 5, p. 203-212.

1984: Till geochemistry in Finland and Canada; Journal of Geochemical Exploration, v. 21, p. 95-117.

Wardlaw, N.C., Stauffer, M.R. and Hoque, M.

1969: Striations, giant grooves and superposed drag folds, Interlake area, Manitoba; Canadian Journal of Earth Sciences, 6, p. 577-593.

Wickenden, R.T.D.

1945: Mesozoic stratigraphy of the eastern plains, Manitoba and Saskatchewan; Geological Survey of Canada, Memoir 239, 87 p.

Appendix I: Results of geochemical analysis on samples from the Balmoral - Komarno Area.

Inwood Till

Sample Number	Cu (ppm)	Pb (ppm)	Zn (ppm)	Ni (ppm)	Co (ppm)	Cr (ppm)	Fe (ppm)	Mn (ppm)	Ba (ppm)	CO_3 (%)
82-SH- 1	30	7	68	37	10	50	11100	260	195	36.3
82-SH- 2	28	8	64	32	11	46	10000	260	195	39.3
82-SH- 3	31	6	68	35	10	53	11100	290	190	39.1
82-SH- 4	28	7	70	36	11	56	11350	240	210	40.1
82-SH- 5	32	6	73	37	12	52	11500	255	220	40.3
82-SH- 6	29	7	69	36	11	52	10900	245	210	40.8
82-SH- 7 b	30	8	66	36	12	49	10400	250	205	37.5
82-SH- 8 b	28	8	63	32	10	48	10200	255	195	40.1
82-SH- 9	30	9	67	34	11	50	10350	275	200	38.0
82-SH-10	30	7	71	37	12	56	10350	255	210	39.4
82-SH-11 b	30	8	68	34	10	50	10200	245	195	38.7
82-SH-12 b	28	7	61	32	11	49	10000	260	185	36.4
82-SH-13 b	29	7	65	34	9	46	10500	255	200	35.5
82-SH-14 b	33	8	70	35	10	49	11500	260	210	39.6
82-SH-15 b	29	10	65	32	10	43	9950	265	205	33.6
82-SH-16 b	41	12	106	51	15	69	18800	380	255	36.6
82-SH-17 b	28	7	64	32	10	48	10400	255	195	37.8
82-SH-18 b	34	6	75	48	12	63	16500	385	220	37.8
82-SH-19	36	5	69	48	10	69	16000	375	205	39.2
82-SH-20	29	6	68	36	10	49	14500	385	185	36.6
82-SH-21 b	32	7	70	42	12	59	16550	340	250	38.3
82-SH-22	20	5	61	33	8	45	13000	340	180	36.2
82-SH-24	31	7	78	35	10	57	16700	345	220	35.9
82-SH-25 b	35	8	89	44	13	63	18950	405	300	34.7
82-SH-26 b	25	7	59	31	9	40	14250	350	215	36.1
82-SH-27 b	33	8	87	42	10	66	19450	365	325	28.3
82-SH-29	28	7	70	31	9	48	14050	405	220	33.3
82-SH-30	26	7	61	29	7	41	13650	350	205	39.9
82-SH-31	37	6	75	39	10	57	15150	370	215	34.5
82-SH-32	33	7	72	32	9	48	15000	350	190	38.0
82-SH-33 b	34	7	68	33	9	53	15150	355	200	39.6
82-SH-34	26	5	55	27	7	41	12400	340	200	36.1
82-SH-35	33	7	66	37	10	57	15200	375	220	37.5
82-SH-36 b	30	7	60	34	10	53	13700	380	215	38.9
82-SH-37 b	32	6	66	32	9	50	14650	350	210	38.5
82-SH-38 b	30	6	62	29	8	41	13250	390	185	32.1
82-SH-39 b	38	7	65	39	10	56	15600	355	230	37.8
82-SH-40	30	7	62	31	7	43	13600	340	185	38.7
82-SH-41	29	6	64	31	9	42	14500	370	200	38.9
82-SH-42 b	28	7	58	28	8	42	12750	360	190	38.2
82-SH-43 b	32	6	63	33	9	51	14250	335	190	39.2
82-SH-44	39	8	67	45	11	64	16900	380	220	38.0
82-SH-45 b	31	6	64	37	8	53	17750	365	185	34.2
82-SH-46	35	7	85	42	12	63	18000	410	240	40.8
82-SH-47 b	29	6	60	30	8	41	13750	365	210	39.2
82-SH-48 b	29	6	63	32	9	43	14600	400	245	39.2
82-SH-49	28	7	65	31	8	53	14250	350	200	39.2
82-SH-50	30	6	67	32	8	48	15000	380	205	39.9
82-SH-51 b	27	6	60	30	9	41	13400	360	200	40.1
82-SH-52 b	28	7	65	31	8	55	13250	360	205	38.7
82-SH-53 b	30	8	67	34	10	58	15000	380	215	39.0
82-SH-54	28	7	62	32	9	51	14250	385	220	39.0
82-SH-55	28	7	62	31	9	54	14400	360	200	38.0
82-SH-56	28	7	60	31	8	51	13700	355	145	40.4
82-SH-57 b	28	6	59	30	8	45	13750	355	200	39.6

Sample Number	Cu (ppm)	Pb (ppm)	Zn (ppm)	Ni (ppm)	Co (ppm)	Cr (ppm)	Fe (ppm)	Mn (ppm)	Ba (ppm)	CO_3 (%)
82-SH-58	26	5	56	31	8	50	13850	330	185	38.2
82-SH-59	23	6	56	31	7	54	12800	350	190	38.0
82-SH-60	25	5	58	30	7	43	12600	345	200	41.3
82-SH-61 b	26	5	65	31	8	80	13800	365	205	38.2
IBO - 1	30	8	65	26	11	60	15350	396	200	40.8
IBO - 2	28	7	63	23	8	56	13300	361	185	41.7
IBO - 3	29	8	68	26	9	60	14500	373	205	42.9
IBO - 4 b	26	8	65	25	8	58	13650	356	175	43.4
IBO - 5	29	17	67	29	10	55	11100	313	274	40.8
IBO - 6 b	24	9	55	22	10	50	11950	380	155	41.4
IBO - 7	28	16	64	27	11	45	10100	327	272	40.1
IBO - 8 b	24	9	67	25	13	56	15250	406	200	41.7
IBO -12 b	37	8	74	35	11	79	17900	415	215	39.7
IBO -13	28	8	64	28	11	60	15000	368	195	40.4
IBO -15	38	7	71	36	12	71	17650	412	215	40.4
IBO -16 b	34	7	68	29	11	56	15300	386	185	42.6
IBO -20 b	30	7	62	27	10	56	13750	381	190	38.0
IBO -21 b	30	7	64	27	9	53	14000	332	195	42.1
IBO -23 b	28	20	67	26	10	50	11750	329	239	42.3
IBO -24 b	29	9	60	25	9	56	13450	337	200	42.3
IBO -26 b	28	6	62	26	9	50	13700	362	180	43.6
IBO -27 b	31	15	67	28	11	50	10850	320	205	41.8
IBO -28 b	32	6	65	30	10	54	15150	387	190	42.9
IBO -29 b	42	17	69	42	12	134	10200	317	198	37.7
IBO -30 b	26	6	57	26	11	48	13400	418	130	42.3
IBO -31 b	34	22	71	30	12	52	12350	336	233	41.1
IBO -35	30	15	68	31	12	50	11600	299	234	41.4
IBO -38	34	7	70	40	11	69	18000	432	200	38.1
IBO -39	33	14	72	32	13	61	13250	322	266	38.9
IBO -40 a	31	6	67	33	10	62	16100	477	210	38.9
IBO -40 b	29	6	64	37	11	68	14500	398	190	38.2
IBO -41	36	8	72	40	12	73	17500	400	191	38.2
IBO -42	36	12	74	33	12	57	13300	327	230	38.6
IBO -43	32	8	66	34	11	60	16300	405	175	36.8
IBO -44	35	15	74	35	13	58	13500	324	232	38.2
IBO -45	28	7	70	34	12	62	17900	413	185	38.2
IBO -50	33	7	70	37	13	64	18150	423	195	34.8
IBO -51 b	32	8	69	31	11	56	16000	370	210	41.4
IBO -52	38	7	72	44	13	81	20500	405	220	37.0
IBO -53	29	9	69	34	11	60	15200	394	210	34.1
IBO -54 b	33	12	72	33	13	51	12150	349	255	39.4
IBO -55 c	34	9	64	30	10	56	15000	370	180	38.2
IBO -57 b	40	11	78	36	11	60	18750	424	190	39.2
IBO -60 b	27	8	61	30	10	56	15000	395	185	42.3
KO - 1 b	29	10	66	35	10	63	14950	406	210	39.2
KO - 2 b	26	8	60	30	9	62	13750	356	180	40.5
KO - 3 b	34	9	67	40	10	73	15950	403	325	37.5
KO - 4 b	25	8	58	28	9	62	13800	415	155	40.6
KO - 5 b	28	5	60	25	8	62	13250	332	185	43.2
KO - 6 b	26	8	57	30	10	53	13500	402	155	44.2
KO - 7 b	42	10	64	31	9	59	15000	373	195	43.4
KO - 8 c	30	10	63	32	9	59	14850	407	195	42.3
KO - 9 b	29	8	61	34	9	63	15100	398	160	42.0
KO -10 b	29	8	60	31	9	55	14150	370	165	43.0
KO -11 b	25	9	59	29	11	55	14100	400	165	42.8
KO -12 b	24	8	57	28	7	53	12500	365	165	44.2
KO -13 b	23	8	49	24	8	51	11750	505	155	42.2

Sample Number	Cu (ppm)	Pb (ppm)	Zn (ppm)	Ni (ppm)	Co (ppm)	Cr (ppm)	Fe (ppm)	Mn (ppm)	Ba (ppm)	CO_3 (%)
KO -14 b	28	9	65	35	10	62	14750	473	190	40.1
KO -15 b	26	6	57	32	9	53	13350	392	170	41.5
KO -16 b	28	5	64	34	11	57	14000	406	185	41.5
KO -17 b	26	5	61	34	10	71	13950	367	165	41.2
KO -18 b	30	5	63	35	11	62	15250	371	175	42.0
KO -19 b	24	5	56	28	8	53	13300	342	145	43.2
KO -20 b	26	7	56	27	9	53	13250	345	130	41.6
KO -21 b	30	7	63	35	10	65	14750	400	165	41.1
KO -22 b	26	7	59	29	9	57	13300	360	155	37.4
KO -23 b	32	8	65	36	10	62	15000	398	165	40.2
KO -24 b	28	8	56	31	9	59	13100	362	145	43.7
KO -25 b	28	8	59	34	10	62	14300	390	165	40.4
KO -26	30	8	63	34	10	59	14900	384	165	41.3
KO -27 b	26	9	57	28	9	55	13200	367	170	41.1
KO -28 b	30	9	63	35	11	63	15500	405	165	39.5
KO -29	27	8	58	31	10	63	14850	370	165	40.2
KO -30 b	30	8	58	33	8	63	15450	356	165	39.5
KO -32 b	27	5	59	24	8	54	14150	350	170	40.6
KO -33 b	22	5	53	25	8	48	12750	342	155	40.9
KO -34 b	28	6	70	34	11	66	16400	415	185	39.7
KO -35 b	24	6	58	24	8	56	13800	304	155	39.2
KO -36 b	25	6	65	28	9	58	14000	346	240	41.6
KO -37 b	24	5	54	24	8	53	13450	378	155	42.3
KO -38 b	24	7	61	24	9	53	13500	372	195	39.7
KO -39 b	25	8	55	25	8	50	13300	378	160	41.8
KO -40 b	30	7	68	34	10	64	16300	371	195	40.6
KO -41	30	9	74	35	11	66	17500	437	195	37.2
KO -42 b	23	7	52	24	8	48	13500	346	150	42.8
KO -43 b	26	8	67	30	10	64	15250	390	190	39.0
KO -44 c	25	6	59	32	11	66	14450	425	190	41.4

Komarno Till

Sample Number	Cu (ppm)	Pb (ppm)	Zn (ppm)	Ni (ppm)	Co (ppm)	Cr (ppm)	Fe (ppm)	Mn (ppm)	Ba (ppm)	CO_3 (%)
82-SH- 8 a	28	9	64	30	11	50	10000	245	190	39.4
82-SH-11 a	26	8	58	33	12	48	9200	265	190	42.8
82-SH-12 a	31	7	63	34	12	53	11150	255	200	38.0
82-SH-13 a	28	8	57	32	11	47	9650	255	210	38.9
82-SH-14 a	31	8	57	33	12	39	9850	305	200	38.5
82-SH-36 a	27	7	54	29	9	42	12400	360	215	38.7
IBO - 4 a	27	8	65	28	10	64	15000	392	205	40.2
IBO - 6 a	31	11	64	26	10	60	14650	368	185	42.2
IBO - 8 a	41	10	82	34	13	73	19300	394	230	41.3
IBO - 9	28	8	73	32	12	75	16400	413	215	38.0
IBO -10	27	8	64	26	11	58	14200	411	195	38.2
IBO -12 a	35	9	86	40	12	77	20000	380	215	39.2
IBO -14 a	38	8	75	41	12	87	19850	348	225	40.6
IBO -16 a	37	7	73	30	11	69	17000	368	195	36.3
IBO -17 a	32	8	69	28	11	60	15000	384	205	41.4
IBO -20 a	32	8	68	32	10	64	15600	340	190	37.5
IBO -21 a	36	6	69	36	11	69	17600	352	250	39.4
IBO -22	39	7	72	40	13	75	18750	415	205	37.5
IBO -23 a	36	9	72	32	10	62	17300	408	215	38.2
IBO -24 a	31	16	75	38	14	62	14150	346	273	38.4
IBO -25 a	37	9	82	40	13	73	21400	419	255	36.4

Sample Number	Cu (ppm)	Pb (ppm)	Zn (ppm)	Ni (ppm)	Co (ppm)	Cr (ppm)	Fe (ppm)	Mn (ppm)	Ba (ppm)	CO_3 (%)
IBO -26 a	30	7	67	33	11	66	16500	379	225	37.0
IBO -27 a	29	12	70	31	11	55	13200	340	231	38.8
IBO -28 a	28	9	90	43	13	75	21500	395	215	34.0
IBO -31 a	39	17	88	38	13	63	16550	349	253	38.8
IBO -32	36	10	88	43	14	77	21200	478	245	37.7
IBO -33	36	7	83	45	12	75	20000	414	205	38.8l
IBO -34	31	17	78	35	15	55	12350	372	229	37.4
IBO -36	60	27	129	61	23	53	13750	354	217	40.9
IBO -46 b	22	8	65	30	10	53	15800	400	175	40.7
IBO -47 a	28	8	89	43	15	75	24000	420	220	37.0
IBO -49 a	38	7	76	42	12	71	18750	419	205	40.3
IBO -54 a	29	8	75	45	13	77	18000	435	240	40.8
IBO -57 a	42	9	80	44	13	79	21000	374	240	38.5
IBO -58 b	34	11	76	38	14	66	16500	381	185	39.2
IBO -59	36	11	85	39	12	73	23000	357	245	38.7
IBO -60 a	36	9	74	39	12	69	19100	395	225	39.2
IBO -61	37	10	77	42	12	73	20000	445	230	39.0
KO - 6 a	27	6	48	30	9	53	13200	415	155	41.1
KO - 9 a	28	10	57	29	9	53	13900	346	165	42.3
KO -11 a	26	8	63	31	10	57	14900	400	175	43.2
KO -13 c	27	8	54	30	9	56	13750	375	155	43.4
KO -18 a	31	6	67	37	12	65	16050	421	175	41.5
KO -20 a	24	6	55	27	9	49	13100	375	145	40.4
KO -34 a	29	6	62	27	11	64	15000	386	180	38.7
KO -42 a	25	7	52	24	10	50	13100	386	155	41.6

Glaciolacustrine Sediments

Sample Number	Cu (ppm)	Pb (ppm)	Zn (ppm)	Ni (ppm)	Co (ppm)	Cr (ppm)	Fe (ppm)	Mn (ppm)	Ba (ppm)	CO_3 (%)
82-SH-28	41	12	108	52	13	74	31500	450	375	29.0
82-SH-48 a	30	6	58	30	7	43	11500	295	305	31.5
IBO -37 a	31	13	74	37	13	59	12950	317	257	37.5
IBO -58 a	65	17	125	63	22	117	53000	636	190	36.8
KO -13 a	42	13	121	53	16	98	37590	565	280	20.7
KO -38 a	38	10	96	43	14	93	35000	355	210	32.5
KO -44 a	35	11	103	42	15	83	31500	399	245	22.8

Drift-ice Turbate

Sample Number	Cu (ppm)	Pb (ppm)	Zn (ppm)	Ni (ppm)	Co (ppm)	Cr (ppm)	Fe (ppm)	Mn (ppm)	Ba (ppm)	CO_3 (%)
82-SH- 7 a	31	8	82	45	13	64	15200	255	245	37.7
82-SH-15 a	31	10	82	43	11	57	13700	290	250	36.2
82-SH-16 a	43	13	100	52	18	69	19250	415	310	30.3
82-SH-17 a	31	8	60	33	12	46	10000	275	245	38.0
82-SH-18 a	29	8	60	34	10	44	9900	215	270	37.8
82-SH-21 a	32	6	63	43	10	50	14750	380	210	39.2
82-SH-23 a	37	10	94	53	15	68	22400	450	250	32.7
82-SH-25 a	37	10	82	41	10	64	17100	315	315	35.9
82-SH-26 a	29	8	64	37	10	50	15000	415	390	32.8
82-SH-27 a	31	8	74	40	10	56	16300	385	325	31.7
82-SH-33 a	42	9	95	44	13	68	22900	400	220	39.2
82-SH-37 a	32	7	63	33	9	51	15300	350	210	36.8
82-SH-38 a	30	6	61	32	10	45	14150	485	230	40.4

Sample Number	Cu (ppm)	Pb (ppm)	Zn (ppm)	Ni (ppm)	Co (ppm)	Cr (ppm)	Fe (ppm)	Mn (ppm)	Ba (ppm)	CO_3 (%)
82-SH-39 a	40	7	75	42	10	59	19350	330	225	35.9
82-SH-42 a	33	5	62	32	10	41	14100	405	215	34.2
82-SH-43 a	37	7	74	35	10	60	18400	285	275	34.9
82-SH-45 a	29	6	55	33	8	45	17750	335	225	38.2
82-SH-47 a	25	7	52	30	7	42	13000	355	255	36.6
82-SH-51 a	40	12	90	52	12	73	23400	345	275	41.1
82-SH-52 a	37	8	74	37	8	58	16750	260	300	38.7
82-SH-53 a	43	11	100	50	13	74	31000	365	295	37.1
82-SH-57 a	38	10	88	43	15	64	23100	385	255	30.5
82-SH-61 a	44	12	118	58	18	46	37500	425	305	32.4
IBO -11	31	9	83	36	12	71	17500	420	230	37.7
IBO -14 b	33	8	67	31	11	62	16300	407	225	40.4
IBO -17 b	37	8	82	49	12	77	19800	367	215	37.7
IBO -18	38	8	78	45	12	81	18000	407	225	37.3
IBO -19	36	7	70	36	11	71	16950	350	195	38.7
IBO -29 a	39	10	88	43	14	71	17850	307	186	36.5
IBO -37 b	27	6	60	27	11	50	14000	370	185	41.9
IBO -46 a	33	8	76	39	12	71	21350	380	240	39.6
IBO -47 b	24	9	80	40	14	71	20000	410	210	38.9
IBO -48	32	7	72	38	13	71	19050	384	210	38.9
IBO -49 b	29	8	70	33	11	58	15000	366	180	41.6
IBO -55 a	41	10	99	56	18	81	22200	390	240	38.0
IBO -55 b	31	10	87	40	13	73	21400	382	195	39.2
IBO -56 a	36	10	90	43	12	77	21500	412	245	35.8
IBO -56 b	35	14	85	36	13	55	13000	328	228	36.7
KO - 1 a	32	10	63	35	9	63	13800	278	215	38.3
KO - 2 a	34	11	72	38	10	69	17500	326	210	35.5
KO - 3 a	44	12	120	58	18	106	39000	410	240	36.2
KO - 4 a	34	12	80	40	11	75	18300	322	320	36.6
KO - 5 a	40	10	98	49	15	90	32000	440	165	32.2
KO - 7 a	43	9	93	47	14	88	31500	444	245	39.2
KO - 8 b	46	14	118	57	19	88	36000	468	245	25.8
KO -10 a	32	6	62	33	9	63	15750	300	230	42.1
KO -12 a	34	13	77	35	11	67	17600	381	235	37.1
KO -14 a	29	7	71	37	13	63	16600	451	185	39.9
KO -15 a	28	7	65	34	10	71	35000	402	160	24.8
KO -16 a	40	8	93	45	15	86	30500	382	240	36.9
KO -17 a	40	10	94	50	16	92	30000	427	205	34.5
KO -19 a	41	11	102	48	16	86	32000	437	225	39.2
KO -21 a	45	13	111	55	17	88	35000	391	215	39.7
KO -22 a	32	8	63	34	10	63	15200	344	200	38.0
KO -23 a	31	8	65	33	10	62	15000	376	170	39.7
KO -24 a	33	7	76	37	12	76	17800	400	155	42.5
KO -25 a	24	7	47	29	10	53	11200	408	165	39.2
KO -27 a	30	8	69	33	10	67	16100	350	185	41.6
KO -28 a	30	9	62	32	10	63	14750	385	180	40.2
KO -30 a	30	9	62	34	11	65	14650	363	185	39.5
KO -32 a	34	10	79	40	11	73	19150	379	205	40.6
KO -33 a	46	21	123	50	17	81	32000	466	250	31.5
KO -35 a	30	9	72	33	11	64	18600	385	360	39.9
KO -36 a	36	9	90	32	13	79	22000	375	260	32.6
KO -37 a	25	6	57	30	10	62	14000	395	160	42.0
KO -39 a	38	10	90	40	14	75	24500	425	240	37.1
KO -40 a	34	10	75	36	12	71	20200	371	215	36.2
KO -43 a	28	9	76	34	12	66	17750	406	215	40.4
KO -44 b	21	16	78	26	13	69	14600	435	200	39.3

Appendix II: Results of geochemical analyses on samples from the Moosehorn - Gypsumville Area

Inwood Till

Sample Number	Cu (ppm)	Pb (ppm)	Zn (ppm)	Ni (ppm)	Co (ppm)	Cr (ppm)	Fe (ppm)	Mn (ppm)	Ba (ppm)	CO_3 (%)
82-MS- 1	35	6	65	40	13	62	9900	290	185	40.0
82-MS- 2	36	7	70	45	14	69	10900	285	190	38.7
82-MS- 3	42	6	83	57	16	96	13500	310	230	43.8
82-MS- 4	42	7	80	56	17	92	13200	325	220	43.2
82-MS- 5	33	8	63	41	14	65	9900	280	180	39.7
82-MS- 6	36	5	64	46	15	76	11000	300	185	40.9
82-MS- 7	50	10	127	68	22	100	35000	435	285	32.3
82-MS- 8 b	38	6	65	52	16	85	11400	290	215	40.2
82-MS- 9	35	6	66	47	14	75	11300	270	225	41.3
82-MS-10 b	38	5	65	55	15	89	12000	290	210	42.0
82-MS-11 b	37	5	69	51	14	82	11650	285	210	43.0
82-MS-12	45	9	91	59	18	91	17100	380	250	37.5
82-MS-13	35	6	69	48	15	79	11850	300	200	40.6
82-MS-14	37	7	76	47	15	69	11850	305	220	39.1
82-MS-15	41	9	86	57	16	87	15000	345	245	40.8
82-MS-16 b	34	7	67	42	13	67	11400	290	205	40.8
82-MS-17 b	50	8	104	64	18	96	20450	400	285	40.0
82-MS-18 b	43	10	100	58	17	86	18600	415	275	36.4
82-MS-19 b	30	6	68	40	13	67	10700	300	200	38.7
82-MS-22 b	30	10	76	38	13	58	11450	320	230	39.5
82-MS-23 b	39	7	83	59	15	92	14150	340	240	38.3
82-MS-24 b	24	8	58	28	10	48	8850	265	160	41.7
82-MS-27 b	27	10	66	32	12	48	10250	270	215	40.4
82-MS-28 b	23	7	57	26	9	38	8600	260	175	43.5
82-MS-29 b	24	8	59	28	10	44	9850	250	175	43.2

Komarno Till

Sample Number	Cu (ppm)	Pb (ppm)	Zn (ppm)	Ni (ppm)	Co (ppm)	Cr (ppm)	Fe (ppm)	Mn (ppm)	Ba (ppm)	CO_3 (%)
82-MS- 8 a	38	7	67	54	16	82	11850	315	215	39.7
82-MS-10 a	29	6	70	56	17	92	12200	300	220	40.6
82-MS-11 a	37	6	68	49	15	75	11400	290	215	42.8
82-MS-16 a	39	8	70	44	14	67	11500	270	240	39.0
82-MS-17 a	49	8	101	60	18	94	19800	410	270	37.6
82-MS-18 a	46	9	99	56	18	82	18400	430	300	35.5
82-MS-19 a	35	9	72	47	16	70	11700	310	220	37.6
82-MS-20 a	42	9	113	57	18	88	21900	450	270	30.7
82-MS-20 b	34	10	97	46	16	75	15500	405	265	34.2
83-GY- 7	44	8	79	56	13	105	17500	344	229	44.0
83-GY- 9 c	38	10	78	55	14	96	14100	354	204	43.5
83-GY-11 b	39	11	74	53	13	101	13300	275	235	43.1

Glaciolacustrine Sediments

Sample Number	Cu (ppm)	Pb (ppm)	Zn (ppm)	Ni (ppm)	Co (ppm)	Cr (ppm)	Fe (ppm)	Mn (ppm)	Ba (ppm)	CO_3 (%)
82-MS-25 b	41	12	121	60	19	81	32000	395	325	14.5
82-MS-30	39	11	119	57	18	82	22700	400	315	30.4
83-GY- 1	40	17	103	51	20	73	20900	604	215	42.8
83-GY- 2	48	18	139	63	26	97	37900	612	204	11.3
83-GY- 3 a	56	12	123	61	20	108	40400	637	409	40.5
83-GY- 3 b	45	7	117	55	20	98	32850	582	460	38.9
83-GY- 4 a	45	6	122	55	20	99	38050	541	338	12.4
83-GY- 4 b	49	5	128	61	22	104	38450	497	196	19.4
83-GY- 5 a	49	6	128	53	19	94	34500	490	282	27.7
83-GY- 5 b	43	12	116	48	16	60	26650	401	205	22.0
83-GY- 6	58	13	128	63	21	110	39900	607	387	39.0
83-GY- 8	45	10	112	42	16	68	30200	504	194	30.7
83-GY- 9 a	39	8	86	47	13	105	21700	438	311	42.1
83-GY- 9 b	38	12	99	42	17	52	24850	474	258	13.0
83-GY-11 a	31	9	74	28	9	36	13850	268	254	20.5
83-GY-12 a	57	15	129	62	22	121	40050	535	309	27.3

Iceberg Turbate

Sample Number	Cu (ppm)	Pb (ppm)	Zn (ppm)	Ni (ppm)	Co (ppm)	Cr (ppm)	Fe (ppm)	Mn (ppm)	Ba (ppm)	CO_3 (%)
82-MS-21 a	39	10	85	46	15	71	13350	245	250	36.7
82-MS-21 b	35	11	105	47	16	77	19250	405	300	26.3
82-MS-22 a	46	9	102	53	16	90	18750	360	275	34.0
82-MS-23 a	39	9	91	57	17	84	14650	380	255	37.0
82-MS-24 a	42	11	112	56	18	87	22000	450	275	34.0
82-MS-25 a	32	10	80	43	13	64	11850	355	200	39.4
82-MS-26 a	44	11	119	59	19	87	31500	480	305	29.3
82-MS-26 b	36	11	93	46	15	72	15300	370	260	33.8
82-MS-27 a	42	10	97	49	15	76	17250	340	265	33.5
82-MS-28 a	44	9	94	57	17	82	17000	385	275	33.4
82-MS-29 a	29	10	65	35	13	46	11300	380	200	40.6
83-GY-10	40	10	104	46	17	58	25000	424	163	27.3
83-GY-12 b	44	14	89	53	16	105	20900	392	230	40.5

Appendix III: Results of geochemical analyses on samples from the Swan Lake - Dawson Bay Area

Older Till

Sample Number	Cu (ppm)	Pb (ppm)	Zn (ppm)	Ni (ppm)	Co (ppm)	Cr (ppm)	Fe (ppm)	Mn (ppm)	Ba (ppm)	CO_3 (%)
SL-83-50 c	43	9	151	34	6	70	33150	432	726	10.1
SL-83-52 b	59	13	157	49	15	69	48500	482	242	13.4
SL-83-53 b	50	14	171	37	10	60	39300	480	200	10.6
SL-83-54 b	45	16	148	33	8	54	37650	388	119	11.0
SL-83-71 b	47	18	143	32	16	63	38150	428	364	12.3

Zelena Till

Sample Number	Cu (ppm)	Pb (ppm)	Zn (ppm)	Ni (ppm)	Co (ppm)	Cr (ppm)	Fe (ppm)	Mn (ppm)	Ba (ppm)	CO_3 (%)
SL-83-18 b	37	18	114	37	23	39	52500	1670	127	18.7
SL-83-19 a	49	11	110	49	14	69	36500	291	169	22.1
SL-83-19 b	42	14	128	30	11	58	29000	719	248	22.5
SL-83-20	52	19	173	54	11	53	42000	1690	276	24.1
SL-83-21	50	17	174	31	12	57	44000	402	381	16.5
SL-83-22	41	17	142	51	18	82	40500	510	373	17.0
SL-83-23	40	17	147	25	10	50	35000	508	269	19.5
SL-83-24 1	36	16	118	33	14	48	31500	713	308	
SL-83-24 2	39	21	116	26	10	47	29500	485	293	
SL-83-24 3	41	22	141	20	11	44	33000	428	280	
SL-83-24 4	39	21	146	20	12	45	32000	539	276	
SL-83-24 5	41	22	154	23	10	46	33500	512	267	
SL-83-24 6	41	20	153	23	11	54	34000	750	232	19.4
SL-83-25 a	52	16	172	44	17	38	27000	405	316	27.1
SL-83-26	48	17	162	31	16	51	38000	511	218	19.6
SL-83-27	44	21	154	47	22	66	38500	1930	218	20.5
SL-83-30	49	15	151	37	16	51	36500	672	289	21.4
SL-83-31 1	44	19	153	49	16	49	46000	437	208	
SL-83-31 2	41	18	126	28	13	45	33500	405	215	
SL-83-31 3	44	15	134	30	11	40	32000	418	218	
SL-83-31 4	41	13	138	32	13	47	33000	511	252	
SL-83-31 5	42	13	142	29	13	42	31500	652	264	19.5
SL-83-32	43	13	147	29	16	44	31500	1410	335	18.5
SL-83-33 1	49	13	147	31	11	42	34500	453	209	
SL-83-33 2	45	9	143	26	9	34	29500	445	239	
SL-83-33 3	42	13	142	22	10	42	30500	462	255	
SL-83-33 4	51	12	157	51	22	47	38500	833	273	
SL-83-33 5	45	11	132	55	22	62	39000	637	211	
SL-83-33 6	37	11	114	25	12	50	29000	447	244	
SL-83-33 7	46	13	157	27	12	56	36500	502	178	23.7
SL-83-34	48	13	154	35	15	51	40500	1760	254	20.6
SL-83-35	45	16	150	31	19	44	35000	761	236	18.5
SL-83-36 a	45	12	140	36	15	45	38500	850	301	21.5
SL-83-37 1	44	10	142	28	9	41	33500	415	253	23.2
SL-83-37 2	45	14	156	21	7	40	37000	317	238	21.4
SL-83-37 3	48	15	156	22	8	44	39500	327	292	20.9
SL-83-37 4	46	18	153	31	12	39	40500	591	281	20.7
SL-83-37 5	44	13	139	33	16	47	36500	843	278	20.5
SL-83-37 6	44	12	139	31	12	58	33500	910	314	20.7
SL-83-38	46	13	144	28	9	47	36000	523	261	19.9
SL-83-39	45	15	152	38	12	48	34500	827	278	18.1
SL-83-40	55	14	158	39	15	64	47500	630	318	18.8
SL-83-43	39	16	112	30	12	43	31500	338	285	27.1

Sample Number	Cu (ppm)	Pb (ppm)	Zn (ppm)	Ni (ppm)	Co (ppm)	Cr (ppm)	Fe (ppm)	Mn (ppm)	Ba (ppm)	CO_3 (%)
SL-83-44	43	11	158	22	9	43	40000	267	171	17.5
SL-83-47 b	68	10	225	74	20	47	57000	391	226	23.5
SL-83-49 b	54	9	166	56	6	52	38200	390	142	19.6
SL-83-51	44	12	133	38	9	52	37650	675	507	23.9
SL-83-55	48	16	174	34	2	43	31100	311	303	17.2
SL-83-58 a	50	11	148	30	2	44	27450	387	167	20.0
SL-83-60 c	49	17	141	32	5	58	28300	466	238	17.6
SL-83-62 b	61	17	153	39	6	66	30550	273	561	18.8
SL-83-63 b	41	17	110	30	8	52	31200	310	190	19.6
SL-83-66 b	42	17	126	41	12	62	34200	575	201	21.5
SL-83-69	52	13	160	33	17	61	37000	368	257	16.6
SL-83-70	53	16	151	38	19	56	38900	482	259	18.0
SL-83-80 b	36	19	100	37	13	43	30650	401	103	25.8
SL-83-81	46	19	146	39	13	51	33350	881	262	21.0
SL-83-82	44	19	148	27	9	51	33350	609	260	20.9
SL-83-83	43	21	139	26	16	50	31800	498	276	18.7
SL-83-84	52	21	136	77	20	45	30000	571	150	26.5

Arran Till

Sample Number	Cu (ppm)	Pb (ppm)	Zn (ppm)	Ni (ppm)	Co (ppm)	Cr (ppm)	Fe (ppm)	Mn (ppm)	Ba (ppm)	CO_3 (%)
SL-83-2	31	10	90	41	11	81	26500	354	230	36.5
SL-83-3 b	27	11	85	44	14	62	27500	396	179	41.2
SL-83-4 c	39	11	106	56	18	71	34500	535	152	38.7
SL-83-9	37	19	97	42	13	51	27500	431	268	42.1
SL-83-11	29	10	84	43	14	63	21000	421	226	38.5
SL-83-12 b	29	11	92	49	14	63	28500	399	193	38.2
SL-83-13 b	44	16	113	56	18	111	34000	369	400	41.2
SL-83-13 c	45	18	110	61	18	69	42000	521	162	38.9
SL-83-16	38	16	95	45	14	63	33000	460	324	40.2
SL-83-17	43	10	113	51	18	119	36500	478	319	38.6
SL-83-42	43	11	103	41	12	72	37000	347	218	33.5
SL-83-47 a	40	9	128	44	15	76	32850	526	296	30.5
SL-83-49 a	56	10	166	48	13	61	59500	568	210	28.0
SL-83-50 b	44	15	122	27	4	53	24000	265	303	34.8
SL-83-52 a	43	7	100	62	13	80	39450	343	159	38.0
SL-83-53 a	55	9	117	54	13	73	36800	371	188	37.8
SL-83-54 a	35	14	94	43	11	71	20400	294	180	43.0
SL-83-56 a	56	14	119	34	12	79	53000	270	162	35.0
SL-83-60 b	51	15	120	50	10	71	27600	557	310	38.2
SL-83-64	51	14	141	40	6	60	35800	356	250	28.6
SL-83-65	44	13	127	42	11	58	34800	453	243	30.7
SL-83-66 c	38	13	99	38	13	56	28450	371	212	32.7
SL-83-67	47	12	143	41	9	62	36250	353	210	26.7
SL-83-68 1	46	14	123	36	13	57	33350	289	201	30.5
SL-83-68 2	48	11	140	40	14	58	32850	299	200	27.1
SL-83-68 3	50	14	148	43	17	61	37300	362	223	26.2
SL-83-68 4	48	18	134	45	17	65	36250	487	221	34.0
SL-83-68 5	36	16	90	45	13	63	22950	319	186	38.7
SL-83-68 6	56	16	151	27	11	68	40400	311	208	30.3
SL-83-72 a	47	15	103	49	17	57	24200	394	203	40.2
SL-83-72 c	47	16	122	44	15	57	28150	448	199	38.3
SL-83-73 b	42	16	107	46	14	56	28900	448	179	35.3
SL-84-1	48	6	138	60	18	60	25200	458	288	42.8
SL-84-2	36	4	103	46	12	64	18900	308	282	41.6
SL-84-3	38	2	120	52	14	79	21250	310	343	40.2

Sample Number	Cu (ppm)	Pb (ppm)	Zn (ppm)	Ni (ppm)	Co (ppm)	Cr (ppm)	Fe (ppm)	Mn (ppm)	Ba (ppm)	CO_3 (%)
SL-84-4	33	4	104	52	17	79	17800	366	265	38.8
SL-84-5	31	7	85	41	13	57	15700	298	280	41.2
SL-84-6	36	6	87	54	17	51	19150	547	254	41.0
SL-84-7	31	6	80	42	13	50	14150	483	321	41.6
SL-84-8	31	3	80	39	10	50	15550	319	272	40.7
SL-84-9	34	7	87	45	14	56	18450	358	319	37.7
SL-84-10	33	5	84	50	14	54	15700	391	258	39.1
SL-84-12	38	4	84	47	14	67	16350	352	304	23.1
SL-84-13	34	5	83	43	14	54	16850	335	242	41.4
SL-84-14	35	9	86	52	14	63	20100	334	180	40.5
SL-84-15	29	2	81	44	9	60	15600	295	292	41.8
SL-84-16	28	3	96	40	10	54	15800	298	282	39.3
SL-84-17	36	2	89	50	11	69	14750	307	219	45.0
SL-84-18	29	2	96	40	11	52	16100	300	211	40.2
SL-84-19	31	3	80	44	11	56	14600	335	248	41.2
SL-84-20	34	2	82	37	12	43	14000	389	278	38.4
SL-84-21	30	3	77	43	12	49	14150	357	226	40.0
SL-84-22	34	3	100	45	11	61	18600	264	132	44.2
SL-84-23	39	3	97	50	13	81	22100	382	262	40.6
SL-84-24	36	7	111	49	14	66	22400	395	283	43.3
SL-84-25	40	4	117	47	12	75	20800	322	236	41.2
SL-84-26	42	2	99	51	14	78	21550	357	283	40.1
SL-84-27	32	4	81	42	11	54	17200	339	243	44.7
SL-84-28	38	3	93	52	14	53	17750	384	200	44.1
SL-84-29	35	3	100	49	15	55	18700	406	199	42.6
SL-84-30	36	6	89	41	10	49	17400	327	211	41.9
SL-84-31	35	5	115	42	9	51	16800	337	199	40.1
SL-84-32 60	36	9	87	51	16	60	20050	415	236	41.9
SL-84-32 100	36	8	90	52	15	62	19300	421	227	41.2
SL-84-32 140	32	9	82	49	11	69	18900	282	191	42.8
SL-84-32 170	35	4	85	51	15	65	18750	333	230	42.2
SL-84-32 200	36	5	90	49	15	65	20600	365	239	39.6
SL-84-33	37	7	106	43	16	59	19550	365	220	42.2
SL-84-34	36	5	97	45	14	64	20750	317	218	39.9
SL-84-35	35	6	93	53	15	58	19100	375	197	39.0
SL-84-36	39	5	98	49	16	64	21550	339	230	
SL-84-37	40	5	95	48	12	53	23050	386	205	40.5
SL-84-38	31	6	83	41	13	55	18050	379	200	40.5
SL-84-39	37	6	98	64	18	64	22700	2560	261	38.5
SL-84-40	33	4	89	45	14	48	17800	407	201	40.1
SL-84-41	38	8	95	52	13	77	20750	327	242	38.7
SL-84-42	40	7	96	49	10	76	22450	286	199	40.3
SL-84-43	40	7	97	46	13	79	19150	339	247	41.2
SL-84-44	41	10	96	58	16	68	21550	603	225	40.3
SL-84-45	33	8	86	45	14	57	16350	458	227	40.7
SL-84-46	34	3	85	54	15	69	17550	301	250	45.5
SL-84-47	33	4	83	44	15	55	17050	338	236	39.8
SL-84-48	37	3	108	53	14	54	18050	323	317	41.7
PR-85-1 b	44	5	83	53	12	50	20300	379	414	41.5
PR-85-3	33	4	78	51	10	52	16200	317	371	42.0
PR-85-5	34	9	78	45	7	76	16450	250	438	36.0
PR-85-7	32	12	84	52	10	62	18850	354	341	36.9
PR-85-8 b	34	8	93	50	10	89	24000	354	313	34.1
PR-85-10 b	35	4	82	48	14	81	19550	385	304	39.9
PR-85-11	28	2	68	45	14	61	15350	374	361	40.3
PR-85-13	37	2	83	54	19	47	19550	485	329	45.5
PR-85-14 b	34	0	82	43	12	44	17450	305	408	42.2
PR-85-15	40	4	83	51	11	43	19700	354	420	42.9

Sample Number	Cu (ppm)	Pb (ppm)	Zn (ppm)	Ni (ppm)	Co (ppm)	Cr (ppm)	Fe (ppm)	Mn (ppm)	Ba (ppm)	CO_3 (%)
PR-85-16	35	2	82	50	9	50	19150	336	416	38.8
PR-85-17 b	37	2	89	47	12	47	18950	323	398	42.2
PR-85-18 b	43	4	87	48	11	45	19550	305	362	42.7
PR-85-19	32	0	78	46	10	51	17150	324	352	42.5
PR-85-21 b	36	0	88	45	12	58	21050	291	351	39.4
PR-85-22	34	0	88	54	13	54	20100	395	340	39.2
PR-85-23 b	36	0	84	47	11	70	17850	307	386	40.6
PR-85-24	32	2	84	46	11	54	18700	341	387	41.3
PR-85-25 b	37	0	82	55	14	67	20250	372	351	41.1
PR-85-26	42	5	113	75	24	58	26650	460	310	38.2
PR-85-27 b	32	0	85	50	14	69	20600	378	341	39.6
PR-85-28	42	0	87	54	15	76	20850	341	362	40.8
PR-85-29	32	0	89	60	21	64	20400	423	373	40.6
PR-85-30	33	0	84	50	17	63	20750	284	348	40.2
PR-85-31	34	0	83	54	17	67	20350	321	315	41.2
PR-85-32	37	0	92	55	19	61	24150	301	320	41.0
PR-85-33	31	5	78	51	14	60	17550	344	398	41.3
PR-85-34	37	5	85	58	16	62	20400	377	371	39.8
PR-85-35	34	7	86	65	17	65	21350	326	255	40.6
PR-85-36	36	6	88	58	16	63	20400	321	338	39.9
PR-85-38	33	4	84	54	12	62	19250	321	367	39.2
PR-85-39	33	0	73	44	11	61	17100	288	321	44.7
PR-85-41	34	6	86	56	14	60	20000	371	331	42.1
PR-85-42	34	7	84	58	17	61	19100	417	391	42.6
PR-85-43	38	13	86	68	22	61	21300	664	333	43.3
PR-85-44	35	5	80	54	10	58	19000	333	393	43.5
PR-85-45	43	7	102	72	20	62	24950	443	288	43.0
PR-85-46	39	17	116	86	24	60	30600	656	229	40.9
PR-85-47	33	7	100	71	21	78	26800	318	272	42.5
PR-85-48	39	10	85	51	11	61	22000	339	342	44.2
PR-85-49 b	31	5	93	63	16	61	22450	432	382	43.5
PR-85-50	37	4	83	58	16	77	21300	404	288	43.5
PR-85-51	34	3	76	49	14	71	18100	338	450	42.5
PR-85-52	35	2	76	51	14	72	19700	345	360	41.8

Iceberg Turbate

Sample Number	Cu (ppm)	Pb (ppm)	Zn (ppm)	Ni (ppm)	Co (ppm)	Cr (ppm)	Fe (ppm)	Mn (ppm)	Ba (ppm)	CO_3 (%)
SL-83-3 a	39	9	100	58	15	73	32500	400	205	42.7
SL-83-4 b	46	11	133	71	20	104	39000	546	257	33.3
SL-83-10 a	49	15	120	50	17	90	38500	510	241	22.0
SL-83-10 b	29	13	82	34	13	53	19500	491	260	41.0
PR-85-1 a	33	7	72	44	10	56	15100	309	417	41.5
PR-85-6	41	11	93	48	8	85	24450	274	368	35.7
PR-85-9	45	9	93	52	14	97	23150	321	322	24.5
PR-85-12	34	0	84	48	14	65	19200	342	349	41.0
PR-85-17 a	35	4	81	41	8	65	16150	248	463	33.8
PR-85-18 a	33	0	79	42	8	67	16900	263	395	36.0
PR-85-20 b	45	2	81	43	11	68	18650	259	326	41.6
PR-85-25 a	43	4	94	48	12	87	24350	300	298	32.4
PR-85-40	32	3	85	51	13	71	19750	321	403	39.7

Postglacial Sediments

Sample Number	Cu (ppm)	Pb (ppm)	Zn (ppm)	Ni (ppm)	Co (ppm)	Cr (ppm)	Fe (ppm)	Mn (ppm)	Ba (ppm)	CO_3 (%)
SL-83-1	65	20	152	47	10	88	50000	600	289	23.3
SL-83-4 a	52	10	160	61	19	75	40000	854	223	25.5
SL-83-4 d	89	16	127	56	15	91	37000	590	329	20.9
SL-83-5 a	47	19	164	53	11	85	35500	480	206	18.7
SL-83-5 b	61	14	145	53	18	101	45500	770	229	18.3
SL-83-5 c	51	17	129	60	17	77	36000	720	216	18.7
SL-83-6 a	57	17	139	50	15	98	45500	440	154	16.9
SL-83-6 b	50	17	125	59	12	77	34500	410	172	17.6
SL-83-7	52	19	126	42	14	89	42000	460	165	20.2
SL-83-8	68	20	132	48	15	86	44000	680	342	25.2
SL-83-12 a	56	16	131	60	19	99	43000	440	263	16.6
SL-83-13 a	39	12	91	52	16	58	35000	477	140	34.4
SL-83-14 a	44	14	97	51	11	95	33500	360	340	36.3
SL-83-14 b	39	13	100	50	14	92	30000	479	217	40.0
SL-83-15	82	19	121	41	11	83	43000	460	541	25.6
SL-83-18 a	39	26	114	48	31	34	25500	845	104	9.1
SL-83-28	46	16	150	44	13	56	25500	219	170	19.8
SL-83-29	45	17	155	29	17	56	33000	489	176	19.1
SL-83-36 b	47	17	160	39	15	65	36500	889	228	
SL-83-46 a	32	10	154	33	11	64	43000	410	117	
SL-83-50 a	41	14	125	37	7	53	34250	324	742	11.0
SL-83-52 c	37	19	154	45	11	56	48000	420	97	5.6
SL-83-56 c	48	11	143	29	4	48	32950	272	219	10.4
SL-83-57	41	18	159	36	7	47	30950	314	231	7.6
SL-83-59	46	17	165	43	8	45	42500	810	259	14.0
SL-83-60 a	36	16	111	33	8	51	22000	303	429	17.6
SL-83-62 a	38	16	129	31	8	57	36150	432	222	9.3
SL-83-63 a	36	14	93	30	8	56	19400	258	305	24.5
SL-83-66 a	44	14	112	41	11	63	27050	361	184	21.0
SL-83-71 a	39	12	116	32	3	38	26500	360	498	19.9
SL-83-72 b	53	21	165	42	11	53	32400	469	211	22.0
SL-83-72 d	39	23	143	33	13	61	35050	202	366	8.6
SL-83-72 e	47	20	136	23	10	46	28400	287	201	10.8
SL-83-73 a	40	24	125	31	13	45	26450	227	195	4.0
SL-83-74	37	12	143	33	7	37	20850	375	635	5.9
SL-83-75 a	29	7	131	32	5	34	26450	288	167	7.0
SL-83-75 b	40	20	132	42	12	56	24600	392	303	27.7
SL-83-80 a	40	22	106	40	13	57	24600	441	264	23.3
SL-84-11	61	17	148	38	16	85	55000	586	162	38.2
PR-85-2 a	49	10	98	60	15	73	26250	484	288	31.7
PR-85-4 a	23	8	64	36	6	48	10550	167	575	43.0
PR-85-8 a	34	9	80	39	8	72	16550	302	566	34.1
PR-85-10 a	39	5	88	51	13	98	21000	325	375	29.6
PR-85-14 a	33	0	71	44	12	64	14800	289	468	39.6
PR-85-20 a	37	5	95	48	11	82	23350	314	373	36.1
PR-85-21 a	45	3	97	53	15	89	24700	345	327	32.8
PR-85-23 a	41	7	101	50	13	87	21650	395	366	26.6
PR-85-27 a	34	2	78	49	11	88	17500	301	400	38.0
PR-85-37	34	9	93	52	16	93	20600	364	312	37.5
PR-85-49 a	31	9	72	56	15	85	16750	330	390	42.0

Cretaceous Bedrock

Sample Number	Cu (ppm)	Pb (ppm)	Zn (ppm)	Ni (ppm)	Co (ppm)	Cr (ppm)	Fe (ppm)	Mn (ppm)	Ba (ppm)	CO_3 (%)
SL-83-25 b	38	13	116	37	20	0	7000	210	1025	
SL-83-48 a	24	24	107	18	5	6	9000	40	371	
SL-83-48 b	67	17	191	50	8	40	28000	180	613	
SL-83-49 c	26	20	120	42	13	38	20500	220	102	
SL-83-56 b	30	16	95	22	6	22	18500	120	235	
SL-83-58 b	31	15	108	38	6	38	22000	350	78	
SL-83-63 c	37	24	46	16	4	50	11500	30	117	
SL-83-73 c	39	21	118	28	6	53	35000	220	174	